University of Stavanger

FACULTY OF SCIENCE AND TECHNOLOGY

Master's Thesis

Study program/specialization: **Petroleum Engineering/ Drilling Technology**	Spring/Autumn semester, 2023 Open
Author: **Queen Mina Peterside**	…… **Queen Mina Peterside**……. (Signature of the author)
Program Coordinator: Supervisor(s): **Mesfin Belayneh**	
Title of bachelor's thesis: ***Effect of Al_2O_3 nanoparticle, Silica Powder microparticle, and Fibers on the newly formulated geopolymer: Experimental and Modelling Studies***	
Credits: 30	
Keywords: Portland cement Geopolymer Silica Powder micro particle Al_2O_3 Nanoparticles UCS Modulus of Elasticity Leakage Absorption Empirical model	Number of pages: ……95…… + Supplemental material/other: 7 Date/year 15/06/2023 Stavanger

ACKNOWLEDGEMENTS

I am privileged to have Mesfin Belayneh Agonafir as my supervisor. The guidance, mentorship, counsel, and support he has offered throughout the course of this thesis have been immeasurable. He has consistently been accessible for discussions on any day of the week, willingly extending his assistance from dawn to dusk. his unwavering commitment to his students is unparalleled and immensely valued.

I also want to thank the University of Stavanger for the opportunity to use their laboratory and materials to carry out this research.

Lastly, my appreciation goes to my husband and family for continuously encouraging me and supporting me during my studies.

ABSTRACT

When the productivity of a reservoir becomes uneconomical, the final fate of the well is to be plugged and abandoned. NORSOK D-10 defines the well integrity criteria and sets criteria for cement properties to reduce the risk level of undesired leakage from the reservoir to the surface.

However, well integrity survey data from the Norwegian Continental Shelf (NCS) shows that out of the seventy-five production and injection wells, cement recorded about an 11% integrity issue rate. Surveys from different countries around the world show that cement failure is one of the major reasons for well integrity failure. This shows that cement does not satisfy the NORSOK D-10 standard's requirement.

Currently, the oil and gas industry is searching for new alternative materials that can be used for plug and abandonment operations. Among others, geopolymer is one of the alternative candidate materials.

Several studies have shown that the addition of nanoparticles and fibers improved the strength and quality of geopolymers. In this thesis work, a total of four experimental test designs have been formulated to investigate the effect of Silica powder, Al_2O_3 nanoparticle solution, carbon fiber, and human hair on the properties of 12M NaOH and 14M NaOH-based neat geopolymer. In addition, the properties of the newly formulated neat geopolymer were compared with Portland G class cement. The geopolymer plugs were cured for 3 and 10 days at 62^{o}C and atmospheric pressure.

Results showed that silica powder increased the strength of the geopolymer with an increase in concentration. The optimum concentrations of Al_2O_3 nanoparticles and fibers have also shown positive impacts on the neat geopolymer. Furthermore, an empirical UCS wave velocity model was developed for the measured data, which showed a good prediction of the test dataset.

TABLE OF CONTENTS

LIST OF FIGURES

LIST OF TABLES

LIST OF ABBREVIATIONS

API = American Petroleum Institute

HSR = High Sulphate Resistant

I.R = Insoluble Residue

ISO = International Organization for Standardization

MSR = Moderate Sulphate Resistant

NCS = Norwegian Continental Shelf

OPC = Ordinary Portland Cement

P&A = Plug and Abandonment

PSA = Petroleum Safety Authority

RPM = Revolution Per Minute

SEM = Scan Electron Microscope

UCS = Uniaxial Compressive Strength

WCR = Water to Cement Ratio

Wt% = Weight percent

%bwoc = Percent by weight of cement

LIST OF SYMBOLS

A = cross-sectional area of the specimen (mm^2)

E = Young´s modulus (GPa)

Fmax = force at the time of failure (N)

G = Shear modulus (GPa)

K = Bulk modulus (GPa)

M = Modulus of Elasticity (GPa)

P = applied force at the moment the sample breaks (N)

Vp = Compressional wave velocity (km/s)

ρ = density (kg/m^3)

τ = Shear stress (Pa)

τ_c = Yield stress (Pa)

μ_c = Viscosity (Pa.s)

γ = Shear rate (sec^{-1})

ΔM = change of mass (g)

1 INTRODUCTION

This MSc thesis presents the experimental and Modelling study of a new geopolymer. The experimental work deals with the formulation of fly ash and alkaline solution binder-based geopolymer. In addition, the impact of Silica Powder micro particle, Al_2O_3 nanoparticles (NP) and binder molar concentration, and fiber-reinforcing additives on the neat geopolymers are also investigated. The geopolymer specimens were cured for 3 days and 10 days at 62^oC temperature. The specimens were characterized by the non-destructive (sonic, mass absorption, rheology, and leakage) and destructive (Uniaxial compressive strength, (UCS)) test methods. Finally, using the UCS and compressional wave velocity data, an empirical model was developed and compared with literature-based models.

1.1 Background

Cement is used in petroleum well construction and during plug and abandonment operations. It is an important barrier element. The primary function of cement among others is to provide Zonal Isolation, Casing Corrosion Protection, and Structural support for the casing can be mentioned. [1].

Figure 1.1 shows a typical well cementing. Cement jobs are categorized as Primary and Secondary. Primary cementing is used to keep the steel pipes called casing in place once they are lowered into a drilled wellbore. cement is poured through the drill strings into the well and up the annulus between the casing and wellbore by the forced pressure of its weight. It is also used to plug so-called lost circulation zones, plugging the vertical well before directional drilling begins and reducing the risk of a blowout. Secondary cementing also called Remedial cementing is used to correct issues that arise during the primary cementing stage or the lifetime of a well. Squeeze cementing is usually used for casing cracks and involves pumping cement slurry down the wellbore at high pressure to fill all spaces that have been identified as troublesome for the normal well operation while plug cementing involves making a plug out of the cement to shut off a hole to block the flow of fluids into and from the wellbore. Plug cementing is also used after the casing is cut at a particular depth in Well abandonment. [2]

For all petroleum well cementing operations, the cement slurry and the cement job quality are the two main factors for the long-term integrity of the wellbore. However, debonding, cracking, and shear failure mechanisms are responsible for increasing the permeability of the cement due to the Pressure and temperature loading.

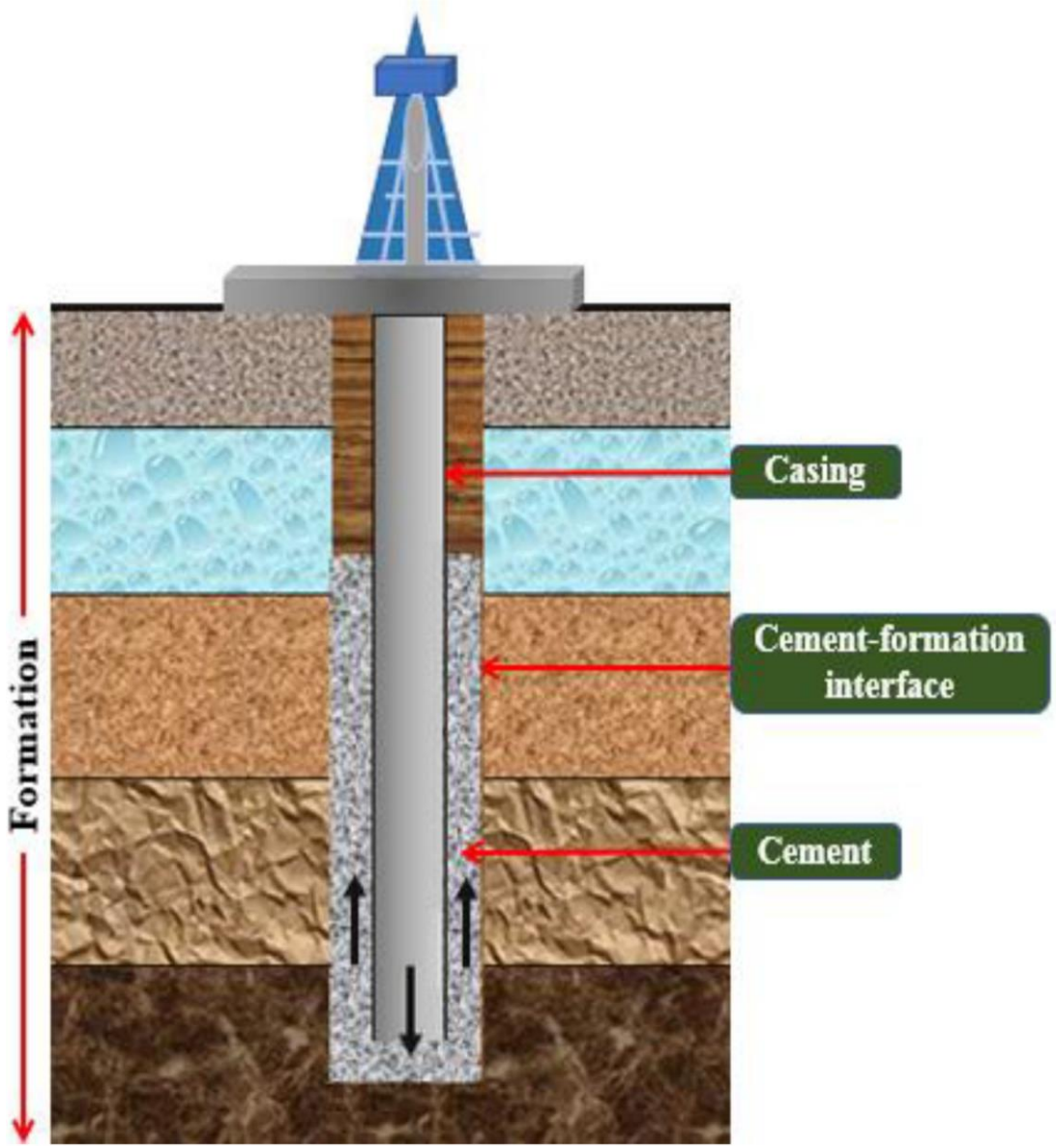

Figure 1.1: Schematic diagram for oil well cementing. [2]

NORSOK D-010 defines Well Integrity as the "*application of technical, operational and organizational solutions to reduce risk of uncontrolled release of formation fluids throughout the life cycle of a well*" [4]. For this, NORSOK D-010 demands a criterion for cement to have properties such as [3]:

- Impermeable

- Long-term Integrity
- Non-shrinking
- Ductile (non-brittle) – able to withstand mechanical loads/impact.
- Resistance to different chemicals/substances (H2S, CO2, and hydrocarbons)
- Wetting, to ensure bonding to steel.

Figure 1.2 shows the application of the cement plug during the plug and abandonment operation. As shown, the plugs comprise primary, secondary, and surface plugs [4].

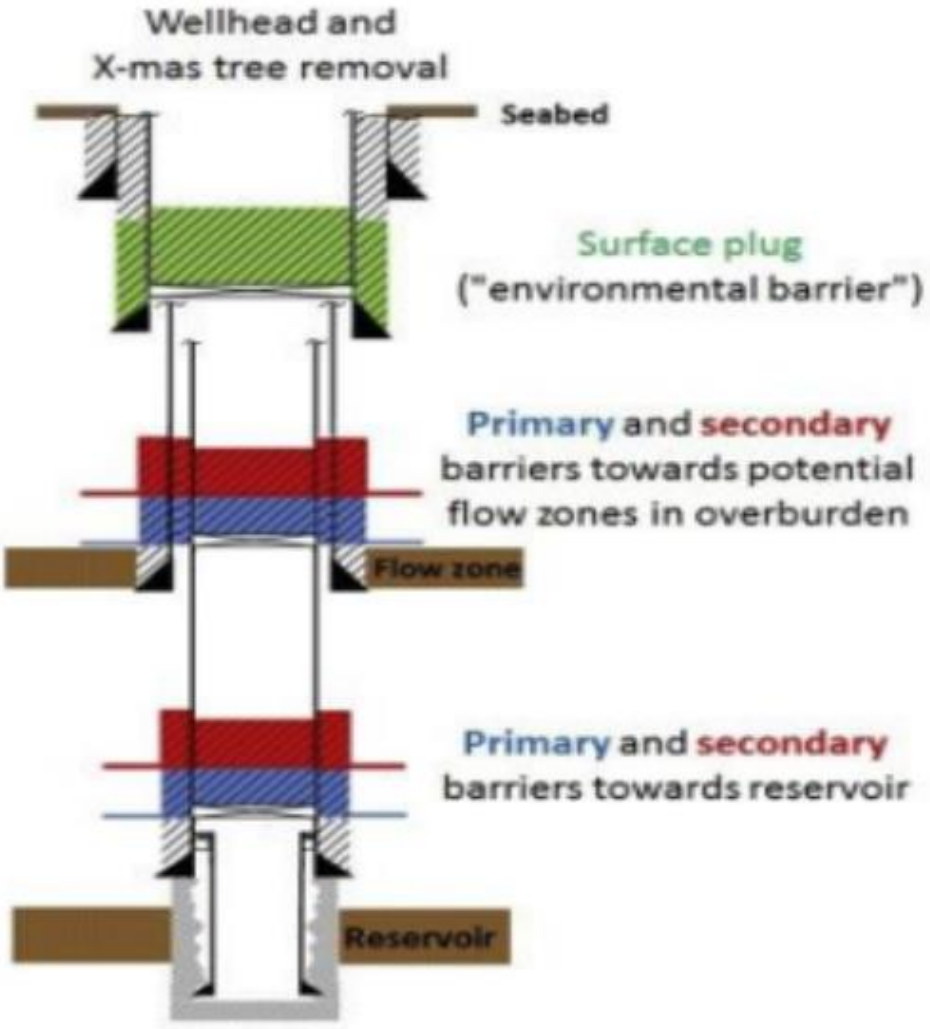

Figure 1.2: Application of cement plug for P&A [4]

Well-integrity issues are usually associated with cement quality, casing corrosion, dynamic drilling and production pressures, and completion and abandonment complexities. primary and secondary barriers are installed to cushion the effect of these issues.

Surveys from different countries around the world show that cement failure is one of the major reasons for well integrity failure. The main aim of maintaining well integrity is to impede accidents from happening. In worst-case scenarios, loss of well integrity could result in loss of lives or severe damage to the environment and oftentimes leads to expensive remedial work.

For example, Vignes & Aadnøy (2008) [5] investigated well integrity issues using a survey based on the evaluation of 21% of the active wells (production and injection wells) on the NCS. Included in the survey was a total of 406 production and injection wells. 323 production (oil and gas) and 83 injection well.

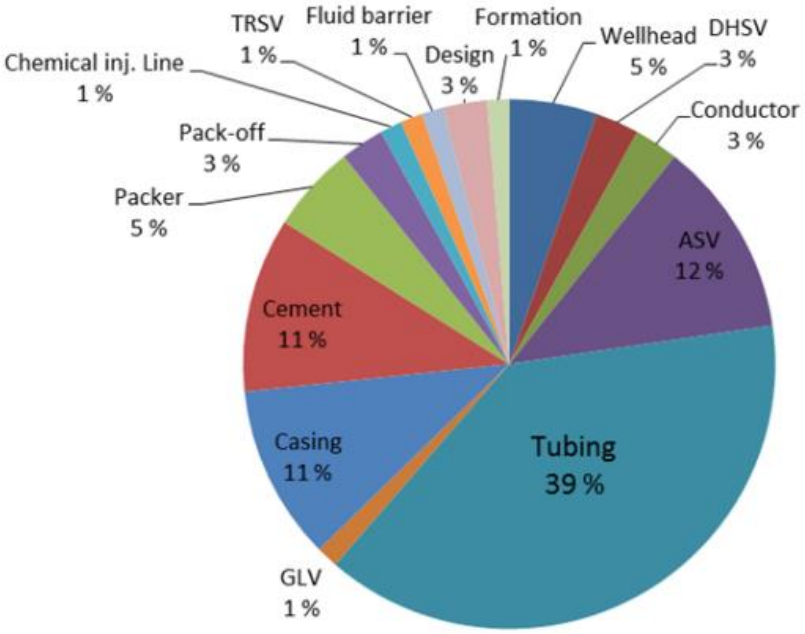

Figure1.3: Well integrity survey in NCS [5]

The well integrity survey results shown in Figure 1.3 indicate that the cement-related issue records about an 11% rate. Most of the integrity problems are within barrier elements such as cement resulting from cement problems such as no cement behind the casing and above the production packer, leaks along cement bonds, or leaks through cement micro annulus.[5]

The survey result showed that cement does not satisfy the standards requirement. Currently, the oil and gas industry are searching for new alterative materials that can be used for plug and abandonment operations. Among others, geopolymer is one of the candidates. This thesis is, therefore, designed for the formulation and characterization of geopolymer and investigates additives that improve the performance of the neat geopolymer.

1.2 Problem Formulation

Sjur (2020) [58] has synthesized 8M NaOH and metasilicate based geopolymer where the precursors are the blending of fly ash and silica fume. However, the properties of geopolymer are affected by several additives, in this thesis work, the synthesis and additive types and concentrations are different from his. Since fly ash contains a high concentration of silica, in this thesis the impact of industrial silica microparticles blended with fly ash precursors as well as a higher concentration of binders-based geopolymer will be synthesized. Then, the impact of additives will be investigated. The issues therefore to be addressed are the impact of additives on the neat geopolymer such as:

- The molar concentration of the alkaline solution
- Silica Powder concentration replacement with fly ash
- Nanoparticles concentration
- Fiber reinforcement.

1.3 Objective

The objective of this thesis work is twofold, namely, to synthesize new neat geopolymers and study the impacts of additives addressed in section 1.2. In addition, to develop an empirical correlation model that relates the uniaxial compressive strength and the compressional wave velocity of the measured dataset.

1.4 Research Design

The research activities implemented in this thesis are outlined in Figure 1.4. The work comprises literature study, experimental and modeling works.

- The literature study part deals with geopolymer research activities such as additives, and the impact of nanoparticles on geopolymer concrete.

- The experimental part presents the synthesis of 12M and 14M NaOH and 40% metasilicate with fly ash as precursor-based new geopolymer synthesis. Then to answer the research questions presented earlier, carbon and human hair fiber, Al_2O_3 nanoparticle, and silica powder effect will be studied. The synthesized plugs and slurry are characterized through destructive, and non-destructive test methods.
- Finally, based on the measured dataset an empirical model will be developed and tested.

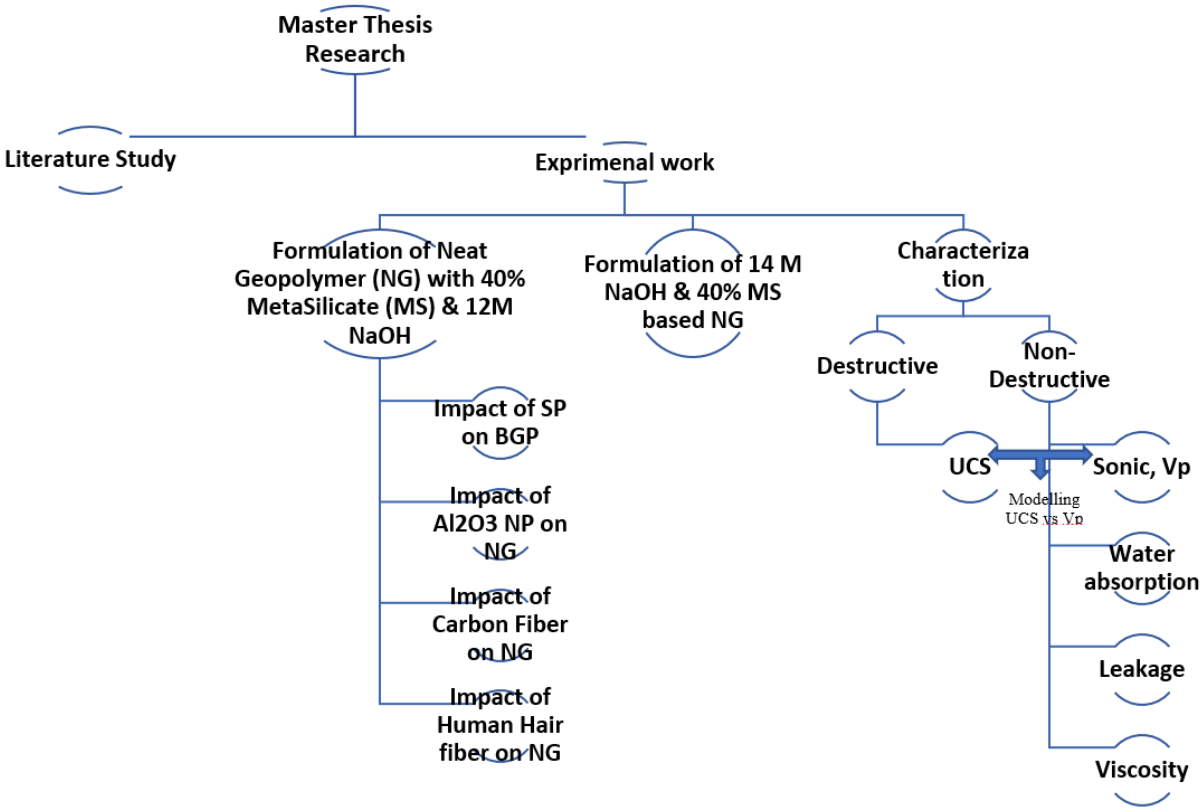

Figure 1.4: Summary of research method implemented in this thesis.

2 LITERATURE SURVEY

This Literature survey aims at giving a background to the subject being reviewed. Previous works done by researchers, methods used, and what they discovered will help to better understand the concept of this research. Also, the information obtained will help with the selection of chemical concentrations and curing temperatures as well.

This research work formulates a geopolymer reference and its property will be compared with the Portland cement.

2.1 Portland Cement

Portland cement is the most used and important type of cement across the world today. It serves as a binding material in building and construction applications and cementing in oil and gas geothermal wells.[6]. It is generally considered to be the most widely consumed construction material after water. It was invented as a product of high-temperature heating together with other materials like clays in a process called calcination. The result of this process is termed clinker. This is further ground into powder to produce Portland cement. The clinker contains four primary minerals: Alite C3S, Belite (C2S), tricalcium aluminate C3A, and tetra calcium aluminoferrite C4AF. Table 2.1 shows the chemical composition of OPC and their corresponding percentage weight.

Table 2.1: Chemical composition of cement

Cement	CaO	Al_2O_3	SiO_2	Fe_2O_3	SO_3	MgO	K_2O	Na_2O	TiO_2	Loss
CSA	42.25	36.46	6.56	2.28	8.92	1.84	0.18	0.24	0.58	0.69
OPC	61.23	5.84	22.32	3.15	2.00	2.02	0.39	0.15	–	1.66

When Portland cement is mixed with water, the product sets in a few hours and hardens over several weeks. The process involved can vary considerably depending upon the mix used and the curing conditions, but a typical concrete mix will set in about 6 hours and achieve a compressive strength of 8MPa in 24 hours. Over time, the strength of the concrete increases to 15 MPa at 3 days, 23 MPa at 1 week, and 41 MPa at 3 months. Though the strength will continue to rise if the water is present for continued hydration, concrete is typically allowed to dry out after a few weeks, and this causes strength growth to stop.[7]

According to ASTM C150, there are generally five types of Portland cement they are.[7]

1. **Type I -** This type of Portland cement is commonly referred to as general-purpose cement. It is wildly used in general construction, especially in the creation of precast, and precast-prestressed concrete structures that will encounter soil or groundwater.
2. **Type II –** Portland cement in this category is recognized for its moderate sulfate resistance and generates relatively low heat during hydration. Its cost is about the same as type I.
3. **Type III –** This has relatively high early strength and is like type I but has finer ground.
4. **Type IV –** This type of Portland cement is generally characterized by its low heat of hydration. It is primarily used for constructing massive concrete structures, that have a low surface-to-volume ratio.
5. **Type V –** This type of Portland cement is used in cases where sulfate resistance is important. It is used in the production of concrete to be exposed to alkali soil and sulfates in groundwater which reacts with (C_3A) and can cause a disruptive explosion.

Table 2.2 shows the five classes of common cement according to the European Committee of Standardization (EN) which comprises Portland cement as a main constituent. These classes are different from the ASTM classes. [7].
A summary of the types of Portland cement is shown in Table 2.2 [7]

Table 2.2: Portland cement types and their constituents

Class	Description	Constituents
CEM I	Portland cement	Comprising Portland cement and up to 5% of minor additional constituents
CEM II	Portland-composite cement	Portland cement and up to 35% of other* single constituents
CEM III	Blast furnace cement	Portland cement and higher percentages of blast furnace slag
CEM IV	Pozzolanic cement	Portland cement and up to 55% of pozzolanic constituents.
CEM V	Composite cement	Portland cement, blast furnace slag or fly ash, and pozzolana

2.2 Geopolymer Concrete

Geopolymer was the name coined by Davidovits in 1978 to refer to materials that are characterized by chains or networks of inorganic molecules. They are inorganic alumino-silicate polymers made by activating various aluminosilicate minerals with different alkaline solutions [8]

Geopolymer materials exhibit amorphous and chemical components that are akin to natural zeolitic material. The process of polymerization involves a chemical reaction between an alkaline solution and source binder materials containing aluminosilicate which results in the formation of a polymeric chain and ring structure composed of Si-O-Al-O linkages as shown in Figure 2.1 [9]

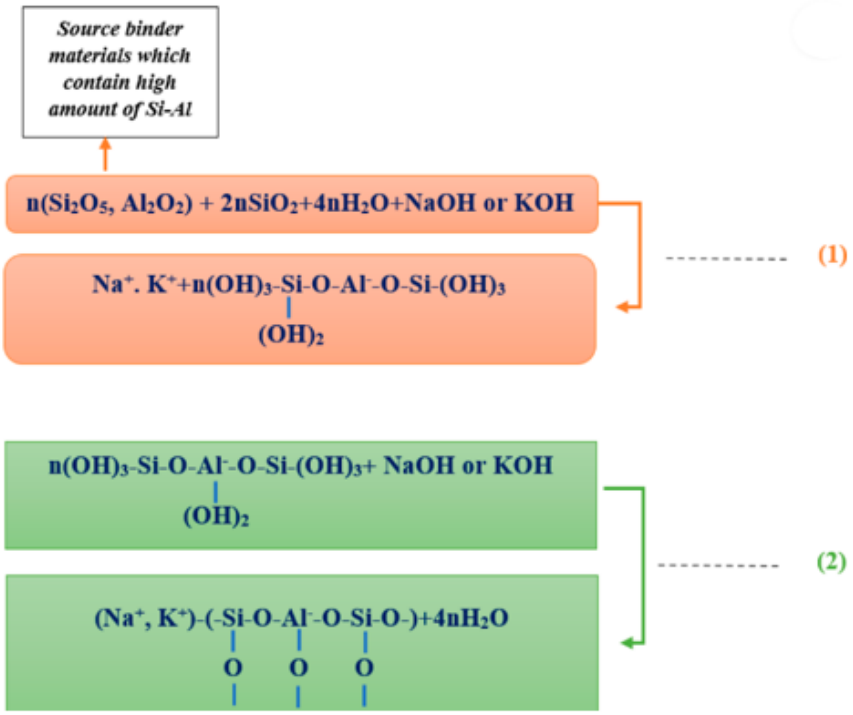

Figure 2.1: Chemical reactions during the geopolymerization process.

Dimas, D et al (2009) suggested that there are three steps involved in the geopolymerization process.[10]

1. Dissolution in alkaline solution.
2. The Diffusion of dissolved ions leads to the formation of compact, coagulated structures.
3. Polycondensation of soluble species to form hydrated products.

Different chemical material constituents are geopolymerized to form geopolymer. Some of the aluminosilicate sources are discussed below.

2.2.1 Fly ash

Fly ash is a finely grained dust consisting mainly of dissolved vitreous particles of spherical shape with a smooth surface. The main components found in most fly ashes include silica oxide(SiO_2), alumina (Al_2O_3), ferric oxide (Fe_2O_3), and calcium oxide (CaO). In addition, minor constituents found in fly ash consist of magnesium oxide (MgO), sulfur trioxide (SO_3), magnesium oxide (MnO_2), titanium dioxide (TiO_2), and unburnt carbon.

Fly ash can be obtained from flue gases of ground or crushed coal or lignite fiber boilers by various methods such as cyclone separation or electrostatic precipitation and is divided into classes C and F. The use of fly ash has attracted a lot of attention in recent years.[11]. Burning bituminous coal yields a commonly found fly ash variant called class F fly ash which has low calcium oxide (CaO) content. Lignite and sub-bituminous coal, on the other hand, used as alternative fuel sources in power generation, result in the production of class C fly ash which has a higher calcium content.[12].

2.2.2 silica powder

Another by-product of aluminosilicate is silica powder. Silica powder is derived as a by-product from the production of silicon metal in arc furnaces. It is obtained from the smoke rising through the furnace chimneys through condensation and collected from the flue gases emitted by arc furnaces. It is finely powdered and possesses high reactivity and holds significant importance in the concrete industry.

Silicon dioxide makes up about 90% of the composition of silica powder and its molecules are spherical with an exceptionally smooth surface so that they are about 100 times softer than cement. A part of the material used in concrete mixtures can be replaced with silica powder, ranging from about 7% to 15% of its weight.

It is an incredibly soft material, consisting of amorphous silica produced as a secondary by-product of silicon.

Its benefits include an increase in the strength of concrete, sulfate resistance, and mechanical corrosion resistance.[13].

Mo et al (2016) investigated the effect of silica powder and cement type on the durability of ultra-high-performance concrete (UHPC). Different cement types were used while varying the quantity of silica powder from 0% to 25% of the cement weight. The result of their study showed that as regards particle distribution, while differences in silica powder content affected the material's packing density differently across the range of

particle size, the resulting particle distributions continue to closely adhere to the optimal packing density despite variations in silica powder content. Test results support this observation, showing very little impact on the durability performance of the tested ultra-high-performance concrete mixes. This signifies that the mix component could potentially be eliminated to reduce cost. However, further studies are important to prove that the removal of silica powder, which is an important element in the mixture, does not affect the material's short-term mechanical properties. More investigation is currently being carried out by the authors to investigate this matter.[14].

Muhammad (2021) studied the effect of silica powder on the bond between building stones and pumice concrete. The primary objective of the research was to investigate the effect of adding silica powder on the bond strength between building stones and pumice lightweight aggregate concrete (PLWAC). Forty concrete-backed stone specimen was used and immersed in a water bath for 28 days, using varying ratios of silica powder.

Table 2.3: Effect of silica content on the compressive strength of the PLWAC.

Concrete compressive strength, MPa	Silica content %			
	0%	**10%**	**15%**	**20%**
Cubic strength*, f_{cu}	14.7	15.7	19.5	17.7
Cylindrical strength**, f'_c	11.76	12.56	15.6	14.16

* Cubic strength: Cubes of 150×150×150mm.

** Cylindrical strength transformed via multiplying f_{cu} by 0.8 to obtain the f'_c of 150×00 mm.

As shown in Figure 2.2, the addition of silica powder to the PLWAC increased compressive strength, bond strength, and concrete shear strength. It was also reported that the increase in the compressive strength was 7% for concrete that had 10% silica powder as against the concrete with zero silica content. This rise continued at about 15% for silica and 32% for concrete.[15]

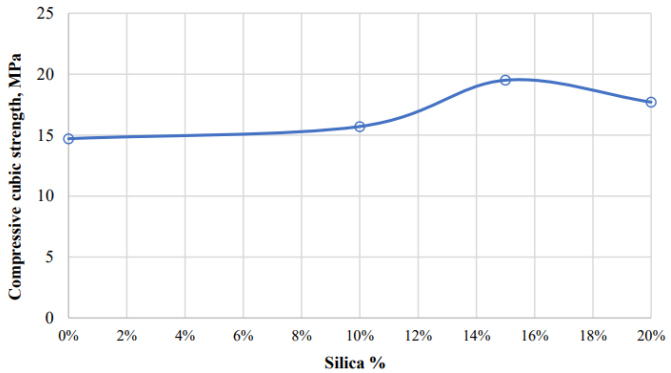

Figure 2.2: Effect of silica powder content on the cubic compressive strength of the PLWAC [15]

The significance of the alkali-to-binder ratio on the mechanical properties of geopolymer concrete cannot be overstated. The strength development of geopolymer concrete depends on NaOH/Na_2SiO_3 ratio, alkaline to binder ratio (A/B), binder type, activator agent type, and curing condition.-The alkali content and Na_2O to Al_2O_3 ratio contribute more efficiently to the formation of the geopolymer phase. The pH increases when the molarity increases, and hence allows the formation of the amorphous phase.

Srinivasa et al (2021) researched the effect of the molarity of sodium hydroxide and the molar ratio of alkaline activator solution on the strength development of geopolymer concrete. Several geopolymer mix designs were formulated with an alkali activator solution. SiO_2/Na_2O in Na_2SiO_3 solution molar ratio was varied from 1.50 to 3.00 for different ratios of Na_2SiO_3/NaOH (2.0, 2.5, and 3.0) while also varying the molarity of NaOH (8M, 10M, 12M, 14M, 16M, and 18M). The study was aimed at observing the various molar ratios on the compressive strength of geopolymer concrete. The proportion of the mixture used was Fly Ash = 450 kg/m^3, Alkali Activator solution (AAS) / Fly ash =0.5, and Na_2SiO_3/NaOH ratios adopted are 2.0, 2.5 and, 3. Table 2.4 shows the different ratios of SiO_3/NaOH in the Alkaline Activator solution used.[16]

Table 2.4: Compressive strengths of geopolymer formulation using various molarities of NaOH and Na_2SiO_3/NaOH ratio=2.0 for different SiO_2/Na_2O ratios. [16]

SiO_2/Na_2O	Compressive Strength (MPa)					
	Na_2SiO_3/NaOH=2.0					
	NaOH Molarity					
	8M	10M	12M	14M	16M	18M
1.50	3.74	4.08	4.26	4.35	5.75	4.89
1.60	4.22	4.60	4.81	4.91	6.49	5.51
1.70	5.71	6.22	6.50	6.64	8.78	7.46
1.80	10.98	11.97	12.51	12.78	16.89	14.35
1.90	13.18	14.37	15.02	15.34	20.27	17.23
2.00	20.42	22.24	23.26	23.74	31.38	26.68
2.10	20.41	22.23	23.25	23.74	31.38	26.67
2.20	19.87	21.65	22.64	23.11	30.55	25.97
2.30	19.38	21.10	22.06	22.53	29.78	25.32
2.40	17.75	19.34	20.22	20.64	27.29	23.19
2.50	11.05	12.04	12.58	12.85	16.98	14.44
2.60	9.42	10.26	10.73	10.95	14.48	12.31
2.70	7.92	8.63	9.02	9.21	12.18	10.35
2..80	6.82	7.43	7.77	7.94	10.49	8.91
2.90	4.80	5.23	5.47	5.58	7.38	6.28
3.00	4.64	5.06	5.29	5.40	7.14	6.06

The result obtained showed in Figure 2.3 that the optimum molar ratio of SiO_2/Na_2O in Na_2SiO_3 solution is found to be around 2.00 to 2.40.

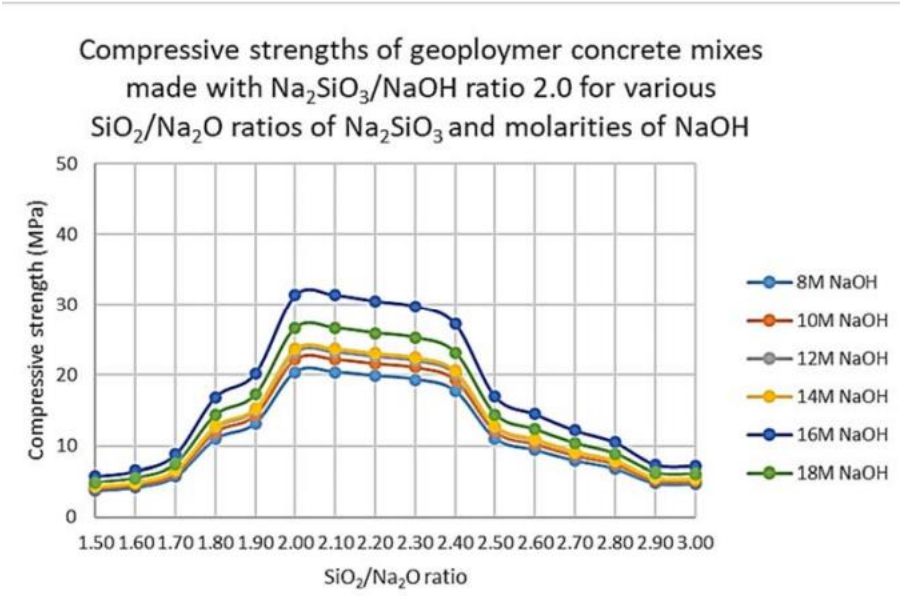

Figure 2.3: Compressive strengths of geopolymer formulated with Na_2SiO_3/NaOH ratio=2.0 for various molarities of NaOH and different SiO_2/Na_2O ratios [16]

Ganesan et al (2019) examined the effect of different activator ratios on the compressive strength of Ground Granulated Blast Furnace Slag (GGBS) based geopolymer concrete. The geopolymer concrete was cured at ambient temperature while studying the effect of different alkaline activator ratios ranging from 0.3, 0.35, 0.4, 0.45, and 0.5 on the strength parameters.

Table 2.5 Mixed proportion of materials used.[17]

Activator Ratio	0.3 (kg/m^3)	0.35 (kg/m^3)	0.4 (kg/m^3)	0.45 (kg/m^3)	0.5 (kg/m^3)
Sodium Silicate	118	138	157	177	196
Sodium hydroxide	47	55	63	71	79
GGBS	550	550	550	550	550
Coarse aggregate	1070	1035	998	962	926
Fine aggregate	559	540	521	503	484
Admixture	5.5	5.5	5.5	5.5	5.5

Observations in Figure 2.4 show that the maximum strength achieved within 3 days by the GGBS is 28.3N/mm^2, while the minimum strength is 13.2N/mm^2 for the activator ratio 0.3 and 0.5 respectively. Also, for 7 days, 14 days, 28 days, and 56 days, the highest strength is found in the activator ratio of 0.3 and the lowest is in the activator ratio of 0.5.

it is noted that increasing the activator ratio results in a decrease in compressive strength.[17]

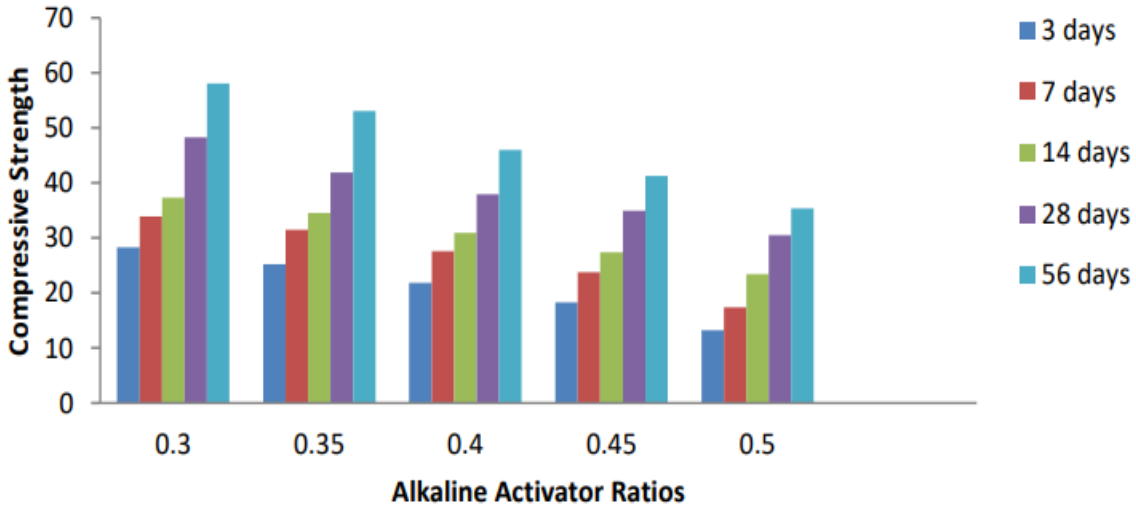

Figure 2.4: Compressive Strength VS alkaline activator ratios.[17]

Based on their experiment, they concluded that the 0.3 activator ratio is the best since the compressive strength is increased by 1.6 times.

2.2.3 Sodium Hydroxide Molarity.

Srinivasa et al (2019) studied the effect of NaOH molarity on the strength development of geopolymer concrete considering 5 Molar ratios ranging from 8M, 10M, 12M, 14M, 16M, and 18 M. For the experiment, fine and smooth particles were mixed for 60 seconds before being added to the geopolymer concrete mix.

Table 2.6: Quantity of NaOH flakes to be added to distilled water to prepare NaOH solution.[16]

Molarity NaOH flakes	NaOH flakes to be added to make NaOH solution (grams)	Molarity of NaOH solution
8M	296	7.4M
10M	364	9.1M
12M	429	10.7M
14M	491	12.3M
16M	552	13.8M
18M	610	15.3M

As the concentration of NaOH plays an important role in the leaching process of Si^{4+} and Al^{3+} ions, a decrease in the molarity of NaOH leads to an increase in the time required for setting. They concluded that the optimum molarity for NaOH is found to be 16M to achieve a strength of range 20-30 MPa.[16]

Sathish et al (2011) Prepared geopolymer samples while varying the molarity of NaOH solution by 12M, 14M, and 16M while adopting two curing methods; hot air oven curing and closed steam curing at 60^{o}C for 24 hours. They kept the Na_2SiO_3 to NaOH constant and used a 0.3 alkaline liquid-to-binder ratio. A total of 126 samples were made and tested for compressive strength using a compressive strength machine. The test result showed an increase in the molarity of NaOH with an increase in compressive strength up to 14M and then a further increase in molarity showed a decrease in the compressive strength.[18]

Mattew et al (2020) [19] researched the effect of the molarity of sodium hydroxide on the aluminosilicate content in the laterite aggregate of laterised geopolymer concrete (LGC) and observed that in contrast to the conventional aggregate, the aluminosilicate content in laterite aggregate goes through a polymerization process with higher values of the molar ratio of sodium hydroxide and then contributes to the additional strength development of LGC. The findings of the current research show a significant improvement in the cube compressive strength of LGC and that by specifically increasing the molarity of sodium hydroxide from 8 to 16, the cube strength of LGC can be increased by an impressive 63%.

2.2.4 Sodium metasilicate

Alkaline activator solution mostly contains sodium or potassium-based silicates which makes it non-user friendly. The need to use solid activators such as sodium metasilicate is necessary to reduce the negative impact of alkaline activators on the compressive strength of geopolymer concrete.

Minhao et al (2020) studied the development of high-strength one-part geopolymer mortar using sodium metasilicate, with mixes investigated over 90 days. Some factors were considered in the mix design which was activator Na_2O to total binder ratio (Na_2O%), M_s, total water to water ratio (w/b), binder content by weight (b%), fineness of metasilicate particles, additional silica content provided by micro silica and curing

conditions. Four mixes M1, M2, M4, and M7 were produced and investigated for compressive strength. It was observed that the compressive strength developed slowly and reached 48 MPa at 28 days. Also, M4 and M7 mix constantly had higher compressive strengths over M1 and M2 over 90 days. The reason was that the metasilicate particle additives were not completely dissolved.[20]

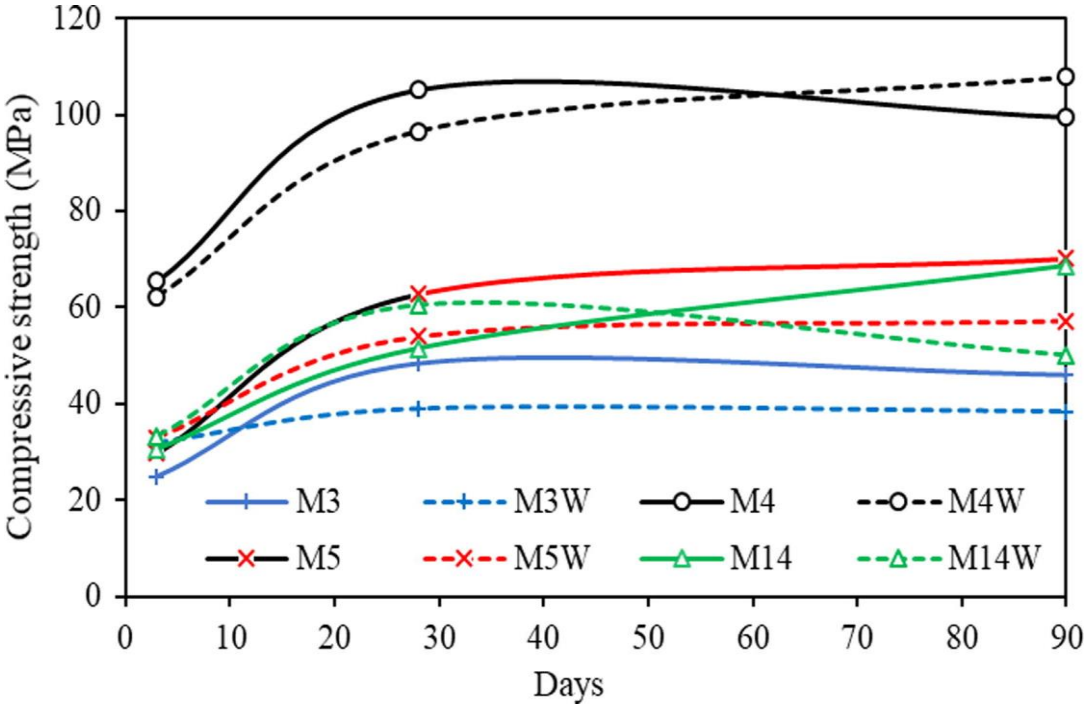

Figure 2.5: Comparison of mixes with different types of activators.[20]

Mohammed et al. (2019) in their study used granular anhydrous sodium metasilicate powder as an alkaline activator in combination with fly ash to produce a binding geopolymer gel [21]. They prepared mixtures containing five concentrations of sodium metasilicate (Na_2SiO_3). The results of their experiment showed that 12wt% of fly-ash concentration of the sodium metasilicate powder resulted in the highest compressive strength which was nearly 50 MPa. In addition, the study found that the flowability of the geopolymer slurry decreased with increasing content of sodium metasilicate. 12wt% Na_2SiO_3 exhibited a 6.7 percent reduction in flowability.

2.2.5 Alkaline activator to solids ratio

The compressive strength of geopolymer slurry is influenced significantly by two factors: the solids-to-liquid ratio and the Na_2SiO_3-to-NaOH ratio. These ratios have a direct impact on the workability of the slurry.

Liew et al (2011) in their research focused on examining how the solids-to-liquid ratio and Na_2SiO_3-to-NaOH ratio affect the synthesis of cement powder and specifically studied their effects on compressive strength. The cement paste derived from the cement powder was tested for compressive strength on the 7^{th} day. The solids-to-liquid ratio varied from 0.4 to 1.2. the highest strength was observed at a solids-to-liquid ratio of 0.8 and as the ratio increased beyond that point, the strength decreased gradually. However, no strength results were recorded for a solids-to-liquid ratio of 0.4 and 1.2. the mixture with the solids-to-liquid ratio of 0.4 showed very low viscosity, making it not suitable for molding. On the other hand, the mixture with a solids-to-liquid ratio of 1.2 had very limited workability, making proper compaction difficult. Therefore, they discovered that the solids-to-liquid ratio of 0.8 provided optimal workability, leading to the highest strength result. Figure 2.6 shows the compressive strength of cement paste from cement powder with various Na_2SiO_3/NaOH ratios.[22]

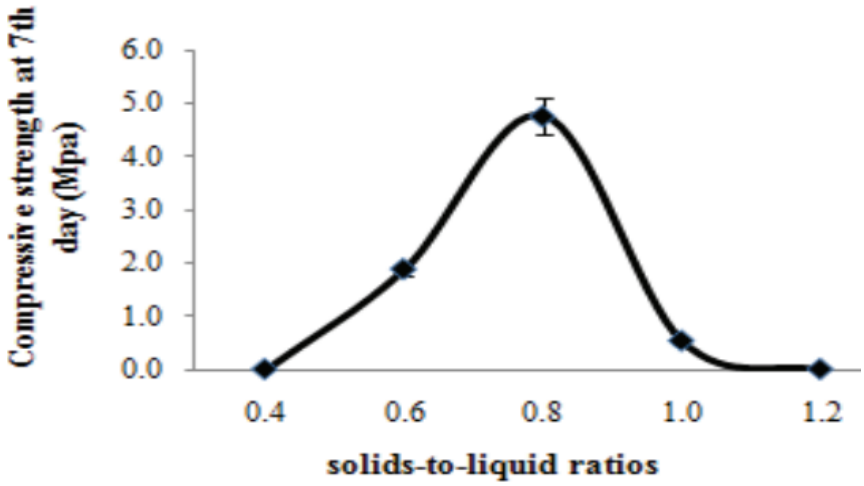

Figure 2.6: Compressive strength at 7th day at various solids-to-liquid (S/L) ratios.[22]

The use of fly ash-based geopolymer concrete instead of Portland cement concrete provides a suitable solution to address environmental issues. Over the past decade, several studies have been carried out to ascertain the properties of the fresh and hardened state of geopolymer concrete that make it a better choice compared to Portland cement concrete. These Properties are discussed below.[23]

2.2.6 Workability

Workability refers to the ease with which freshly made concrete can be moved, placed, and compressed into a dense mass. Geopolymer concrete freshly produced has a firm texture and glossy appearance.[24]. Hardjito (2004) reported that the workability of

geopolymer concrete could be improved without causing segregation or reduction in compressive strength with the addition of a naphthalene-based superplasticizer. The maximum workable flow obtained within the range of 95-145mm depends on the mass ratio of NaOH and Na_2SiO_3.[25].

Shankar et al (2012) reported that the workability of geopolymer concrete mixture reduces as the strength of concrete and molarity of NaOH increases because of a reduction in the ratio of water to geopolymer solids as well as a decrease in water.[26].

Yasir et al (2015) also reported that the workability of the geopolymer concrete increases with an increase in the alkaline solution to fly ash ratio. However, a mixture with an alkaline solution to fly ash ratio of less than 0.3 was found to be very stiff. They concluded that it was possible to improve the workability of fly ash-based geopolymer concrete by adding up to 4% naphthalene-based superplasticizer (by mass of fly ash). However, a slight reduction in compressive strength was observed after adding 2% of the superplasticizer.[27]

2.2.7 compressive Strength

The compressive strength of geopolymer concrete does not change over time but a longer curing period, increased water content, and high temperatures up to 75°C improve the geopolymerization process and result in an increase in compressive strength.[24]. Joseph et al (2020) from their findings concluded that the compressive strength of geopolymer concrete showed an increase with the increase in temperature up to 100°C but decreased thereafter. This was likely due to the loss of moisture from the concrete. A further study showed that by choosing the curing temperature and curing period adequately, it could be feasible to achieve high early strength in geopolymer concrete. The report specifically indicated that 96.4% of the 28-day strength could be achieved within just 7 days by conducting 24 hours of curing at 100°C. [28]

Palomo et al (1999) [29] reported that prolonged curing at elevated temperatures can have a negative effect on compressive strength as it can cause the granular structure to collapse resulting in excessive shrinkage. They also discovered from their research that the compressive strength of geopolymer concrete tends to increase with an increase in alkali to fly ash ratio up to 0.55 and Na_2SiO_3/NaOH up to 2.5, and beyond these values, the

compressive strength decreases. It was observed that the rise in compressive strength was mainly because of sodium silicate content on the change of geopolymer's structure.
Chindaprasita et al (2018) investigated the setting time and compressive strength of alkali-activated calcium-based fly ash geopolymer concrete under ambient temperature, using three calcium ionic materials such as Portland cement (PC), calcium hydroxide (CH) and calcium oxide (CaO) such as Portland cement (PC), calcium hydroxide (CH) and calcium oxide (CaO). They reported that incorporating PC, CH, and CaO in the geopolymer concrete is a very crucial prerequisite for repair material. These additives significantly improved the compressive strength, whereas the compressive strength was decreased due to the incorporation of CaO in alkali-activated high calcium fly-ash-based geopolymer concrete. The study further concluded that 5% PC and 5–15% CH incorporation in alkali-activated fly ash-based geopolymer is suitable as a replacement for repair materials.[30]

Nath et al (2017) investigated low calcium fly ash-based geopolymer concrete with some additives: GGBFS, OPC, and hydrated lime under ambient curing temperature. The study found that the compressive strength of geopolymer concrete mixes due to incorporating additives has significantly improved when compared to control concrete. The flexural strength of geopolymer concrete cured at ambient temperature was higher than that of normal concrete with ordinary Portland cement for the same compressive strength. However, the modulus of elasticity of the geopolymer concrete was lower than the control concrete.[31]

Singh et al (2016) conducted research on the impact of activator concentration on the strength, interfacial transition zone (ITZ), and shrinkage of fly ash/slag-based geopolymer concrete during ambient temperature curing. Their research discovered that above 14M activator concentration, because of the rigid microstructure and variation in phase composition at the interface of bulk matrix and aggregate, the compressive strength was reduced. In addition, after 6 months, the drying shrinkage of geopolymer concrete was significantly lower than ordinary Portland cement due to its prevailing zeolitic characteristics. They also discovered that at room temperature, The geopolymer achieved the necessary setting and hardening at optimum activator concentration.[32]

2.2.8 Density

Hadjito et al (2005) in their research discovered that for geopolymer concrete made with granite coarse aggregate, the unit weight was found to be between 2330-2430 kg/m^3.[33] Furthermore, Olivia et al (2011) reported that the density of geopolymer concrete slurry ranged from 2248-2294 kg/m^3 which is close to the density of Portland cement and typically falls between 2200 -2600 kg/m^3.[34]

2.2.9 Shrinkage

Wallah (2009) studied the drying shrinkage of heat-cured fly ash-based geopolymer concrete using low-calcium fly ash as its source material, alkaline solution, and aggregates which are normally used for ordinary Portland cement concrete. This research was carried out using four series of test specimens that had different compressive strengths. They reported that a low drying shrinkage was produced when fly ash-based geopolymer concrete was cured under heat and was close to 100 micro strains after 1 year period compared to the range of 500-600 micro strains typically observed in ordinary Portland-based concrete. Moreover, it was reported that the shrinkage strain values did not show any significant difference among the slurries with varying compressive strengths and curing types.[35]

Hardjito et al (2005) reported that in heating during curing, the amount of water remaining in the micro-pores of the hardened geopolymer concrete was insignificant. This was because most of the water released during the chemical reaction may be evaporated during the heat curing process, which leads to lower drying shrinkage in geopolymer concrete compared to other types of concrete.[33]

2.2.10 Durability

Sulfate attack is a crucial issue regarding the durability and serviceability of geopolymer materials used in oil wells. Previous experiences with Portland cement and blended cement concretes showed cases of concrete degradation when subjected to sulfate attack in various environments.

Geopolymer-based materials have better resistance to acid attack when compared to Portland-based materials due to their low amount of calcium.

Wallah et al (2006) [36] in their study reported that low calcium fly ash-based geopolymer concrete samples cured for 24 hours at 60ºC and later exposed to 5% sodium sulfate solution for about 1 year, did not show any damage on their surface. They exhibited very good resistance against sulfate attacks. In addition, no significant changes were observed in the compressive strength and weight of the samples over one year of exposure.
The short-term resistance of cementitious clay-Portland cement and clay-high calcium fly ash (FA) geopolymer systems prepared using silty clay as a major component against 5wt% sodium sulfate and 5wt% magnesium sulfate solutions was investigated by Sukmak et al (2015). They observed that upon exposure to sulfate environments for 240 days, the compressive strength of the geopolymer concrete reduced by 10.8% and 21.6% in Na_2SO_4 and $MgSO_4$ solutions respectively. After exposure to a sulfate environment, the formation of ettringite, gypsum, and brucite was noticed, and the C-S-H phase disappeared while the ettringite phase formed.[37]

It is common knowledge that the mechanisms of attack by sulphuric acid and magnesium are different. Conventional concretes are usually not able to withstand prolonged exposure to high concentrations of these solutions which then leads to decalcification of the C-H-S components. As a result, OPC concrete surface becomes soft and could be removed, exposing the underlying layers of concrete to deterioration. At the same time, the attack by magnesium sulfate results in the decalcification of C-H-S components, leading to loss of adhesion and strength in the concrete. Heat-cured fly ash-based geopolymer concrete exhibits very good resistance to acid and sulfate attacks when compared to conventional concrete.

Shankar et al (2012) investigated to examine the impact of sulfuric acid on the weight and strength of geopolymer concrete (GPC). The GPC samples were immersed in a 10% sulfuric acid solution for 45 days, 7 days after casting. The changes in weight and strength were continuously monitored throughout testing. The results obtained showed that there were no visible cracks or alterations in the shape of the GPC samples. However, in the initial period of exposure, white powder deposits were observed which gradually hardened over time. It was also observed that the compressive strength experienced a reduction from 7% to 23% while the split tensile strength showed a reduction of 8% to 45% followed by a slight weight loss.[38]

Bakharev (2005) studied the durability of class F-fly ash-based geopolymer when exposed to a sulfate environment. Three different tests were used to determine the resistance of geopolymer material It involved the immersion of the materials in 5% solutions of sodium sulfate, magnesium sulfate, and a combination of 5% sodium sulfate and 5% magnesium sulfate over 5 months. The weight evolution, compressive strength, degradation products, and microstructural changes were analyzed carefully and studied throughout the testing period. The study revealed that in the case of low performance geopolymers, the deterioration was mainly through the crystallization of zeolites. On the other hand, high-performance geopolymers experienced deterioration because of the formation of fissures within the amorphous polymer matrix. In addition, it was found that when samples prepared with sodium hydroxide solution and high temperature are cured and immersed in sulfate solution, the compressive strength was improved by 4-12%.[39]

Wallah et al (2006) carried out a study to investigate the performance of low calcium fly ash-based geopolymer concrete samples taking account of weight loss and residual compressive strength when exposed to different concentrations of 0.5%,1%, and 2% of sulfuric acid over 1 year, after casting for 24 hours at 60°C curing. Visual observations showed that the surface of the plugs exhibited minimal damage and comparatively lower mass loss (3%) in geopolymer concrete as compared to concrete made with ordinary Portland cement. The deterioration in compressive strength was also observed when exposed to acid attack and its intensity depends on the acid concentration and exposure period.[36]

2.3 Effect Of Nanoparticle on Geopolymer

Incorporating suitable nanoparticles such as nano-silica and nano alumina in geopolymers not only enhances nucleation sites for aluminosilicate reactions but may act as a component of these reactions.[40]. Ali et al. (2014) conducted a review of various nanoparticles and their effects on modifying geopolymer properties [41]. The authors concluded that the incorporation of nanoparticles in geopolymer increases the compressive strength of specimens.

Geopolymers are shown to have high strength in the range of 40-80^{o}C and have a structure consisting of aluminosilicate due to polymeric reactions [40]. For a greater amount of geopolymeric reactions, the properties of geopolymers are improved, leading to increased

strength and reduction in water absorption.[40]. At high temperatures, a properly designed mixture can even give compressive strength higher than conventional Portland class G cement [41]. Generally, a drawdown with geopolymer exhibits low strength development at ambient curing temperature [41]. Researchers have explored various ways to enhance the strength with additives like slag, lime, and ultra-fine fly ash. Incorporating 1–2% nanoparticles has been found to improve the compressive strength, flexural strength, and elastic modulus of the considered pastes.[40].

A wide range of nanoparticles exist, and they affect geopolymer and other cement binder materials in several ways. Some Previous Research work has been conducted on Al_2O_3 and its effect on altering the characteristics of the geopolymer.

Tanakorn et al. (2016) revealed that the addition of nano-Al_2O_3 into fly ash geopolymer paste results in only a slight reduction in setting time [42]. The Addition of 1–2% nanoparticles has been shown to improve the compressive strength, flexural strength, and elastic modulus of pastes by promoting the formation of additional calcium silicate Hydrate (CSH) as well as calcium aluminosilicate hydrate (CASH) and sodium aluminosilicate hydrate (NASH) or geopolymer gel in geopolymer matrix. Additionally, nano-Al_2O_3 has been found to improve the shear bond strength between concrete substrate and geopolymer.

Nanoparticles were added to fly ash at the dosages of 0%, 1%, 2%, and 3% by weight. The sodium hydroxide concentration of 10 molars, sodium silicate to sodium hydroxide weight ratio of 2.0, the alkaline liquid/binder ratio of 0.60, and curing at an ambient temperature of 23^{o}C were used in all mixtures. Results showed that the addition of nano-Al_2O_3 improved the shear bond strength between concrete substrate and geopolymer. 2% nano-Al_2O_3 cured for 28 days at 45^{o}C slant shear angle 20.61 MPa compared with 10.73 MPa of the control.

The effect of mixing micro-Al_2O_3 and another nanoparticle such as micro-SiO_2 on the strength of geopolymer paste was investigated in a study by Mehmet Kaya (2021). NaOH was used as an activator together with ceramic powder used in ceramic production was used in the study.[43]

Micro SiO_2 and Al_2O_3 were added to the ceramic Powder by weight in ratios of 3%, 6%, and 9%. NaOH was used after being cooled to room temperature by mixing with the required water mixture. The water content in the mixture was determined as 0.30 and placed in standard molds measuring 40 mm×40 mm×160 mm. The molds were then wrapped in a fireproof oven bag and kept in an oven at 105°C for 24 h. The samples were taken out of the oven, mold removed, and then kept at room temperature for 7 days and 28 days. Control samples produced with ceramic Powder only were compared with samples containing micro SiO_2 and micro Al_2O_3.

The compressive strength results of the samples showed that an increase in compressive strength between 3.53 and 17.97 MPa was observed with the increase of the SiO_2 / Al_2O_3 ratio in the sample. It was concluded after conducting regression analysis that the optimum mixing ratio for geopolymer paste was 1.60% for SiO_2/ Al_2O_3, 8.52% for (SiO_2 + Al_2O_3)/Ceramic Powder, and 6.74% for Na

2.4 Fibre Effect on Geopolymer

Extensive research has been carried out dedicated to investigating the influence of the different fiber types on the mechanical properties of geopolymer concrete. The type of fiber used to enhance the performance of geopolymer concrete can be divided into two categories, artificial and natural Fibers. To address the issues of brittleness and easy cracking of geopolymer concrete, incorporating various fiber types into geopolymer concrete has become a popular method in engineering applications.

2.4.1 Steel Fiber

Steel Fibers are widely added to geopolymer concrete due to their high density, low cost, and high tensile strength. The most common shapes for sections in geopolymer concrete are circular, square, and rectangular.

Research has proven that the addition of steel fibers can effectively manage the creation and propagation of cracks, thus improving the crack resistance of geopolymer concrete, which is prone to brittleness. The key characteristics of steel fibers that are commonly used in geopolymer concrete research are outlined in Table 2.7 [44]

Table 2.7. Basic Properties of steel fiber

Types	Length (mm)	Diameter (mm)	Tensile Strength (MPa)	Elastic Modulus (GPa)	Density ρ/(g/cm^3)	Ref.
Hooked end	13	0.20	2000	200	7.85	[3]
	30	0.56	1100	200	7.85	[59]
	35	0.55	1350	210	--	[60]
Crimped	25	0.50	900–1250	200–210	--	[52]
	25	0.50	2670	--	--	[61]
Straight	13	0.16	2500	200	7.90	[62]
	15	0.12	1200	200	7.80	[63]
	10	0.12	1200	200	7.80	[63]

2.4.2 Inorganic Fiber

Inorganic Fiber is a classification of chemical fibers made from minerals. The most common types of inorganic fibers are Basalt fiber, glass fiber, and carbon fiber. Basalt fiber is made up of basalt gravel, is environmentally friendly, and has good mechanical properties. Carbon fiber is a type of lightweight and high-strength inorganic fiber material, composed primarily of carbon atoms. Glass fiber is an inorganic, non-metallic substance known for its excellent performance attributes including very high resistance to heat, good insulation, excellent mechanical strength, and notable corrosion resistance. However, it has some disadvantages which include limited wear resistance and brittleness. [44]

Table 2.8. Basic mechanical properties of typical inorganic fibers

Types	Length (mm)	Diameter (μm)	Tensile Strength (MPa)	Elastic Modulus (GPa)	Density ρ/(g/cm^3)	Ref.
Basalt	15	50	2830	83.9	2.70	[63]
	6	--	1450	88	2.63	[79]
Carbon	12	7	4000	242	--	[80]
	6	7	3950	238	1.70	[81]
	5–10	7	3530	230	--	[82]
	10	7	4558	231	1.82	[71]
Glass	6	20	1700	72	2.68	[81]
	12	12	2500	--	1.81	[61]
	6	100	1700	72	1.76	[83]

2.4.3 Synthetic Fiber

Synthetic fiber is primarily composed of macromolecular compounds. The addition of synthetic fiber into concrete can significantly impede the formation and propagation of concrete cracks thereby enhancing the toughness of the material. The commonly used

synthetic fibers are polyethylene (PE) fiber, polypropylene (PP) fiber, and polyvinyl alcohol (PVA) fiber.[44]

Table 2.9. Basic mechanical properties of typical synthetic fibers

Types	Length (mm)	Diameter (mm)	Tensile Strength (MPa)	Elastic Modulus (GPa)	Density ρ/(g/cm^3)	Ref.
PPFs	3–19	0.017	461	4.9	0.91	[3]
	6	0.035	400	3.5	0.91	[45]
	12	0.040	480	5.0	0.91	[87]
	6–50	--	310–600	3.5–6.5	0.91–0.95	[47]
PVAFs	12	0.020	1400–1600	35.0–39.0	1.26–1.29	[87]
	30	0.660	800	29.0	1.30	[59]
	12	0.015	1560	29.5	1.30	[88]
	12	0.040	1600	40.0	1.30	[89]
PEFs	--	0.020	2900	116	0.97	[64]
	6/12	0.022	3360	115	0.97	[6]

2.4.4 Natural Fiber

Natural fibers are primarily derived from three main sources: plant, animal, and mineral. Plant fiber is obtained from various parts of the plant body primarily composed of cellulose, hemicellulose, and lignin. Animal fiber is derived from human hair, animal hair, feathers, or insect secretions and is primarily composed of proteins. Mineral fiber is obtained from fibrous mineral rocks and is composed mainly of various oxides such as silica and alumina.[44]

Table 2.10: Basic Mechanical Properties of Natural Fibers

Types	Density (g/cm^3)	Tensile Strength (MPa)	Elastic Modulus (GPa)	Elongation %
Abaca fiber	1.50	400	12.00	3.0–10.0
Bamboo fiber	1.10	500	35.91	1.4
Banana leaf fiber	1.35	600	17.85	3.4
Coconut leaf fiber	1.15	500	2.50	20.0
Coconut shell fiber	1.20	175	4.00–6.00	30.0
Cotton fiber	1.60	287–597	5.50–12.60	7.0–8.0
Flax fiber	1.50	800–1500	27.60–80.00	1.2–3.2
Hemp fiber	1.48	550–900	70.00	2.0–4.0
Jute fiber	1.46	393–800	10.00–30.00	1.5–1.8
Red hemp fiber	1.45	930	53.00	1.6
Ramie fiber	1.50	220–938	44.00–128.00	2.0–3.8
Sisal fiber	1.45	530–640	9.4.00–22.00	3.0–7.0
Cork fiber	1.50	1000	40.00	4.4
Silk fiber	1.30	100–1500	5.00–25.00	15.0–60.0
Feather fiber	0.90	100–203	3.00–10.00	6.9

Dong et al (2020) Carried out research to determine the possibility of a negative effect of natural fibers such as jute on the compressive strength of ultra-high-performance concrete at ambient and high temperatures. Compressive tests were performed on 50mm cube plugs after being exposed to varying temperatures ranging from room temperature to 200°C, 400°C, 600°C, and 800°C. The plugs were subjected to controlled heating using an electrical furnace, with a slow heating rate of 0.5°C per minute. Reaching the desired temperature, the plugs were held at constant temperature for 2 hours. It was determined through the experiment that this heating rate and conditioning time allowed the samples to achieve a stable and uniform thermal state. They recorded the peak loads and compressive strength as the mean of three plugs.

Results obtained showed an increase in compressive strength of the ultra-high-performance concrete after exposure to a temperature of 200°C and decreased when the temperature was higher than 400°C. with a density of 3 kg/m^3 of jute fibers, the UHPC exhibited comparable compressive strength across all temperatures. However, when the jute fiber dosage was increased to 5 kg/m^3 and 10 kg/m^3, a reduction in compressive strength was observed in the UHPC at room temperature. Also, as the temperature increased above 400°C, the reduction in compressive strength became more pronounced with higher fiber dosage.[45]

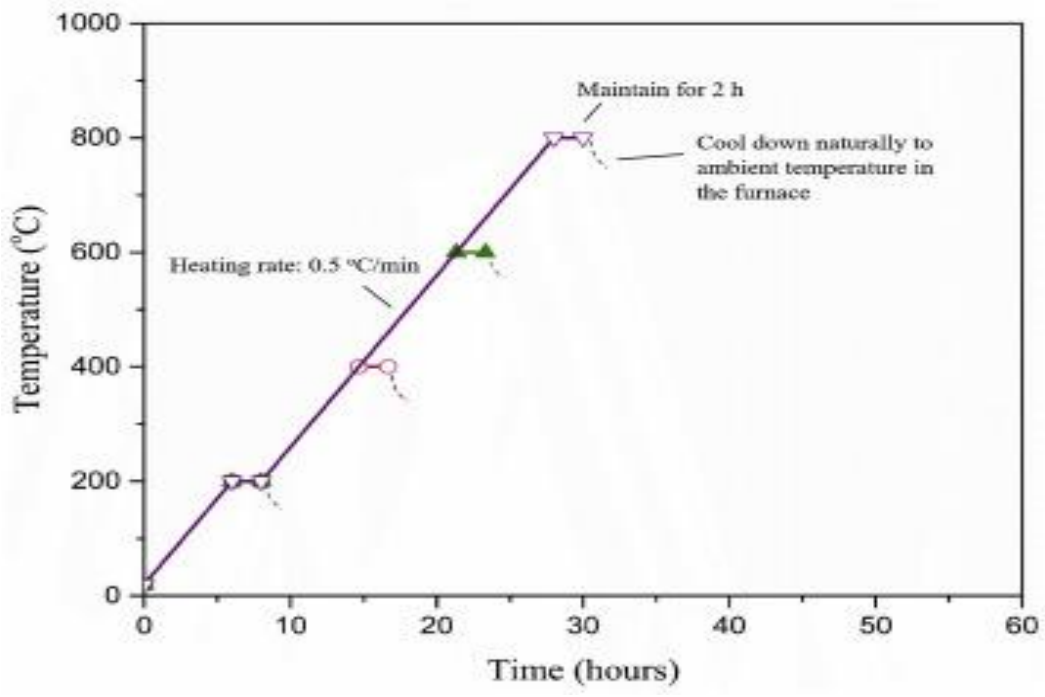

Figure 2.7: Heating curve employed for measuring the residual compressive strength of the samples.[46]

Marzena et al (2022) studied the effects of varying types of fibers on cement composites. Natural fibers such as cotton, sisal, jute, ramie, and bamboo, as well as synthetic fibers including polymer and polypropylene, were investigated in this study. It was observed that the fibers had an impact on the consistency of the mixture, resulting in a change of up to 15%. During the test for flexural strength on the composite materials, the samples showed variations of approximately 8% which depended on the type of fiber used. Findings also indicated that the use of natural fibers had a positive effect on compressive strength, increasing by 27%, while synthetic fibers led to a decrease of 4% in compressive strength.[47]

3 EXPERIMENTAL WORKS

3.1 Materials

In the subsequent sub-section, the chemical and physical properties of the materials are presented alongside the corresponding company providers.

The investigation in this study is based on the formulation of a new geopolymer which is synthesized by mixing non-cementitious solids (silica powder, fly ash) and alkaline activators (12M and 14M NaOH, Na_2SiO_3). The effect of nanoparticles and Fibers on the base geopolymer was also evaluated.

3.1.1 Fly Ash

Low-calcium (CaO, lime) fly ash class F was used in this thesis, shown in Figure 3.1. Usually, fly ash has the composition in Table 3.1. The chemical was provided by NORCEM AS [48].

Figure 3.1: Fly ash class F.

Table 3.1: Typical fly ash composition [49].

SiO	Al_2O_3	Fe_2O_2	CaO	MgO	SO_3	Na_sO & K_2O
54.90	25.80	6.90	8.70	1.80	0.60	0.60

3.1.2 Silica Powder

The silica powder was purchased from Sigma- Aldrich.it is composed of sand and white quartz in powdered form. It is white with quartz has 99.5% of the total composition and has a molecular weight of 60.08g/mol. It is used as an additive in combination with fly ash to improve the strength of the geopolymer slurry. Figure 3.2 shows the Silica powder.

Figure 3.2: Silica powder.

3.1.3 NaOH

NaOH pellets of 97% purity of 12M NaOH and 14M solution were made by mixing with water. NaOH pellets were bought from Sigma-Aldrich [50], Sodium hydroxide (98.5-100.5%) of 2.13 g/cm^3 (20°C) had the colour of white pellets. Figure 3.3 shows the pellets and the 14 M and 12 M NaOH solution.

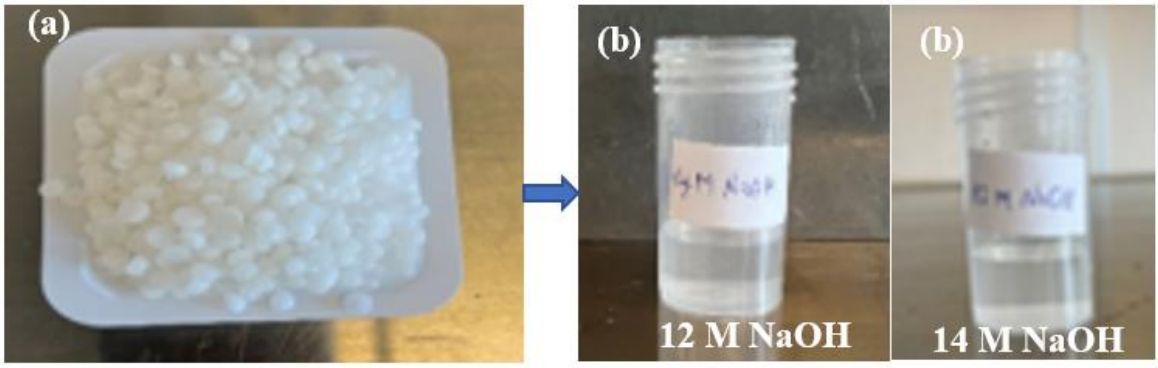

Figure 3.3: a) NaOH in pellets state (b) 12M and 14M NaOH solution

3.1.4 Silicate/sodium hydroxide ratio

Different literature was consulted to decide the optimum Silicate /sodium hydroxide ratio to use in different NaOH molar concentrations for this experiment. For instance, Manvendra et al (2020) reported that in the case of the alkaline ratio, 2.5 got the optimum point of engineering strength among all ratios of the sodium silicate to sodium hydroxide used in their research.[51]

3.1.5 WATER

Fresh water was used which was available from the faucet in the laboratory. It was used with the assumption that the water was clean and void of any contaminations.

3.1.6 Nano-Al_2O_3

The nano aluminum oxide was purchased from US research nanomaterials incorporated. The particles are 100% alpha and have an average particle size (APS) of 80nm with a purity of 99+%. The nanoparticles are white and are fully dispersed in water with a concentration of 20wt% in which the nanoparticles have a density of 3,97 g/cm^3. [52]

Figure 3.4: Nano Al_2O_3

3.1.7 Fiber

Nanoparticles and fibers have been employed in geopolymer composites to enhance their flexural strength. There are many factors to consider before the selection of fiber type. One of such is the compatibility of material properties with the application. For this research, two fiber types were used. They are.

- Carbon fiber (Synthetic fiber)
- Human hair (Natural fiber)

Carbon fiber(CF).

Carbon fiber is a thin filamentous material and is primarily made up of carbon atoms. These carbon atoms are bonded together in microscopic crystals that show an alignment along the fiber's long axis. This crystal alignment arrangement adds a high level of strength to the fiber relative to its size.[53].

The carbon fiber used in this experiment was sourced by my thesis supervisor for past experiments and the details of the materials' characterization were unfortunately unavailable. The fiber is visually black and lightweight. It looks like a fine strand of hair as sown in Figure 3.5. The fiber was cut accordingly to enable even dispersion in the geopolymer slurry.

Figure 3.5: Carbon fiber

Human hair (HH).

The human hair used for this experiment was solely 100% cut out from my supervisor's head as shown in Figure 3.6. He was gracious to allow me to use it. The hair is weightier than carbon fiber and has a coarse feel. It was cut into smaller strands to allow for easy dispersion in the geopolymer slurry.

Figure 3.6: a) my supervisor's head with hair b) the cut strands of hair

3.1.8 Cement

The cement used was provided by NORCEM and is a high sulfate resistant (HSR) API class G type cement. The chemical composition of the cement is shown in Figure 3.7b.

Figure 3.7a: Portland G-class Cement Powder

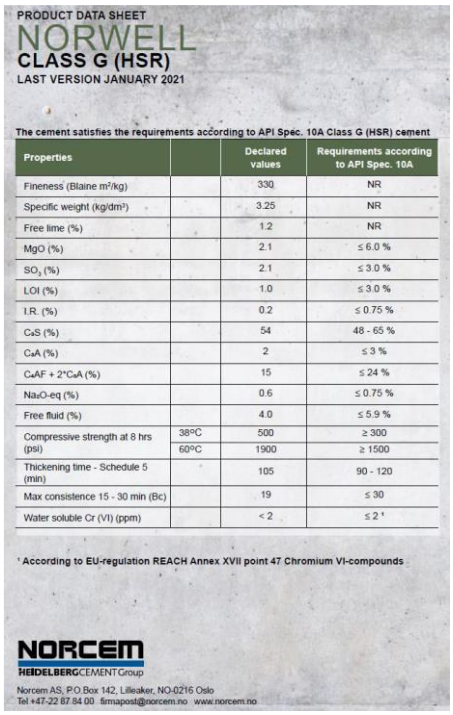

PRODUCT DATA SHEET

NORWELL

CLASS G (HSR)

LAST VERSION JANUARY 2021

The cement satisfies the requirements according to API Spec. 10A Class G (HSR) cement

Properties		Declared values	Requirements according to API Spec. 10A
Fineness (Blaine m²/kg)		330	NR
Specific weight (kg/dm³)		3.25	NR
Free lime (%)		1.2	NR
MgO (%)		2.1	≤ 6.0 %
SO_3 (%)		2.1	≤ 3.0 %
LOI (%)		1.0	≤ 3.0 %
I.R. (%)		0.2	≤ 0.75 %
C_3S (%)		54	48 - 65 %
C_3A (%)		2	≤ 3 %
$C_4AF + 2*C_3A$ (%)		15	≤ 24 %
Na_2O-eq (%)		0.6	≤ 0.75 %
Free fluid (%)		4.0	≤ 5.9 %
Compressive strength at 8 hrs (psi)	38°C	500	≥ 300
	60°C	1900	≥ 1500
Thickening time - Schedule 5 (min)		105	90 - 120
Max consistence 15 - 30 min (Bc)		19	≤ 30
Water soluble Cr (VI) (ppm)		< 2	≤ 2 [1]

[1] According to EU-regulation REACH Annex XVII point 47 Chromium VI-compounds

NORCEM

HEIDELBERGCEMENT Group

Norcem AS, P.O.Box 142, Lilleaker, NO-0216 Oslo

Tel +47-22 87 84 00 firmapost@norcem.no www.norcem.no

Figure 3.7b: Cement and it's composition.

3.1.9 Mold

Figure 3.8 is the mould used for the geopolymer, and cement slurry is plastic cylinders with a measured diameter of 34,50mm and a length of 69,25mm. The geopolymer slurry was poured directly into the cylinders but had to be coated with a thin layer of oil which acts as a lubricant in the case of the cement slurry to allow for easy retrieval of the plug. All cylindrical moulds are then cut open with a sharp knife to allow for retrieval of the plugs for further testing.

Figure 3.8: slurry mold

3.2 Characterization Methods

This subsection presents the experimental work characterization methods including destructive and non-destructive. The measurement principles, equipment, and theories to characterize geopolymer plugs and slurries are presented. Figure 3.9 shows the summary of the characterization methods.

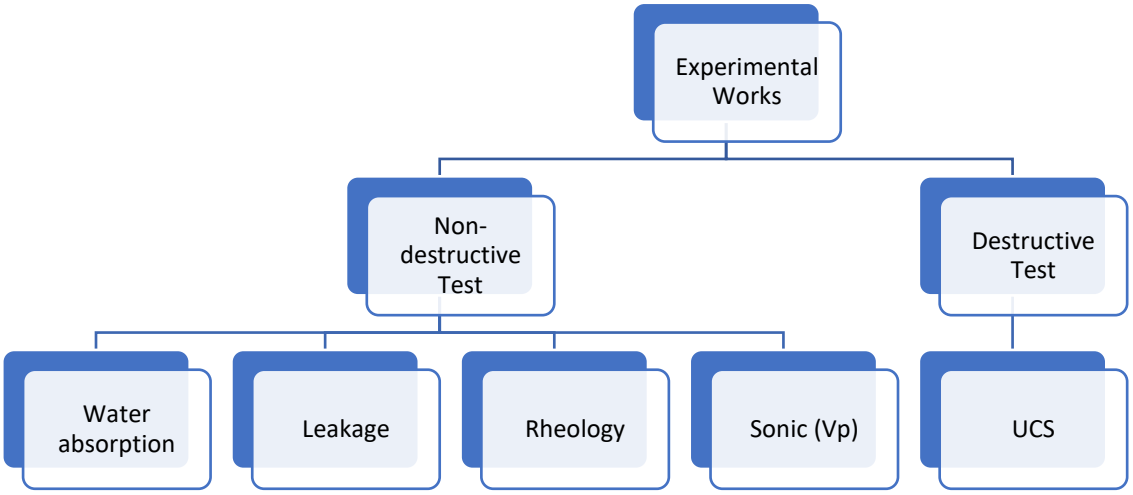

Figure 3.9: Geopolymers Characterization methods used in this thesis work.

3.2.1 Destructive Test

The main equipment which was used for crushing all the geopolymer and cement plugs was a specially customized hand-operated hydraulic shop press (UCS machine) purchased from Biltema Stavanger. It was equipped with a load sensor which allowed for accurate recording of load data to ensure correct output. It was connected to a computer with the aid of data acquisition software (DAQ), with which the computer collected all the load measurements.

It was important to ensure that the top and bottom surfaces of the plugs were flat to avoid point loading before starting any testing. This requirement was applied both during the destructive and non-destructive tests. To ensure the flatness, a spirit level was used, and the samples were then positioned on a small circular stage under the load cell. The load cell was then slowly lowered to a position just above the cement plugs. For safety purposes, a plastic protective cover was carefully placed in front of the plug to serve as a safeguard against concrete splinters and dust that might contain nanoparticles. Then,

manual loading of the concrete plug commenced and continued until the plug was yielded and crushed.

The compressive machines shown in Figure 3.10 can withstand a maximum force of 30 KN. Force load to the hydraulic crushing machine is applied to the plugs by manual hand-pumping by the operator.

Figure 3.10: Hand-operated hydraulic shop press

The Standard Force vs. %Deformation plot shown as an example in Figure 3.11 is the output from the destructive UCS machine. In converting the force-deformation to stress-strain, one can also determine the material properties such as Young's modulus (E). Except for the UCS, due to the failure of the deformation sensor, unfortunately, the Youngs modulus of the plugs was not calculated and presented in this thesis.

Using the peak force load ($Fmax$), and dividing by cross-sectional area (A), the uniaxial compressive strength (σ) can be calculated as: [53]

$$\sigma = \frac{Fmax}{A} \qquad 3.1$$

Uniaxial compressive strength (UCS) refers to the highest compressive stress applied to a sample before cracking or failing. This is also known as unconfined compressive strength because there is no confining stress on the sample during the test.

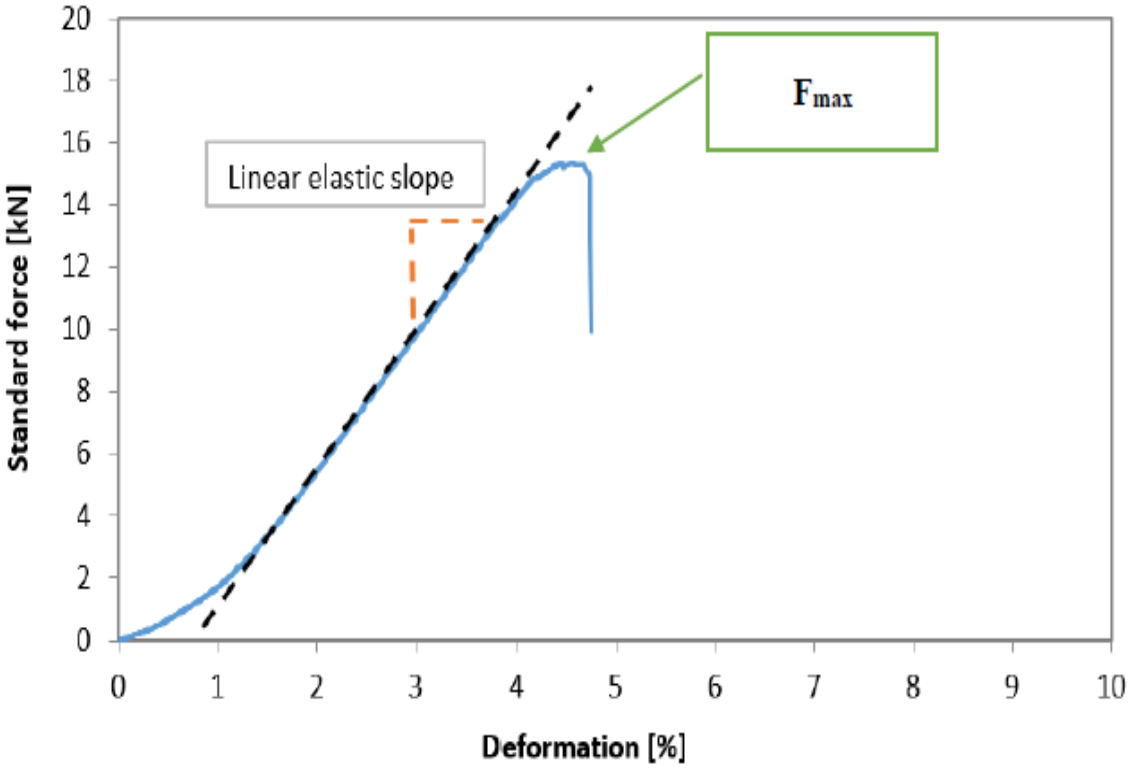

Figure 3.11: Example of Standard Force vs. %Deformation curve from UCS machine.

3.2.2 Non-Destructive Tests

The non-destructive tests were carried out on the geopolymer and cement plugs before the destructive test.

3.2.2.1 Rheology

The study of materials' deformation and flow characteristics is known as Rheology. For this research, rheology is defined as the scientific field that attempts to determine intrinsic fluid properties, mainly viscosity. This is important for establishing the relationship between the shear rate and the shear stress which is responsible for fluid movement [54]. Acquiring rheological data for geopolymer and cement slurry is very important as these parameters play a crucial role in determining the workability of the slurry.

Rheology experimental procedure

Figure 3.12 is an OFITE 8-Speed viscometer, which was used for the rheology experiment procedure. The geopolymer and cement slurry were thoroughly mixed to achieve a smooth mixture before pouring into the measurement cup. Thereafter, viscosity readings were recorded for 300, 200, 100, 60, 30, 6, and 3 RPM. It is worth noting that testing the

geopolymer and cement slurries at 600RPM was omitted as it is not a practical measurement for cementation.

Figure 3.12 shows the OFITE viscometer used to measure the viscosity of the cement and geopolymer slurries.

Figure 3.12: OFITE viscometer used to measure the rheology of geopolymer cement slurry.

Rheology model

Several well-established rheological models are available for characterizing the rheology of materials. However, the Casson rheological model stands out in the context of evaluating the rheology of cement slurry. This model will be given due consideration in this thesis as it holds significant relevance [59].

$$\sqrt{\tau} + \sqrt{\mu_c . \gamma}, for\ \tau < \tau_c \qquad 3.2$$

$$\gamma = 0, for\ \tau \geq \tau_c$$

Where:

- τ=Shear stress, [lbf100 ft^2]
- τ_c=Casson yield stress, [lbf100 ft^2]
- μ_c=Casson plastic viscosity, [lbf·sec/100 ft^2]
- γ=Shear rate, [sec^{-1}]

3.2.2.2 Geometrical parameters

Diameter and Length

To obtain precise data in geometric parameters, a vernier caliper is used to measure the outer diameters and lengths of the cement plugs. From these measurements, the cross-sectional areas and volumes of the cement plugs were directly calculated. For the calculation of the cross-sectional area and volume respectively, the following formulas were employed.

$$A_{\text{cross-section}} = \frac{\pi}{4} \cdot \left(\frac{OD}{1000}\right)^2 \quad 3.3$$

$$V = \frac{\pi}{4} \cdot \left(\frac{OD}{1000}\right)^2 \cdot \left(\frac{L_O}{1000}\right) \quad 3.4$$

Where:

$A_{\text{cross-section}}$ = cross−sectional area of cement plug, (m^2)
OD =Outer diameter (mm)
V =Volume (m^3)
L_0 = Original plug length (mm)

Mass and density

The mass of the plugs was measured with weight balance and the density was calculated using mass and the volume as

$$\rho = \frac{m}{V} \quad 3.5$$

Where:

ρ = Density, (kg/m^3)
m =Mass, (kg)
V = Volume, (m^3)

3.2.2.2 Sonic

As shown in Figure 3.13, the Pundit 7 sonic device is used to measure the transit time of P-waves through the geopolymer plugs. The sample plug was tightly positioned between

two sensors with one transmitting the compressional sound wave and the other receiving it. Before each set of measurements, the apparatus was calibrated using a silicon plug with a predetermined travel time of 25μs.

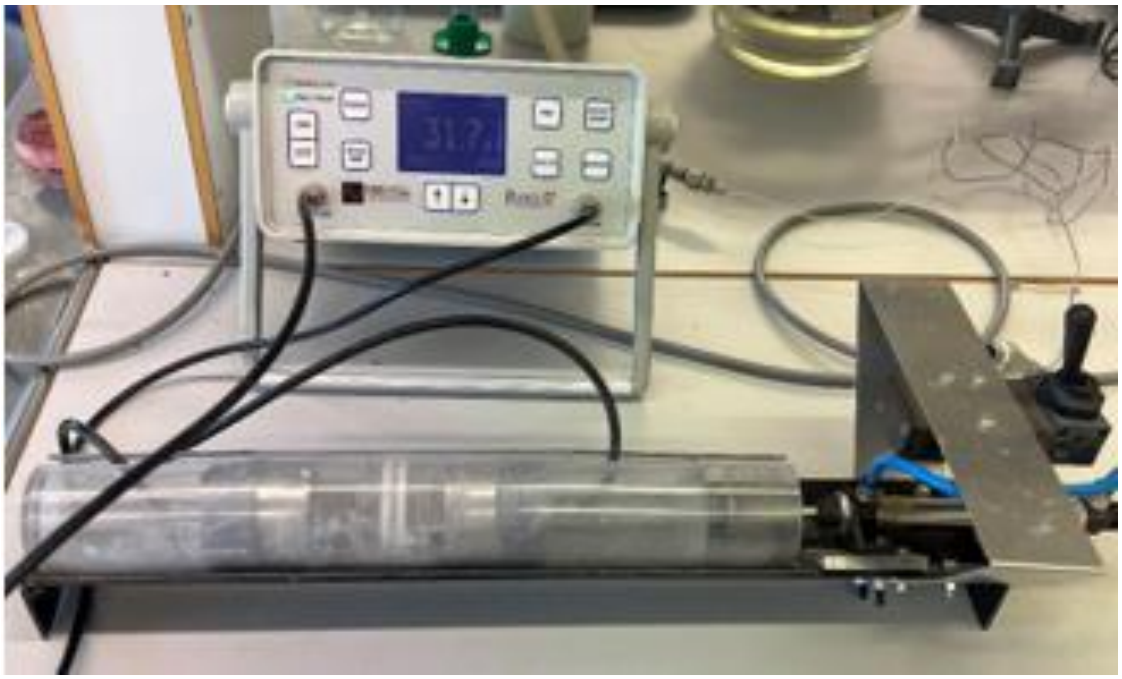

Figure 3.13: CNS Farnell Pundit 7 ultrasonic measurement device

The compressional sonic wave velocity (or P-wave velocity), can be measured from the travel time through the length of the plugs using the formula:

$$V_p = \frac{l}{t} \qquad 3.6$$

Where vp is the P-wave velocity (m/s), l is the length of the specimen (m), t is the P-wave's traveling time (sec).

The compressional wave velocity can be used to relate the elastic and physical properties of the core plug using the equation [55]:

$$V_p = \sqrt{\frac{K+\frac{4}{3}G}{\rho}} \qquad 3.7$$

Where K is the bulk modulus (GPa), G is the shear modulus (GPa) and ρ is the density (kg/m^3).

The bulk modulus (K) characterizes the material's ability to withstand the volumetric change with hydrostatic load, whereas the shear modulus (G) is the resistance to the angular deformation resulting from applying shear loading.

$$M = K + \frac{4}{3}\,G \tag{3.8}$$

Where M is the modulus of elasticity (GPa).

The modulus of elasticity can be calculated from the P-wave velocity and the density with the following equation:

$$M = K + \frac{4}{3}\,G = {v^2}_p\,\rho * 10^{-9} \tag{3.9}$$

3.2.2.3 Water Absorption

One crucial requirement for the cement properties according to NORSOK D-010 is that cement shall be impermeable. Permeability is the measure of the ability of a rock to allow fluids to flow through it, determined by the rock's pore structure and connectivity. The permeability of a core plug is determined from lab flooding experiments as well as the application of Darcy's law. However, due to limited equipment in this thesis, the degree of mass fluid absorption under room temperature and pressure was used to compare the degree of internal pore structure.

The mass change between the consecutive days is calculated as:

$$\Delta M = \frac{M_{t+1} - M_t}{M_t} * 100 \tag{3.10}$$

Where ΔM is the change in mass (%), Mt is the mass at time t, and Mt+1 is the mass at time t+1

Figure 3.14: Water absorption process diagram

3.2.2.5 Leakage Test

12M of neat geopolymer and 0.44 of class G cement were prepared. The geopolymer and cement slurries were poured into a steel pipes with one end open, and left to set for 24 hours before being cured in an oven for 3 days at 62^{O}C. It was then filled with water after cooling for a short time under running water. Measurements for leakage, mass absorption, and water evaporation were then taken after 24hrs. This cycle was repeated for oven curing for 48hrs, 72hrs, 96hrs, and 120hrs under the same conditions. The top of the pipe is covered with aluminum foil to reduce water evaporation during the length of the testing. The test setup is shown in Figure 3.15.

Figure 3.15: Leakage test setup

The test design matrix aims to study and compare the effect of heat treatment on the leakage rates of geopolymer and cement. The heating cycle (3 days, 3+3 days, and 3+3+4 days) is shown in Figure 3.16.

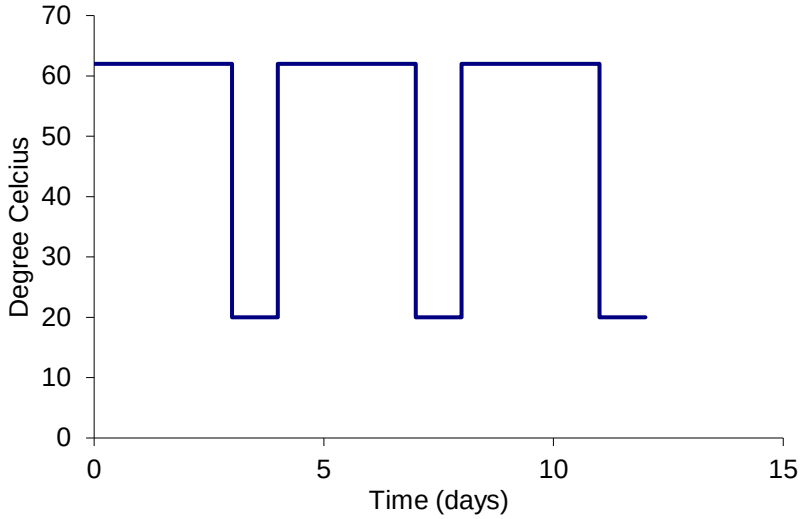

Figure 3.16: Heating cycles on the plugs in 62°C vs days.

3.3 . UCS predictive empirical models

In literature, several empirical models relate destructive test data (UCS) with non-destructive data (compressional wave velocity, Vp). For instance, in a petroleum drilling well, based on North Sea rock-extracted shale formation, Horsrud developed UCS-vs Vp as [56]

$$UCS\ (MPa) = 0.77V_p^{2.93} \qquad 3.11$$

Where V_p is the compressional wave velocity in km/s

The model is still utilized for the estimation of the uniaxial compressive strength of drilling formation based on compressional sonic travel time log data. However, its performance will be evaluated.

For cement-based plugs, Nerhus (2020) has conducted several tests on cement plugs and tested both uniaxial compressive strength and compressive wave velocity. The empirical model reads: [57]

$$UCS\ (MPa) = 0.0954V_p^{4.7184} \qquad 3.12$$

Where Vp is in km/s

3.4 Slurry and plug preparation.

3.4.1 Composition of geopolymer preparation

The methods used to prepare and mix chemicals to make the geopolymer sample plugs are described below. It is important to note that while making all the test batches, the first three plugs were reference plugs that had no additives and a set of three was prepared for each concentration of additives. Also, the solid contents were put in a mixing container, followed by the addition of the liquid components including the nanoparticles and fibers into the mixture, thoroughly combined to achieve a smooth consistency, and then poured into molds. The molds containing the slurries were then cured at room temperature for 24hrs before and after being cured in the oven at 62^{o}C for the designated number of days.

For all the geopolymer slurries prepared, 40% clear homemade sodium metasilicate was used. The choice to use this is a reference from Sjur [58]. It was discovered that using this percentage concentration gave the best result. Because this research is based on Sjur's findings, the decision to use the 40% clear concentration was to achieve optimum results. The process of preparing the 40% clear solution was a bit complex and time-consuming. The liquid preparation started by weighing up 200g of solid anhydrous sodium metasilicate powder and 500g of water into different jars. Solid anhydrous sodium metasilicate is then gradually poured into the jar containing the weighed water while stirring with a stirring rod. At this point, most of the solid particles are not dissolved. To achieve a clear solution, a heat bath is applied at this point.

The heat bath was prepared by first boiling some water in an electric cooker using a metal bucket. The sodium metasilicate solution is then transferred to the heat bath and stirred continuously until a 40% clear solution is achieved. The heat bath temperature was kept at 95-75^{o}C for 1 hour. The heat bath process is illustrated in Figure 3.17.

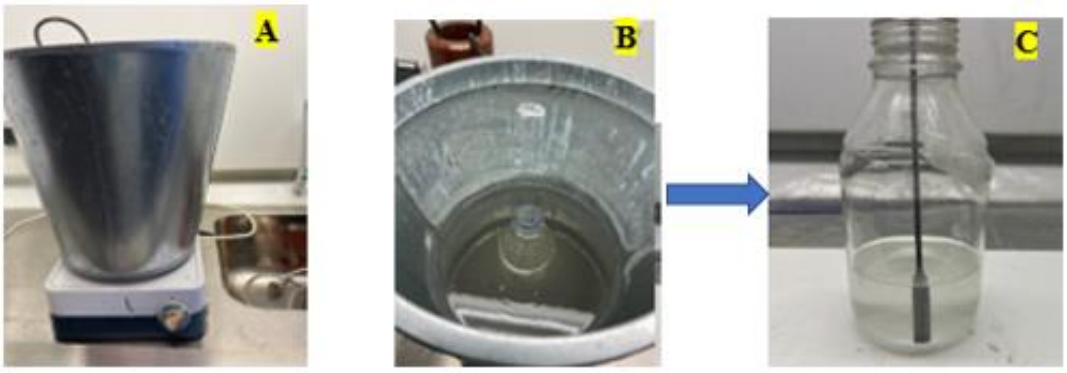

Figure 3.17: A) Heat bath setup. B) Liquid sodium metasilicate deeply immersed in the hot water bath C) Crystal clear 40% solution after the heating process

At the point of achieving a completely clear solution (40%), the heat bath is turned off and the solution is allowed to cool for 24 hours before use.

12M NaOH solution.

In the preparation of the 12M NaOH solution, a NaOH stock solution calculator was used to calculate the ratio of water to NaOH pellets to be used. For this experiment, 240g of NaOH pellets were weighed in a collector plate and 500g of water was weighed in a jar. The solid NaOH pellets were then gradually emptied into the jar containing the water and were continuously stirred until all the solid particles were completely dissolved to produce a clear solution. This solution was then left for 24 hours to allow for a complete dissolution of particles before use.

14M NaOH solution

The same procedure outlined above was used to prepare the 14M NaOH solution. The NaOH molar calculator was used to determine the ratio of water to NaOH pellets to be used. For this case, 200g of NaOH pellets was used with 500g of water. The clear NaOH solution achieved was also left for 24 hours to allow for a complete dissolution of particles before use.

Silicate/sodium hydroxide ratio

Different literature was consulted to decide the optimum Silicate /sodium hydroxide ratio to use in different NaOH molar concentrations for this experiment. For instance, Manvendra et al (2020) [50] reported that in the case of the alkaline ratio, 2.5 got the

optimum point of engineering strength among all ratios of the sodium silicate to sodium hydroxide used in their research.

Base geopolymer synthesis

The base geopolymer was synthesized using precursor solid (fly ash) and binders (alkaline solution and sodium hydroxide). The criteria for the qualification of the base geopolymers is by checking their pumpability. This was done by measuring the viscosity. Since the binders are very strong and the slurry was very viscous, several attempts were done to thin the slurry by adding extra water.

3.4.2 Neat Geopolymer Slurry preparation

For the qualification of the slurry composition, viscosity, and curing temperature qualifying factors were considered.

Viscosity determines the pumpability of the slurry. For this, we set criteria that the viscometer of the slurry should have a dial reading value of 300 RPM. It is a customary practice that cement uses 300 RPM as the maximum and measured the dial reading until 300 RPM to characterize the viscosity of the slurry.

3.4.2.1 Test for pumpability.

To formulate a reference Geopolymer that is pumpable (12M NaOH + 40% clear Silicate + 202g of Fly Ash), different water ratios were used for the different Rpm speeds applied. The results obtained are tabulated in Table 3.2.

Table 3.2: Data from pumpability test of geopolymer slurry

Extra water	**600**	**300**	**200**	**100**	**60**	**30**	**6**	**3**
0	N/A	N/A	N/A	80				
5	N/A	N/A	255					
10	N/A	265	177	89	54	28	6.5	4.5

The result is a 0.52 fluid-to-solid ratio in 2.5 silicate/NaOH ratio blended with 10 g extra water.

Table 3.3: Geopolymer slurry additives and composition

Additives	Ref
FA	202
Silica Powder	-
Silicate	75
12M NaOH	30
Extra water	10

To formulate a reference Geopolymer that is pumpable (14M NaOH + 40% clear Silicate + 202g of Fly Ash), the same process used for 12M was used and the same result was achieved. Subsequent slurries are prepared with the workable ratio obtained above. The various additives are added after the fly ash, Silicate/sodium hydroxide, and water ratios are combined thoroughly to achieve a smooth consistency. This is then poured into the mold as shown in Figure 3.18, which is always 3 for each mixture ratio for this research work.

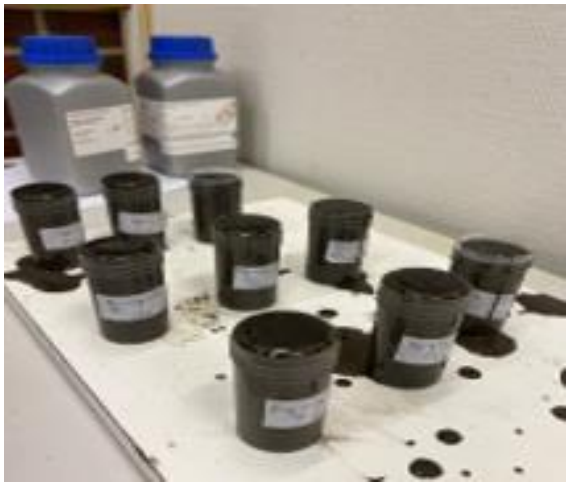

Figure 3.18: Geopolymer slurry filling in plastic mould

3.4.2.2 Test for Curing temperature.

Previous studies (Sjur 2020) [58] have shown that the maximum strength of geopolymer was obtained when the temperature was about 62^{o}C. In this thesis work, as shown in figure 3.19, the comparison between plugs cured at high temperature (105^{o}C) and moderate temperature(62^{o}C), the condition of the plug at 105^{o}C results in cracks, and on

the other hand the plug at 62ºC is in good condition. Therefore, 62ºC is selected in this thesis work.

Figure 3.19: (a) Condition of plugs at 105^{O}C and (b) plug at 62^{O}C.

The molds containing the slurries are left in the air for 24 hours and then transferred to the oven to cure at 62ºC for the allocated time frame as shown in Figure 3.20.

Figure 3.20: Oven used for curing plugs.

Subsequently, the molds were retrieved from the oven and the plugs were retrieved from the molds, polished, and left to air for 24 hours.

Polishing after curing

All the geopolymer and Portland cement plugs underwent a sandpaper (P120) polishing process after being cut to achieve a horizontal top surface. Figure 3.21 shows sandpaper

used to polish the surface. It was important to go through this process to ensure a uniform base during compressive testing as any unevenness could result in the generation of significant stress in the inclined portion of the plugs, thereby yielding a wrong result. To reduce uncertainties arising from point load effects, a small water leveler was used to ensure the horizontal orientation of the top surface as shown in Figure 3.22. Also, a complementary test was carried out by flipping the plug upside down to further ensure the accuracy of the testing process.

Figure 3.21: Sandpaper used for making the top surface of the plugs horizontal after cutting.

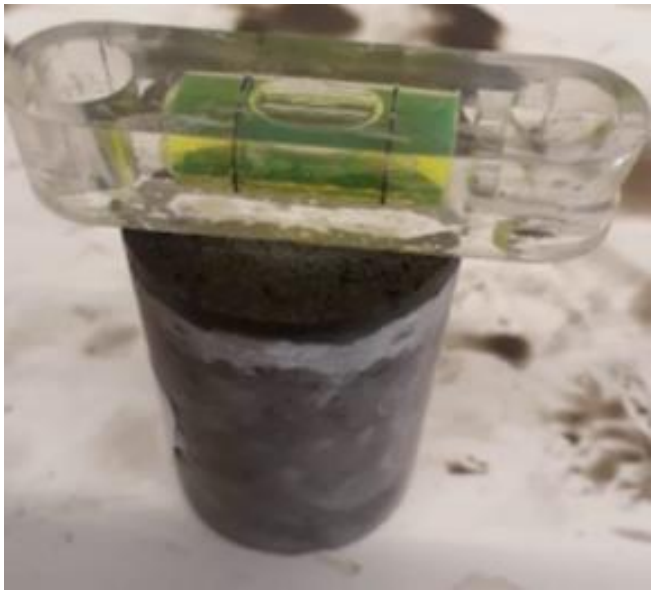

Figure 3.22: Water leveller on plugs top surface.

3.5 Experimental test designs

This thesis synthesized geopolymer and evaluated the impact of nanoparticles, different Fiber Types, silica powder, and the molar concentration of NaOH. In addition, a 0.44 water-cement ratio of G-class cement was prepared and compared with the geopolymer.

3.5.1 Test Design 1- Silica Powder in 12 M NaOH-based Neat Geopolymer

As shown in Table 3.1, fly ash contains about 54.9% Silica (SiO_2) [49]. To study the effect of rock-based additives in geopolymers, quartz was selected for the study since the mineral is Silica.

Objective: In this design, the objective was to investigate the impact of silica power on the base 12M NaOH neat geopolymer. Table 3.4 shows the test matrix design 1.

Table 3.4: Formulation of test matrix design 1.

Additives	Ref	Ref +5g SP	Ref +10g SP	Ref +20g SP
FA	202	197	192	182
Silica Powder	-	5	10	20
Silicate	75	75	75	75
12 M NaOH	30	30	30	30
Extra water	10	10	10	10

3.5.2 Test Design 2- Silica Powder in 12 M and 14 M NaOH Geopolymer

Objective: In this design, the objective was to investigate the impact of silica power on the base geopolymers. 12 and 14 M concentrations of NaOH were compared. The effects of various concentrations of NaOH on the inter-particle gelation of fly ash (Alida Abdullah et al.) and Sodium hydroxide effect on the mechanical properties of fly-ash slag-based geopolymer concrete (Manvendra Verma) [51], gave rise to this decision.
Table 3.5 shows the test matrix design 2.

Table 3.5: Formulation of test matrix design 2

Additives	Ref	Ref +5g SP	Ref +10g SP
FA	202	197	192
Silica Powder	-	5	10
Silicate	75	75	75
12 M or 14M NaOH	30	30	30
Extra water	10	10	10

3.5.3 Test Design 3-Al_2O_3 nanoparticles in Neat 12M Geopolymer

The design idea is to improve the weak geopolymer with an increasingly small concentration of nanoparticles. Though a wide range of nanoparticles exists, from previous research, adding nanoparticles such as Al_2O_3 has been shown to improve the performance of geopolymers. As previously discussed in Chapter 2, a study carried out by Tanakorn et al. (2016) showed that the addition of nano-Al_2O_3 into fly ash geopolymer paste made a positive impact on its properties. Table 3.6 shows the test matrix design 3.

Table 3.6: Formulation of test matrix design 3

Additives	Ref	Ref +0.1g NP	Ref +0.3g NP	Ref +0.5g NP
FA	202	202	202	202
Al2O3 NP	-	0.1	0.3	0.5
Silicate	75	75	75	75
12 M NaOH	30	30	30	30
Extra water	10	10	10	10

3.5.4 Test Design 4-Carbon and Human Hair Fiber in 12M-based Geopolymer

The design idea is to investigate the effect of both synthetic and natural fiber on 12M geopolymer. Carbon fiber (CF) and human hair (HH) were used. The use of human hair is a novel design that aims at producing an original and cheap alternative to other forms of additives if it works. The weight of Fly ash using each of the fiber types was kept constant at 202g, this was because the weight of the fiber additives was assumed not to make much of a difference to the total weight of the slurry. The test matrix design for 12M geopolymer with carbon fiber and 12M geopolymer with Human hair is shown in Table 3.7.

Table 3.7: Formulation of test matrix design 4

Additives	Ref	Ref +0.1g CF	Ref +0.3g CF	Ref +0.1g HH	Ref +0.3g HH
FA	202	202	202	202	202
CF	-	0.1	0.3	-	-
HH	-	-	-	0.1	0.3
Silicate	75	75	75	75	75
12 M NaOH	30	30	30	30	30
Extra water	10	10	10	10	10

4 RESULTS AND DISCUSSION

In this chapter, the results of the various tests (destructive and non-destructive) carried out on the geopolymer plugs will be discussed.
Discussions will be based on the UCS, and Modulus of elasticity results obtained from the destructive and non-destructive tests. All plugs used for the test were left in the air 24 hours before and after curing in an oven at 62^{o}C.

It is important to analyze the uniaxial compressive strength (UCS) of geopolymer cement to determine its load-carrying capacity and ability to withstand harsh environments. A higher UCS value translates to higher strength of the geopolymer cement which proves that the geopolymer cement is good.

Results reported in this thesis are the average of 3 samples of each of the test designs.

4.1 Effect of Silicate Powder in 12M-based Geopolymer

4.1.1 UCS

To further test the UCS strength of 12 M NaOH reference geopolymer cement plugs, the plugs were further cured for 10 days to compare with the results obtained from the previous test for 3 days. This design aims to compare between 12M at 3 days and 12M at 10 days.

From Figure 4.1 curing at 62^{o}C for 10 days gave a good UCS result. It can thus be observed that the strength of the 12M geopolymer cement mixture increases with an increase in curing time. It is generally expected that the increase in the mass of silica powder added to the reference geopolymer plug will correspond to an increase in the UCS strength of the plug. Adding 5g of silica powder does not show an impact on the neat geopolymer cement.

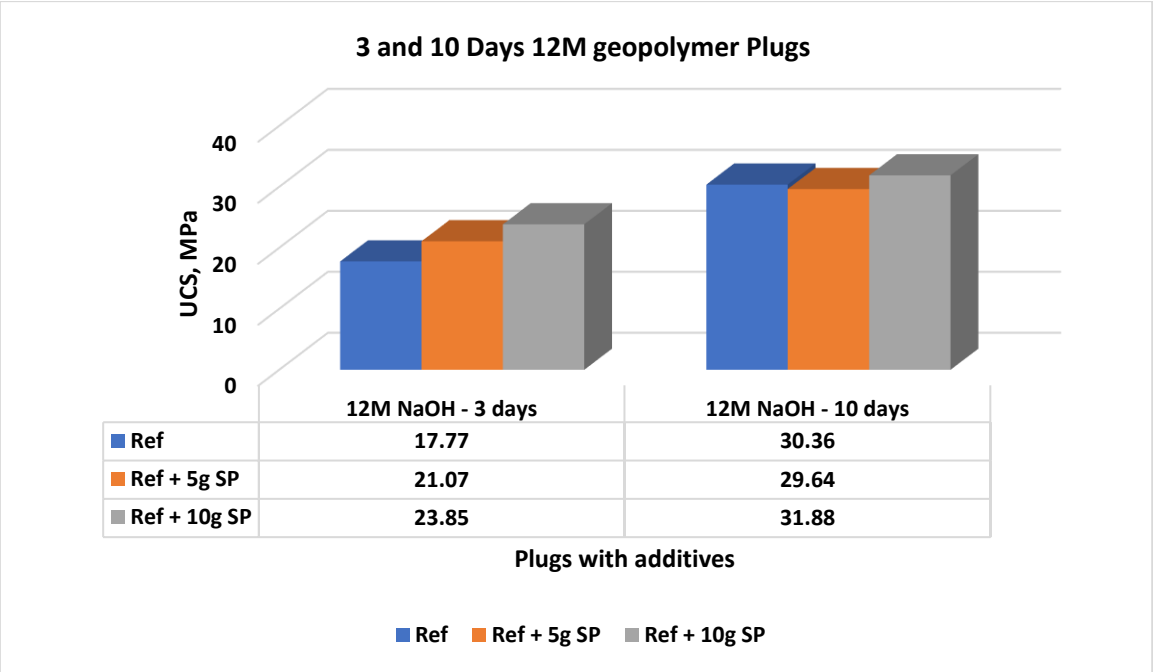

Figure 4.1: UCS for the effect of silica powder on 12M geopolymers.

4.1.2 Modulus of elasticity

The results obtained show that the stiffness of the geopolymer did not significantly improve with an increase in curing time. The neat geopolymer plugs at 10 days showed only about 9.3% improvement in stiffness compared with the same for 3 days while Ref + 5g SP and Ref +10g for 10 days showed 6% and 6.48% respectively. The result did not also follow the expected trend when compared with the UCS values obtained above.

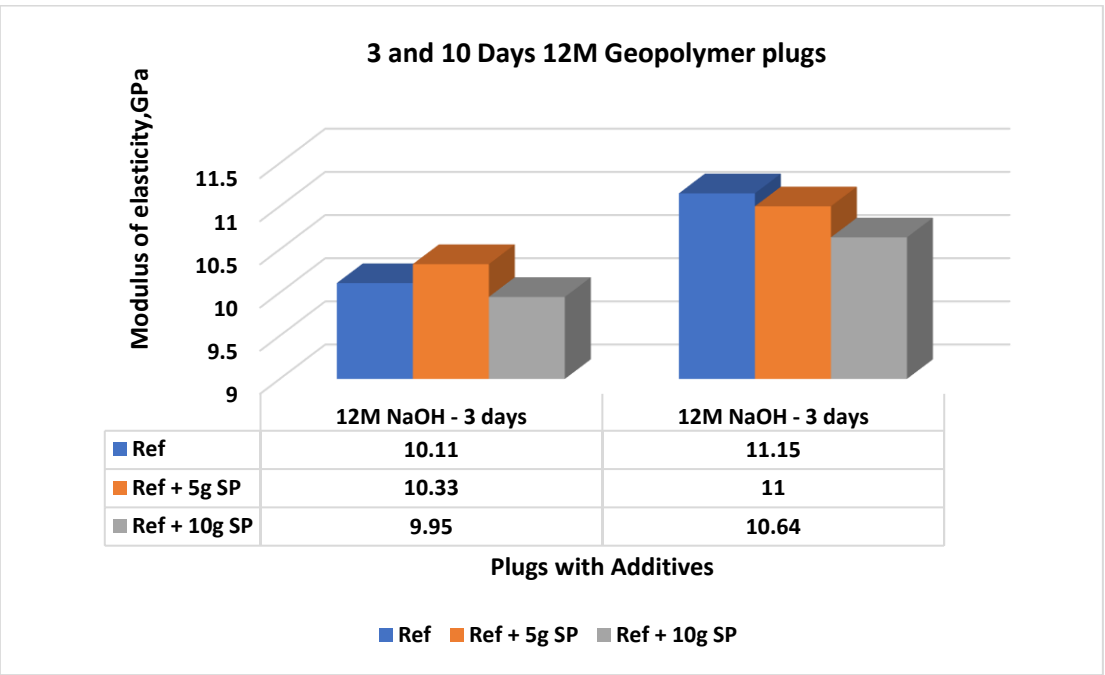

Figure 4.2: modulus of elasticity for the effect of silica powder on 12M geopolymers.

4.2 Effect of Silica Powder in 12 M and 14 M NaOH-based Geopolymer

4.2.1 UCS

Figure 4.3 displays the UCS result of 12M and 14M geopolymer plugs that contain Silica powder in increasing values of 0g, 5g, and 10g respectively, and cured at 62^{o}C for 3 days. Different color codes are used to differentiate the plugs with reference to their percentage Silica powder ratios.

The 12M plugs when crushed after 3 days in the oven and 2 days in the air showed a steady increase in strength and an increase in Silica powder mass. Improvements in each of the plugs with respect to the previous plugs were fairly the same.

The 14M plugs without silica powder showed a remarkable UCS strength compared to the plugs with 5g silica powder. The plugs containing 10g also showed a good UCS strength but were not satisfactory when compared with the neat geopolymer reference plug because it was expected that the high amount of Silica Powder will cause a significant shoot-up in the UCS strength.

The result obtained from the 14M with 5g Silica powder was not satisfactory, Hence the need to repeat the test to ensure that every possibility of error was ruled out. The result obtained is shown in Figure 4.3.

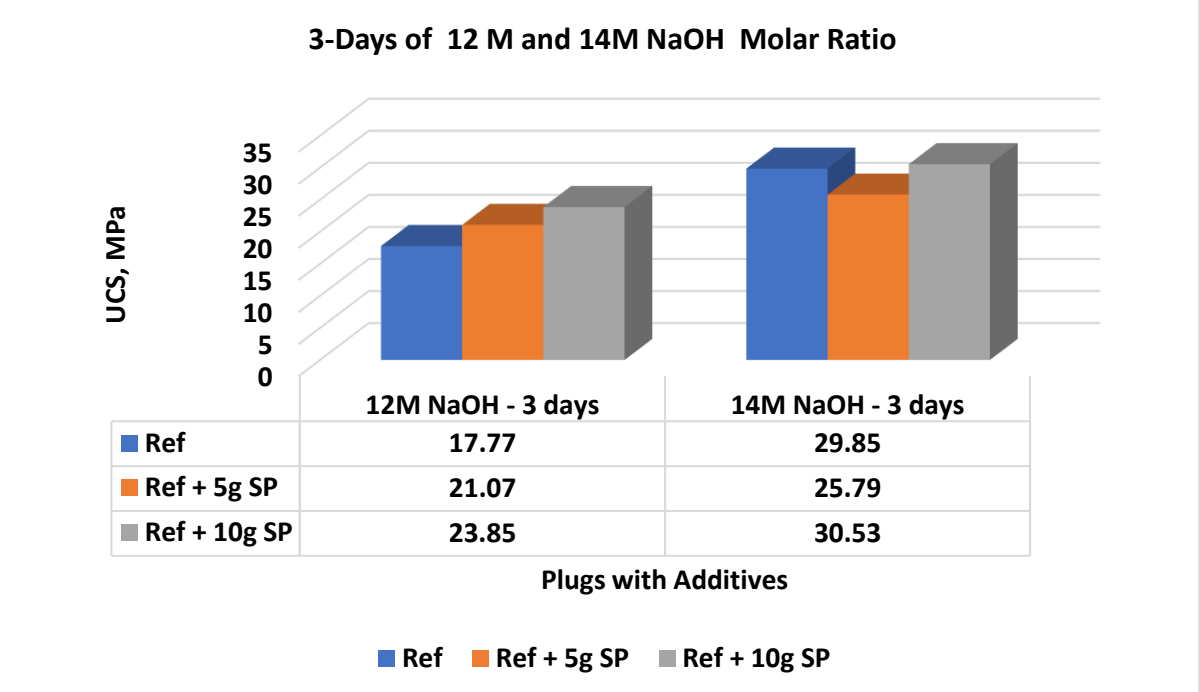

Figure 4.3: UCS for the effect of silica powder on 12M and 14M geopolymers.

The graph above shows no significant change from the previous result obtained from the original test with 5g for 14M NaOH, therefore it was safe to conclude that 5g of silica powder in the 14M reference geopolymer plug did not make a positive impact in the UCS of the sample.

It is safe to conclude that when using 12M, the best option will be to use a high mass of silica powder (10g) while 14M will be better off without silica powder as an additive.

4.2.2 Modulus of elasticity

Properties of an ideal geopolymer plug should include high stiffness with ductility but this is not always true. High stiffness can help geopolymer plugs withstand any permanent deformation that might occur because of a harsh downhole environment.

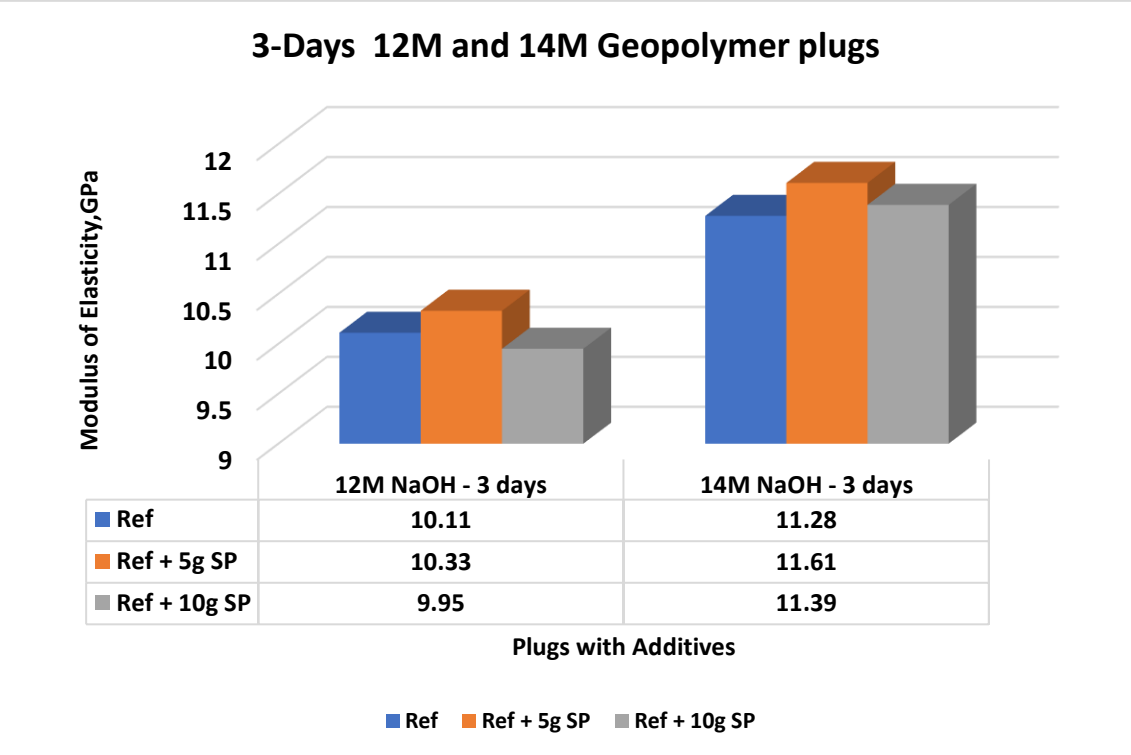

Figure 4.4: Modulus of elasticity for the effect of silica powder on 12M and 14M geopolymers.

From Figure 4.4, it is shown that after curing for 12M geopolymer plugs cured at 3 days did not show good modulus of elasticity results. The molar ratio is observed to have a positive impact on the stiffness of the geopolymer plug with 14M having a trend than 12M geopolymer plugs. The addition of 5g of silica powder improved the stiffness of the geopolymer plug with about 2% which does not make much of an impact. With 10g Silica powder, the 12M geopolymer plug showed an even more decrease in stiffness than the

reference 12M geopolymer plug. The result did not follow the expected trend when compared with the UCS results obtained above. It is expected that when UCS increases, the modulus of elasticity should also increase.

The 14M plugs did not also give a good result. The UCS and modulus of elasticity obtained were almost the same and did not follow the expected trend. The Ref + 5g Silica powder plug gave a poor stiffness value.

4.3 Effect of Al_2O_3 Nanoparticles in 12M NaOH-based Geopolymer

4.3.1 UCS

As previously discussed in Chapter 2, adding nanoparticles to neat geopolymer reference slurry increases its compressive strength.

Using reference 12M NaOH sample with 17.771 as the base, Al_2O_3 Nanoparticles were added to the sample in increasing masses of 0.1g, 0.3g, and 0.5g for 3 days and were compared with the results for 10 days. The results are shown in Figure 4.4.

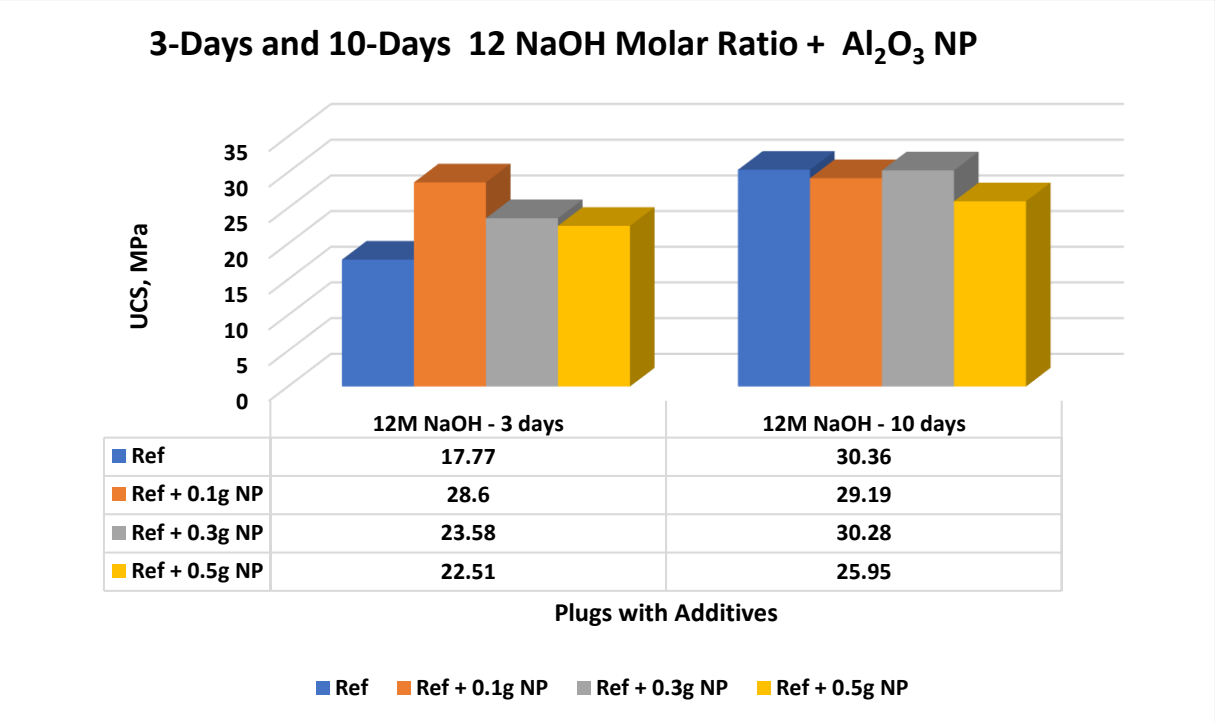

Figure 4.4: UCS for the effect of AL_2O_3 on 12M geopolymers.

It can be observed that the plugs cured for 10 days showed stronger UCS values than the plugs cured for 3 days. It can however not be said that this rise in strength is evenly distributed. As shown in the diagram. There is a significant shoot-up in UCS from when

0.1g of Al_2O_3 when compared with the neat plug. However, the strength decreases as more grams of Al_2O_3 (0.3g and 0.5g) are added to the neat geopolymer sample. This trend is visible in both the samples cured at 3 days and 10 days respectively.

As shown in the diagram, nanoparticles in higher molar ratios do not make a significant impact on geopolymer cement. Comparing the Ref + 0.1 Al_2O_3 plugs for 3 days and 10 days, the improvement in strength is insignificant, which is less than 1.0 MPa.

4.3.2 Modulus of elasticity

It can be said that stiffness improved without the addition of Al_2O_3 to the neat geopolymer slurry cured for 10 days compared to that of 3 days. The results obtained for 3 days and 10 days with the addition of Al_2O_3 nanoparticles do not make so much of an impact and when compared with the UCS results do not follow the expected trend.

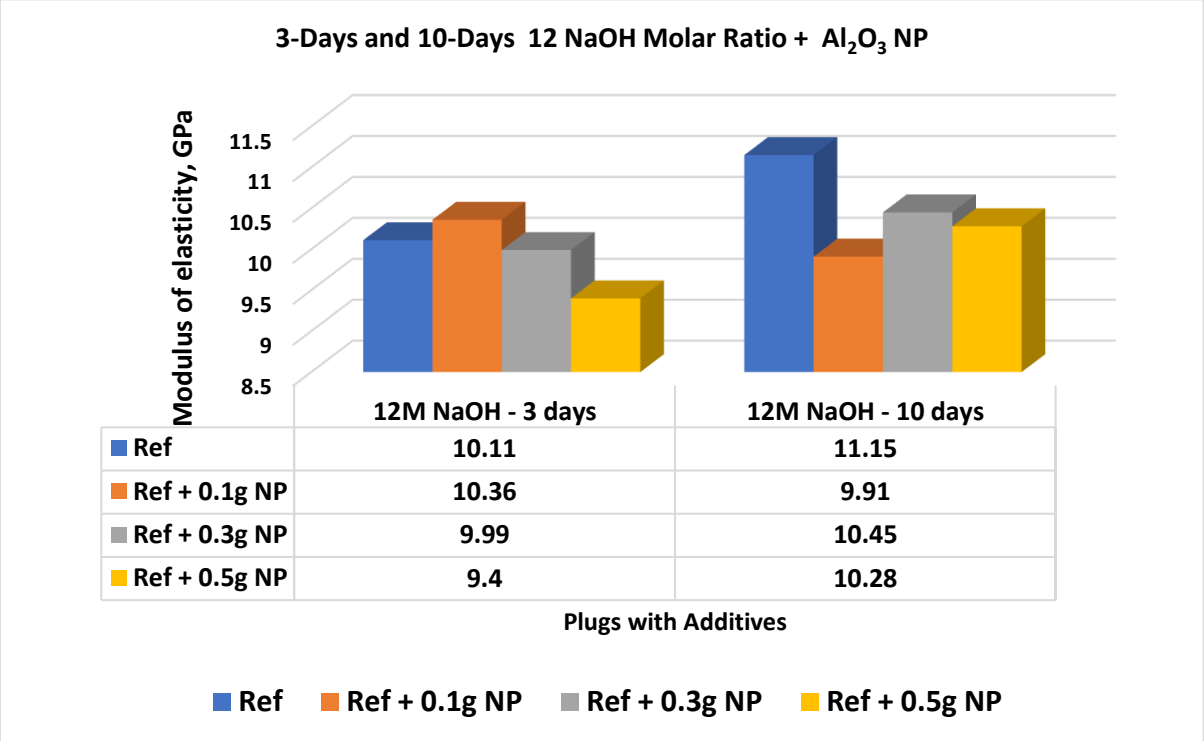

Figure 4.5: Modulus of elasticity for the effect of Al_2O_3 on 12M geopolymers.

4.4 Comparison between neat geopolymer and OPC

4.4.1 UCS

To investigate the strength of geopolymer further, the results obtained from the 12M neat geopolymer slurry at 3 days and 10 days in the oven were compared with cement. After

being instructed by my supervisor, the neat geopolymer was prepared and tested with one of the 2023 Bachelor Students, who is working on a different cement research project. The cement slurry was achieved by mixing 227g of cement + 100g of water which resulted in a 0.44 water-cement ratio (WCR) of the G-class cement. The result obtained is shown in Figure 4.6.

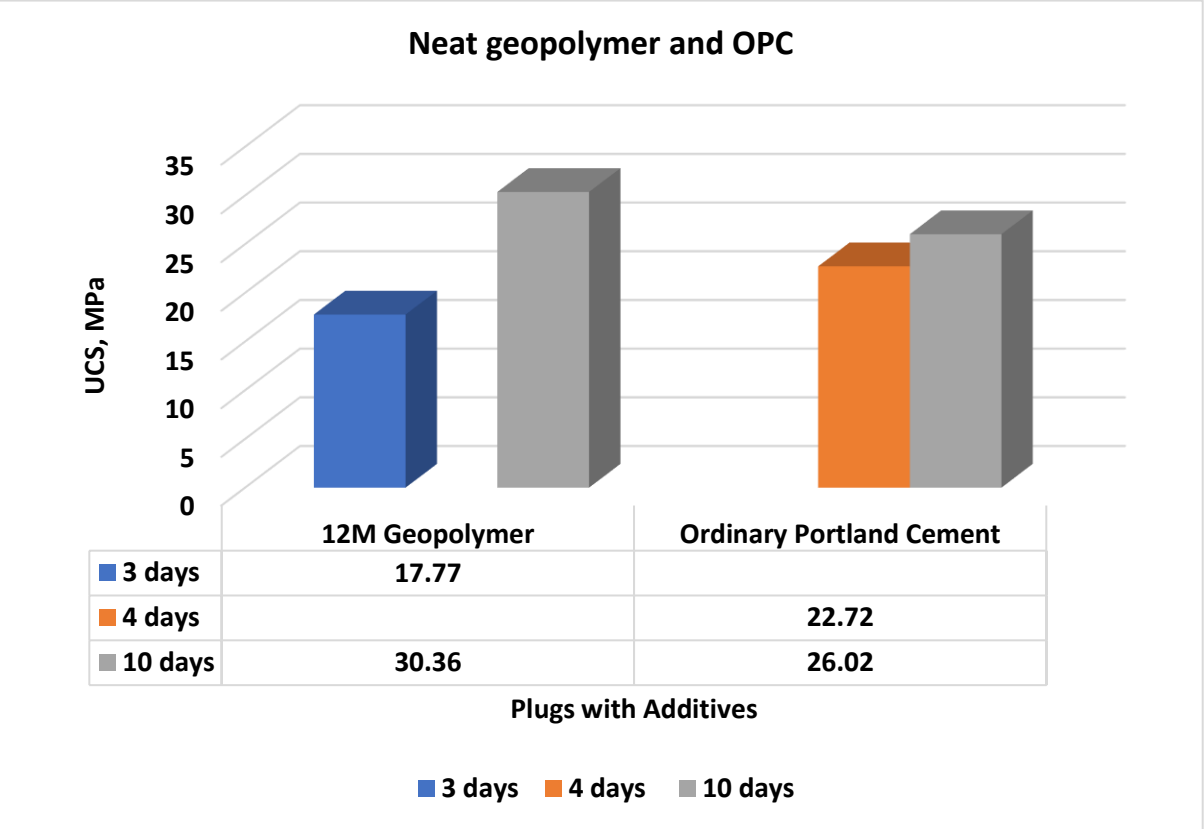

Figure 4.6: UCS comparing neat geopolymer and OPC.

The diagram shows that geopolymer concrete generally has higher strength than Ordinary Portland cement. The compressive strength for geopolymer shows a significant increase in strength from 3 to 10 days of curing. Ordinary Portland cement shows a decrease in compressive strength with an increase in curing days from 4 to 10 days.

4.4.2 Modulus of elasticity

Ordinary Portland cement generally showed better stiffness than neat geopolymer cement. The graph shows that stiffness for ordinary Portland cement increases with an increase in the curing days of the plug. The geopolymer cement also shows good stiffness since it follows the expected trend for modulus of elasticity when compared to UCS.

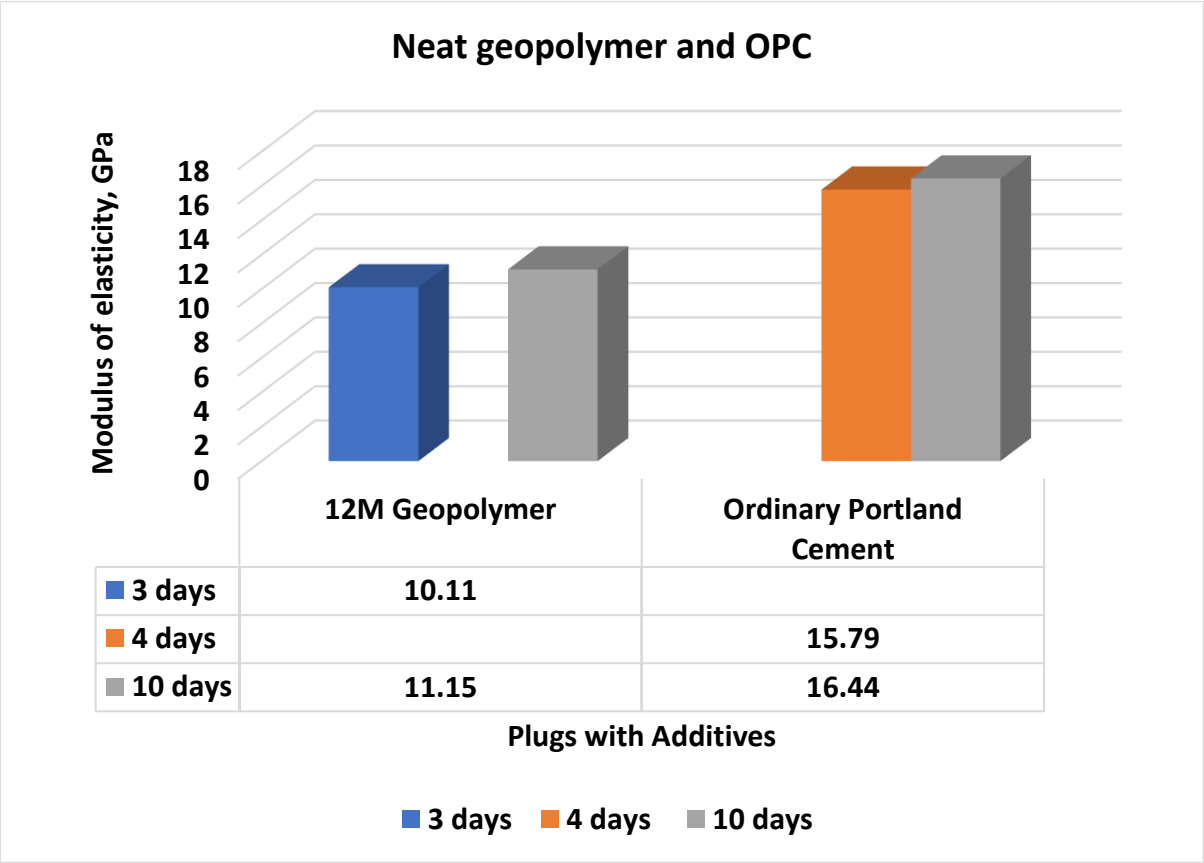

Figure 4.7: Modulus of elasticity comparing neat geopolymer and OPC

4.5 Effect of Carbon Fiber and Human Hair in 12M NaOH-based Geopolymer

The effect of additives on the strength of geopolymer concrete was investigated. Carbon fiber, and human hair were used. The use of human hair for this kind of test is the first of its kind. My supervisor graciously donated some of his hair to be used for this experimental work. The different types of fibers were added to the geopolymer mixture in tiny bits and stirred continuously until dissolved in the slurry. Carbon fiber is easily dissolved, unlike human hair. It was also observed that both fibers thickened the slurry and therefore reducing the quantity of the mixture obtained.

4.5.1 UCS

Figure 4.8 shows the results of the UCS test carried out on the plugs. It is observed from Figure 4.8 that adding 0.1g of CF to the neat geopolymer gives about a 19% increase in the strength of the plug compared to the same quantity of HH when added to the neat geopolymer concrete. But an increase to 0.3g shows the HH plugs have greater strength than their CF counterpart.

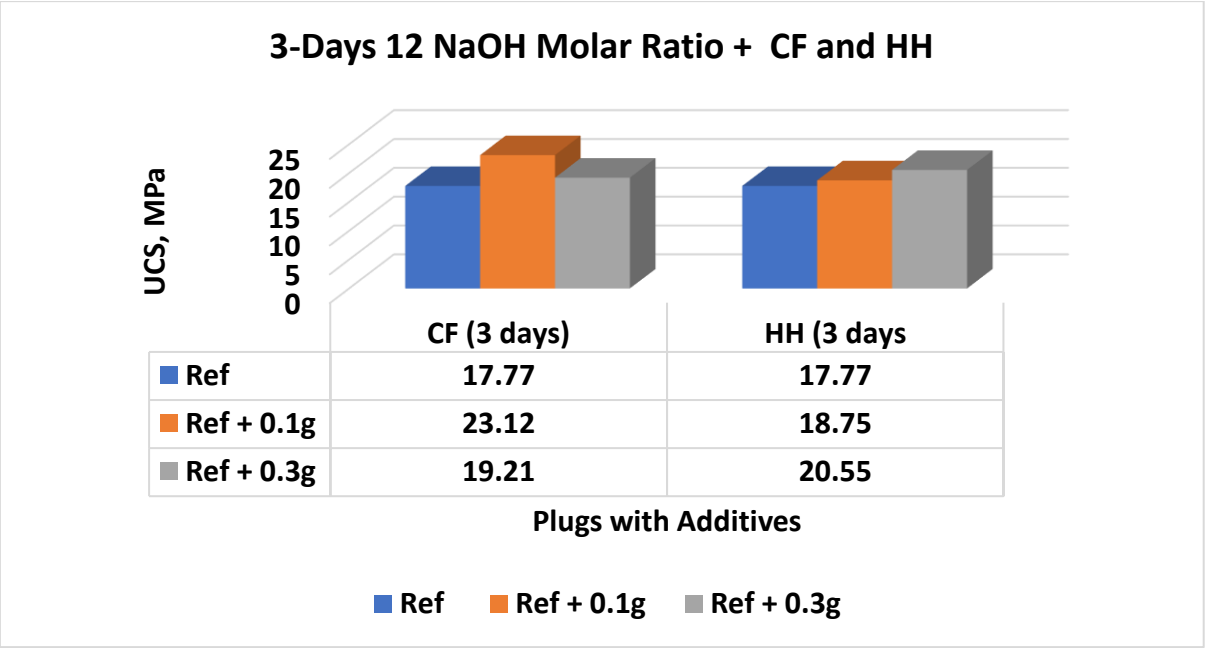

Figure 4.8: UCS comparing human hair and carbon fiber on 12M geopolymer.

4.5.2 Modulus of elasticity

The plugs containing both CF and HF did not generally show good stiffness, but the HH plugs showed better stiffness development than the CF plugs. Only the neat geopolymer plugs gave a good stiffness result.

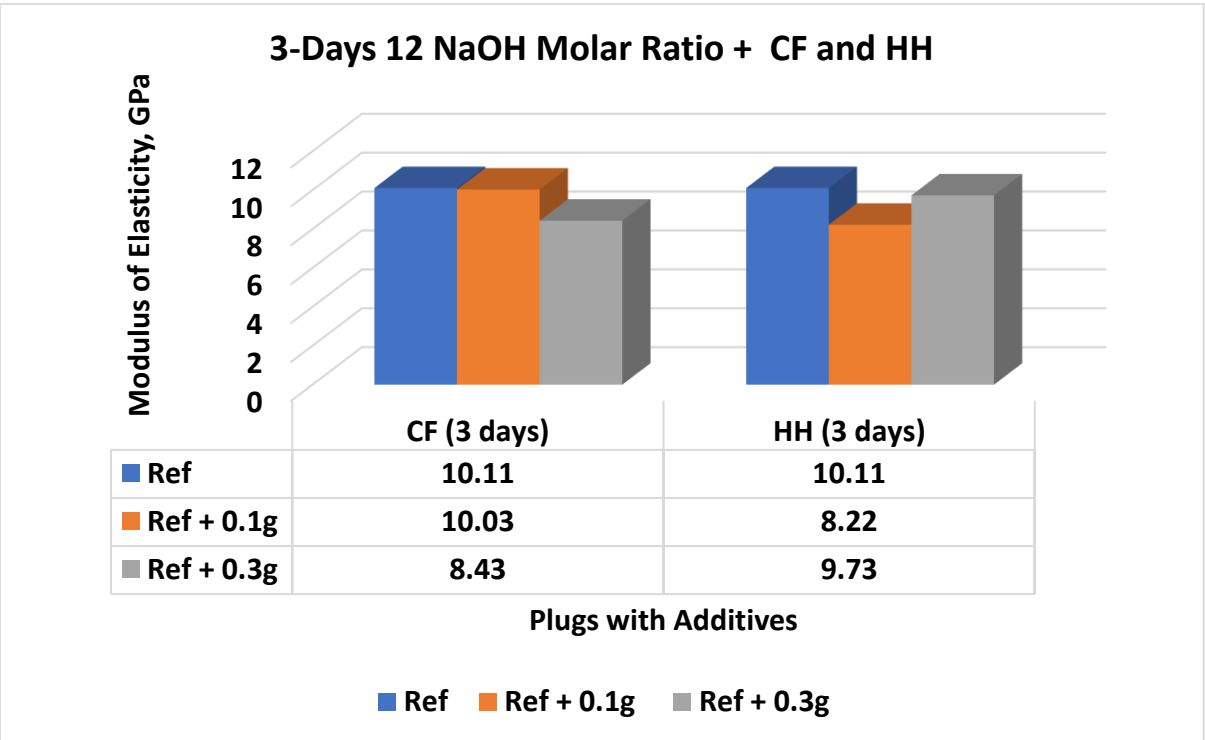

Figure 4.9: Modulus of elasticity comparing human hair and carbon fiber on 12M geopolymer.

4.6 Further investigation of the best system

To check which system is best for oil well cementing, 12M neat geopolymer slurry, and 0.44 neat class G cements were prepared and were subjected to water absorption and leakage tests.

The plugs were immersed completely in water after being cured for 3 days in the oven at 62^{o}C and thereafter left in the air for 24 hours. The plugs were measured in 24-hour intervals for 5 days.

4.6.1 Water Absorption

Figure 4.10 shows that after the first 24 hours, the water absorption in the geopolymer plug continually decreased while the cement plug continues to absorb water though it is observed that the rate of absorption declines steadily until day 5. The negative change observed after 48 hours in the mass of the geopolymer plug might be because after 24 hours, the plug becomes completely saturated, and further immersion in water leads to some of the parts breaking off and not being captured during measurement.

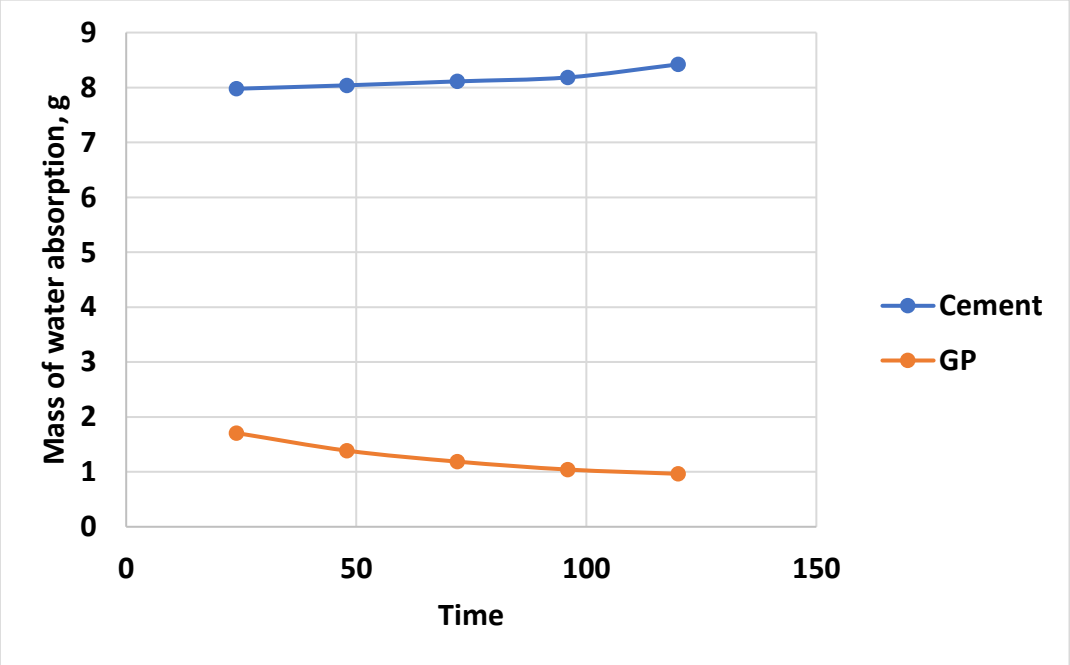

Figure 4.10: Mass of water absorption versus time of geopolymer and cement plugs.

4.6.2 Leakage testing of the best system.

As previously described in Chapter 3, the leakage test measurements were taken at 3 days, 3+3 days, and 3+3+4 days. The results obtained for the zero additive geopolymer and cement samples are tabulated in Table 4.1 and Table 4.2, respectively.

Table 4.1: Geopolymer leakage test data

Curing Time	Weight of added water	Weight of fluid leaked	Weight of water absorbed	Weight of fluid evaporated
3 days	25.5	0.00	2.45	0.67
3 + 3 days	27.39	0.00	5.36	0.11
3 + 3 + 4 days	26.33	0.00	6.32	0.15

Table 4.2: Cement leakage test data

Curing Time	Weight of added water	Weight of fluid leaked	Weight of water absorbed	Weight of fluid evaporated
3 days	22.7	0.00	10.36	0.21
3 + 3 days	24.13	0.00	7.62	0.30
3 + 3 + 4 days	24.67	0.00	6.64	0.39

Several measurements were taken after each test cycle, but the important ones were the amount of water absorbed and the amount of fluid absorbed by the plugs at the end of each cycle. An interesting observation in the samples shows that the amount of water absorbed by the geopolymer sample increases after each heat cycle while for the cement sample, the amount of water absorbed decreases after each heat cycle. To be able to understand the different trends exhibited by the various samples, a closer look at the samples showed cracks in the geopolymer sample while the cement sample had no visible cracks. It is assumed that the cracks in the geopolymer sample were responsible for the increase in water absorption at the end of each heat cycle. It is safe to say that geopolymer undergoes quicker degradation with an increase in heat when compared to cement.

It is also noticeably clear that for all the data measurements, the amount of water that leaked through for the various samples is zero.

The water evaporation measured for each sample is very small and insignificant though the geopolymer sample recorded a high amount of water evaporation at the end of the first heat cycle when compared to the cement sample. Though it is not certain what might be responsible for this, it is likely that the open end of the steel pipe might not have been properly closed which allowed for higher evaporation of the fluid.

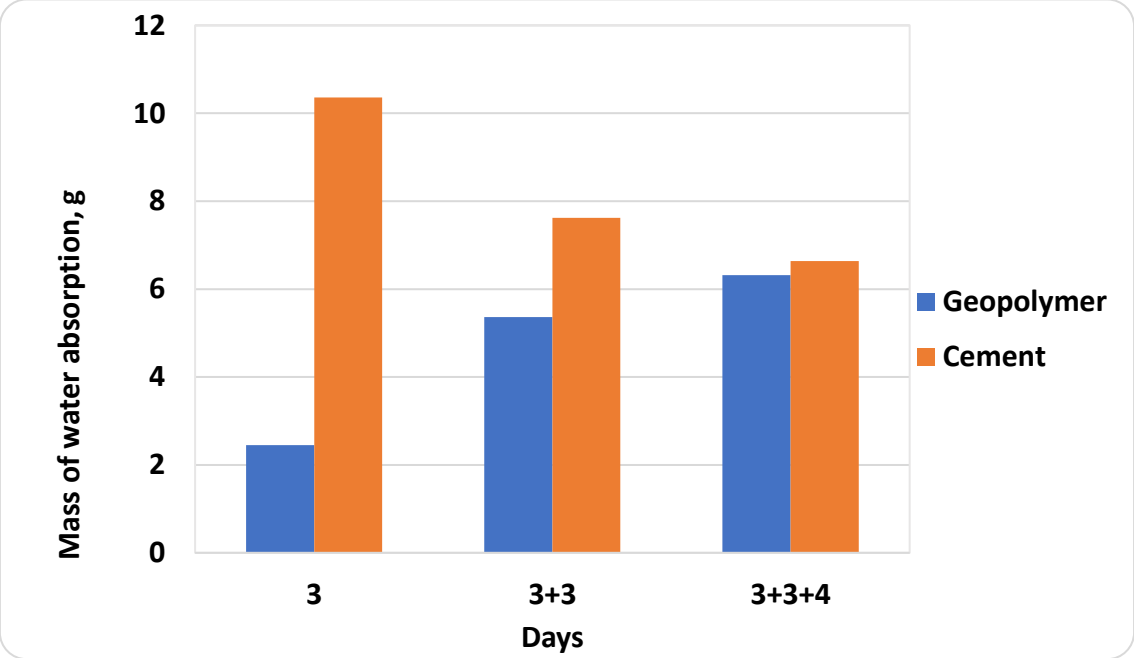

Figure 4.11: Mass of water absorption versus time of geopolymer and cement plugs in the pipe.

Figure 4.11 shows that both samples recorded almost the same amount of water absorption at the end of the final heat cycle. The geopolymer sample showed a trend of steady decline with each heat cycle while the cement sample showed a steady increase in water absorption with each heat cycle.

4.6.3 Rheological properties of geopolymer

Rheology helps to understand how the slurry will flow or deform under applied force and this makes it an important factor to consider in fluid transportation. The yield stress of the geopolymer and cement slurries are some of the rheological properties that are investigated to obtain maximum material properties during molding. Torsional stress is applied to the material and the varying degree of resistance to the stress is recorded. The viscosity of the Geopolymer is compared with cement.

Figure 4.12 displays the measured viscometer responses of the two systems. As shown, the geopolymer system exhibits higher shear rheology compared to the cement system for almost all measured points. At very low shear rates (less than 50 sec^{-1}), the cement system showed a higher shear rate than the geopolymer system and then begins to steadily decline at higher values until about 510 sec^{-1} where the highest difference is observed.

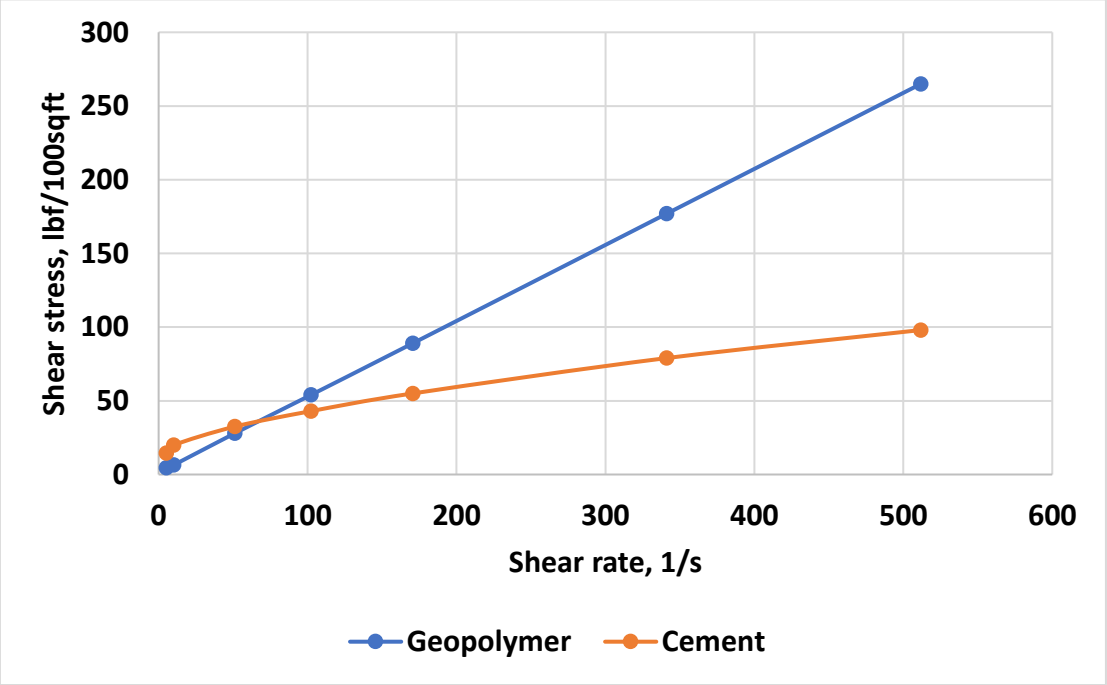

Figure 4.12: Shear stress and a shear rate of geopolymer and cement

Using the viscometer-measured data (Figure 4.12) and the Casson rheology model (Eq. 3.2), the viscosity parameters are calculated. The Casson yield stress of the two systems (geopolymer and cement) is shown in Figure 4.13. It is observed that the control system exhibits very low yield stress compared to the cement system. This means that the geopolymer system will require more force to initiate flow, unlike the cement slurry. This is beneficial as the geopolymer cement will not easily deform under high load.

The Casson plastic viscosity of the geopolymer and cement systems is shown in Figure 4.14. It is observed that the geopolymer system has higher values than the cement system. This means that the geopolymer system has a higher resistance to flow than the cement system and thus needs more pumping power to initiate motions. This is a valuable property as it ensures proper transport and hole cleaning which is very important in cementing jobs.

A better way of determining and understanding rheological properties is through simulations using simulation software but unfortunately, this was not done due to time constraints.

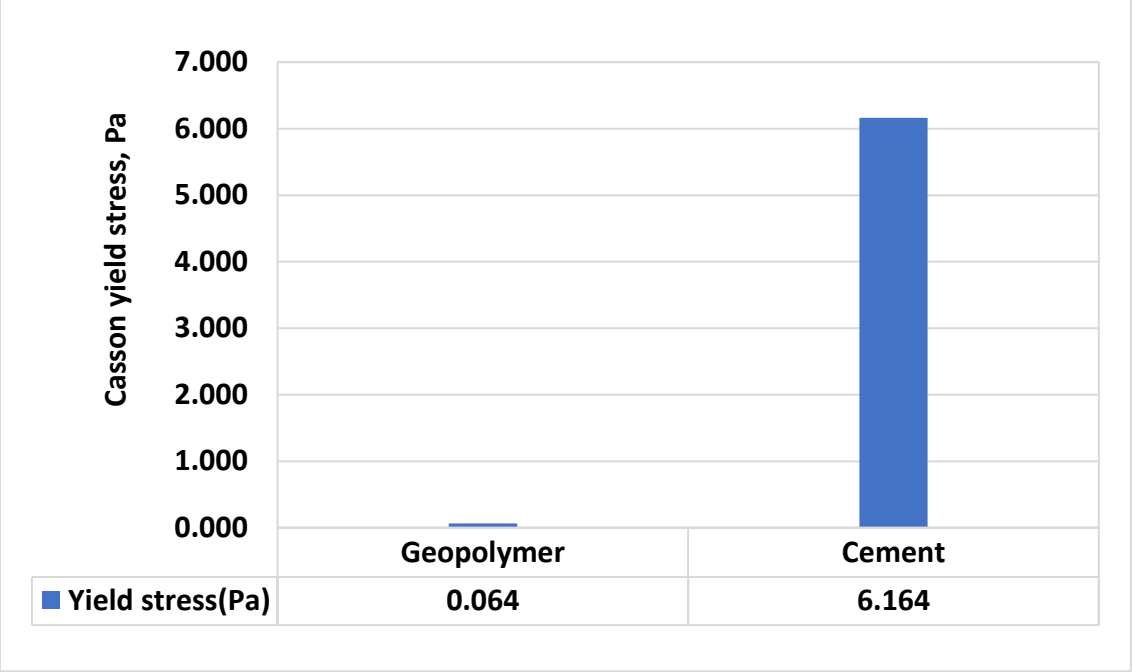

Figure 4.13: Casson yield stress of the geopolymer and cement plugs.

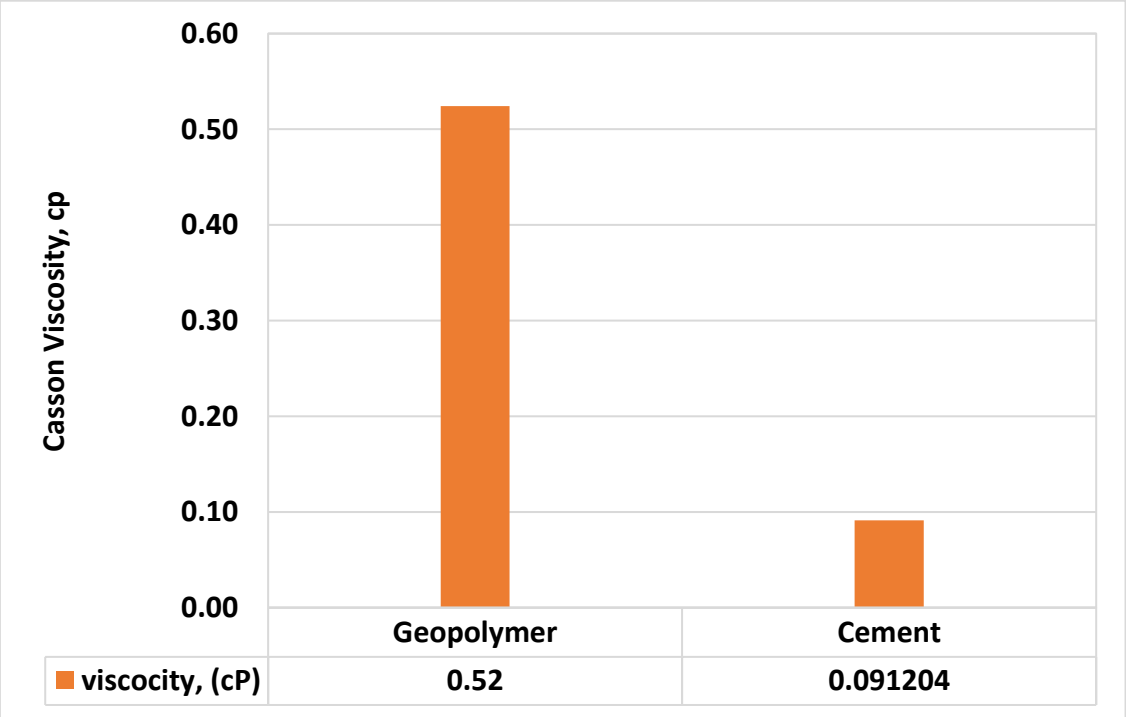

Figure 4.14: Casson plastic viscosity of the geopolymer and cement plugs

4.7 Uncertainties and Challenges

Test For absorption

After some days in the water bath, the mass of the geopolymer plug remained unchanged at about 72 hours and a decline in mass was noticed with an increase in the time of the water bath process. It was not certain what was responsible for this as some particles were noticed at the base of the water bath which might have broken off the geopolymer plug and was likely responsible for the decline in mass.

Human Error

Human error is one of the factors that can cause uncertainties during experiments. For example, measuring error during sonic transit measuring time. There is a chance that plugs did not get in full contact with the emitter and receiver during sonic measurement which can influence the accuracy of the sonic reading. Also, during the measurement of the mass of the materials used for the slurry preparation, it was difficult to get the exact measurement, a difference of + or – 0.01g was experienced which could have affected the results obtained from the testing of the plugs. Some other errors may have been experienced during the tests as humans are not perfect and prone to making mistakes.

Slurry Preparation

The process for mixing the slurry for each test batch involved weighing up the required amount of the constituents, mixing them all up in a container, stirring until a homogeneous slurry is obtained, and pouring them into the molds. A paper towel is then used to wipe the container used before mixing the next batch. It is worth noting that this does not guarantee that there are zero residues in the container and may affect the results obtained.

Also, because the slurry was prepared by hand, it was not guaranteed that all the solid particles were completely dissolved which may have also affected the results obtained at the end of the test.

Carbon fiber.

As earlier stated, the carbon fiber used for this experiment was purchased by my supervisor for previous students, and information was not obtained for it. The manner of

storage and length of time which it has been stored in the laboratory might have a potential impact on the results obtained.

Plug preparation.

While preparing the plugs for test for UCS, sandpaper and a water level was used to ensure the flatness of the plug surfaces to avoid point load. While great care was employed to ensure that error was eliminated, there might exist a possibility that some uncertainties regarding the quality of the polishing process were not completely ruled out. For some of the plugs, the process of achieving the desired flatness resulted in reducing the length of the plugs to a great extent which could have also affected the UCS result obtained.

Repetition of experiments

It is important to carry out tests multiple times to ensure the accuracy of the results obtained but due to time and material constraints, only three plugs per additive were prepared and the mean of the three plugs was used as the result. It would have been better if more samples were collected to ensure that the result was accurate. It is proposed that more plugs and tests should be carried out to ensure better accuracy if time and finances allow.

Dispersion of nanoparticles and fiber

In previous literature consulted, the use of ultrasonic dispersion method is employed to properly distribute the nanoparticles and fibers in the slurry. For this thesis, the nanoparticles and fibers were dispersed in the slurry by continuous stirring by hand and thus making it debatable if the elements were properly and equally distributed in the geopolymer slurries.

5 MODELING AND TESTING

5.1 Empirical model development

In section 3.3, Shale rock-based (Horsrud, 2001) and cement-based (Nerhus, 2020) empirical UCS-vs Vp models are presented.

Similarly, in this thesis work, based on the limited dataset, an empirical model is developed using 70% of the geopolymer experimental data and using the model to estimate 30% of the UCS by inputting the non-destructive, compressional wave velocity.

Figure 5.1 shows the correlation between the destructive test data (UCS) and non-destructive (compressional wave velocity) data points. The y-axis shows the UCS while the x-axis is the compressional wave velocity. The empirical model reads.

$$\mathbf{UCS\ (MPa) = 0.0694V_p^{6.4014}} \qquad 3.13$$

Where V_p is the compressional wave velocity in km/s

The power law function which corresponds to the regression value has a coefficient of determination (R^2) of 0.7067.

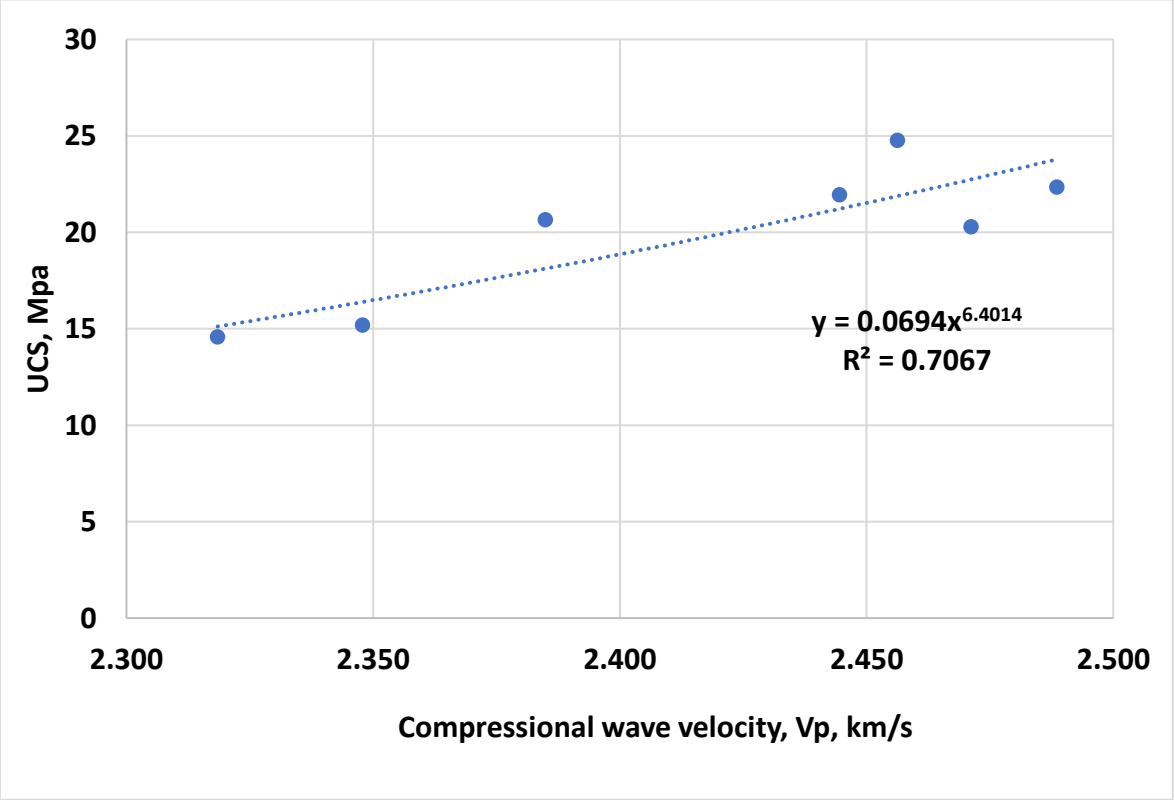

Figure 5.1 Measured Geopolymer's UCS vs Vp data and modeling

5.2 Model Testing

The literature empirical models (Horsrud, and Nerus) will be compared with this thesis model using the training dataset. Figure 5.2 shows the result. As shown, for the first batch and every other batch, Nehus and Horsrud underestimated the UCS value by a large margin. In contrast, Nerhus (2020) reported that when testing for UCS test values, Horsrud overestimated the actual UCS by a reasonable margin for all test batches. For the first test batch, the model developed in this thesis, Mina (2023) captures the experimental data very well but slightly underestimates the UCS of the plugs for the rest of the test batches with a small difference.

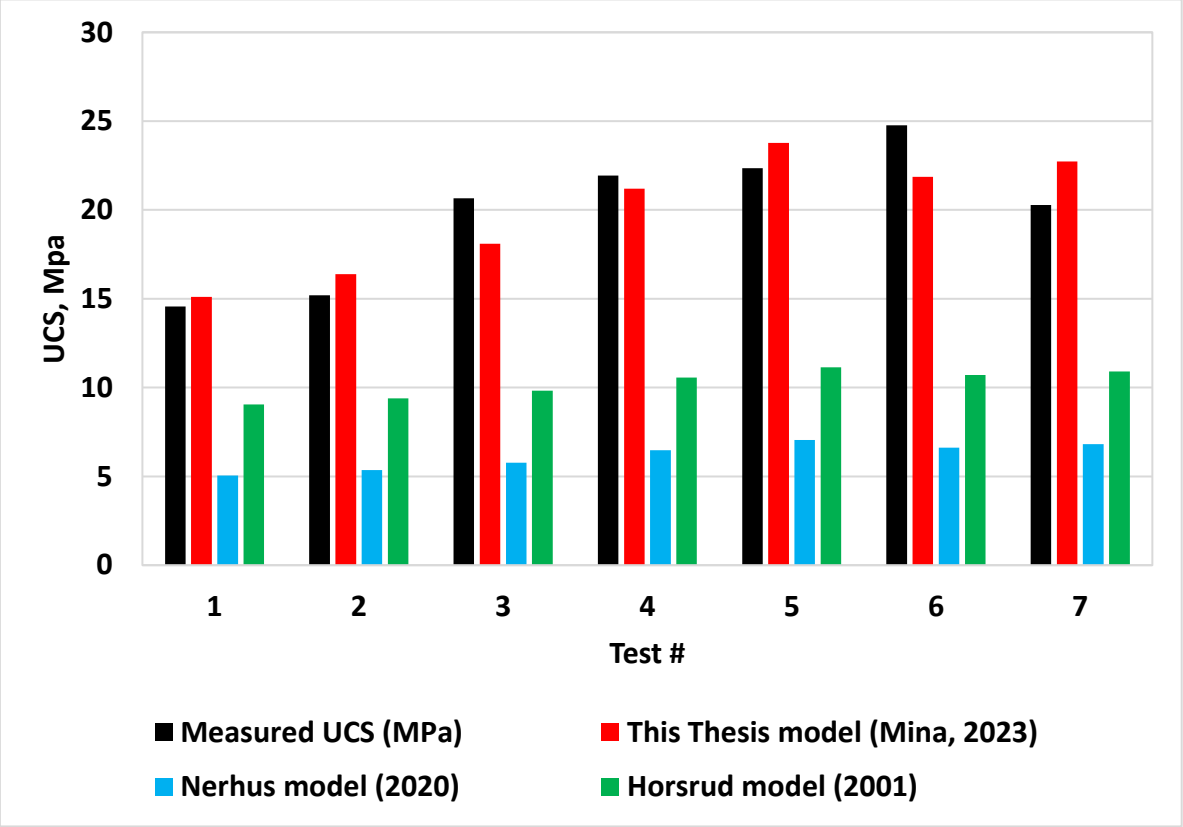

Figure 5.2 Models testing using 70% training dataset.

5.3 Comparison of Models

Further, the three models are using the 30% unseen test data. Figure 5.3 shows the comparison result.

This thesis (Mina 2023) generally performed better than Nerhus's (2020) and Horsrud's (2001) model when compared with the measured UCS. In summary, the new model developed based on the UCS data from this thesis is more precise than Nerhus and

Horsrud. It is safe to say that the new model developed in this thesis can be used as a model for future comparisons.

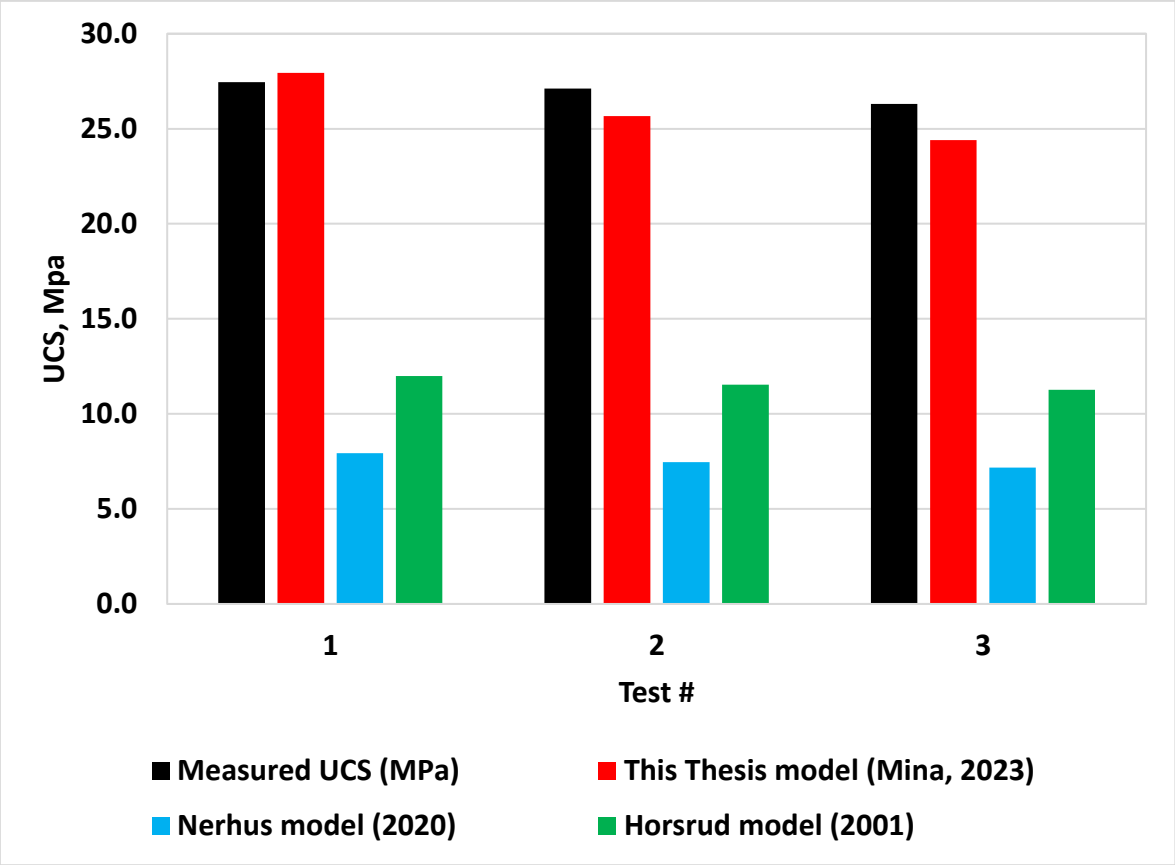

Figure 5.3 Models validation using 30% of the testing dataset

6 SUMMARY AND CONCLUSION

A total of four experimental test designs were formulated to study the effect of silica powder, NaOH molar concentration, Al_3O_2 nanoparticles, carbon fiber, and human hair fibers on the neat geopolymer. The properties of the neat geopolymer and Ordinary Portland G-class cement are compared. The experimental tests will be summarized based on the best UCS results obtained from the test designs. Table 6.1-Table 6.6 show the summary of the results obtained from 3 days and 10 days cured at 62°C and atmospheric pressure.

Table 6.1: Test Design 1: Effect of Silica Powder in 12 M NaOH-based Neat Geopolymer

Geopolymer	NaOH molar concentration	Curing age days	Best dosage additives, g	Neat GP UCS, MPa	Best additive modified GP, UCS, MPa	% Change With Respect to Neat GP
Neat GP	12 M	3		17.77		
	12M	10		30.36		
GP with SP	12M	3	10g SP		23.85	**34.2**
	12M	10	10g SP		31.88	**5.0**

Table 6.2: Test Design 2a: Effect of Molar Ratio 12M and 14M for 3 days

Geopolymer	NaOH molar concentration	Curing age	Best dosage of additives, g	Neat GP UCS, MPa	Best additive modified GP, UCS, MPa	% Change With Respect to 12 M based GP
Neat GP	12 M	3	-	17.77	-	**67.98**
	14M	3	-	29.85	-	

Table 6.3: Test Design 2b: Effect of SP on 12M and 14M Molar Ratio for 3 days

Geopolymer	NaOH molar concentration	Curing age	Best dosage of additives, g	Neat GP UCS, MPa	Best additive modified GP, UCS, MPa	% Change With Respect to 12 M based GP
GP with SP	12M	3	10g SP		23.85	**28.0**
	14M	3	10g SP		30.53	

Table 6.4: Test Design 3: Effect of Nanoparticles on 12M NaOH-Based Geopolymer

Geopolymer	NaOH molar concentration	Curing age, days	Best dosage additives, g	Neat GP UCS, MPa	Best additive modified GP, UCS, MPa	% Change With Respect to Neat GP
Neat GP	12 M	3	-	17.77		
	12M	10		30.36		
GP with Al_2O_3 NP	12M	3	0.1 g Al_2O_3		28.6	**60.9**
	12M	10	0.3 g Al2O3		30.28	**-0.3**

Table 6.5: Test Design 4: Effect of Carbon fiber (CF) and Human hair (HH) on 12M for 3 Days

Geopolymer	NaOH molar concentration	Curing age, days	Best dosage additives, g	Neat GP UCS, MPa	Best additive modified GP, UCS, MPa	% Change With Respect to Neat GP
Neat GP	12 M	3	-	17.77		
GP with CF	12M	3	0.1 g CF		23.12	**30.1**
GP with HH	12M	3	0.3 g HH		20.54	**15.6**

Table 6.6: Comparison between 12 and 14 M NaOH-based neat geopolymers and OPC.

Curing days	GP		OPC	% Neat GP Change With Respect to Neat OPC
	Molar Conc.	UCS	UCS	
10	12M NaOH	30.36	26.02	**14.30**
10	14M NaOH	29.85	26.02	**12.83**

The main observations obtained from the experimental works are summarized as:

- For all tested silica powder blended geopolymers and cured for 3 days, the silica powder additives increased the UCS of the neat geopolymer. The UCS increment was linear as the concentration increased. On the other hand, for 10 days of curing plugs, the UCS values increment was non-linear. It was observed that the 5g SP additives decreased the UCS of the neat geopolymer by about 1 MPa, but the 10g SP increased the UCS by about 1.5 MP. The reason for the 5g SP plugs anomaly could likely be caused by some defects on the plug's surfaces or due to anomalies during the slurry preparation. The impact of the SP on the modulus of elasticity

was linearly and decreasing trend. The results were not the same trend for the modulus of elasticity as this had a decreasing trend with the addition of silica powder. Due to the short research period, more repeat tests were not conducted for verification purposes. Despite the results, the observation will open further investigation and the authors will therefore suggest future work.

- After 3 days of curing, the UCS of 12 M NaOH-based neat geopolymer increased when the SP concentration increased by 5g and 10 g. On the other hand, the UCS of 14 M NaOH-based neat geopolymer decreased and increased for SP 5g and 10 g, respectively. The molar concentration had an increasing trend with 12M of NaOH while the 14M had varying UCS results. Generally, the 14 M NaOH-based geopolymer was stronger than the 12 M NaOH-based geopolymer. The modulus of elasticity for both molar ratios had a steady decrease with a higher mass of silica powder (10g).

- The addition of Al_3O_2 nanoparticles increased the strength of the geopolymer but there was no defined consistency trend with the various additive concentration for each respective curing age. The control plugs gave better Modulus of elasticity results than the plugs with nanoparticles for both curing ages except for 0.1g of nanoparticle additive for 3 days which gave a higher UCS value. Up to the considered curing days, temperature, and pressure, the general observation is that the nanoparticle-free plugs exhibited better strength than the ones without the nanoparticle blended geopolymer additive with an increase in curing time. The reason could be that the nanoparticle solution might have delayed the hydration process. However, over time, one may achieve different results. The author suggests future work for further investigation with a higher curing time.

- Carbon fiber showed to increase the UCS strength of geopolymer in a moderate dosage of 0.1g but further increase reduced the strength by about 16%. The human hair showed a linear increase in UCS of the geopolymer as concentration increased. Therefore, based on the trend, it can be said that further investigation with an increase in the mass of human hair may or may not increase the UCS strength of the geopolymer. The observation will open a research work for further investigation. The modulus of elasticity decreased for all the analyzed fiber types.

- It is also observed that at the considered curing temperature, and days, the newly formulated neat geopolymer is stronger than the ordinary Portland cement.

- Taking a mean of all the results obtained, it was clear that the properties of the plugs tend to further increase with an increase in concentration and curing age.

- The Plugs Water absorption trends results showed that the neat geopolymer performed better than cement.

- The test for leakage with neat geopolymer slurry and neat class-G cement slurry showed that at the beginning of the cycle for the leakage test, geopolymer had better performance than cement. Over time with further cycles, the fluid absorption rate for cement experienced a steady increase while that of geopolymer continued to decrease linearly with both having zero leakage. By visual inspection, the structural makeup of the geopolymer looks very dense. Therefore, the author feels that the performance of geopolymer will even further improve with an increase in leakage test cycles. However, the authors suggest further investigation.

- Though the geopolymer slurry recorded a slow start when compared with the cement slurry, results show that it had an increased shear strength while reducing Casson yield stress. This shows that geopolymer slurry is a stronger and more durable cementing material compared to class G cement.

- Without the need to permanently crush the plugs, a practical UCS model was created in this thesis work to predict the unconfined compressive strength by using wave velocity. The effectiveness of this newly developed model was confirmed by the coefficient of determination R^2 of 0.7067 which showed a good ability to accurately capture UCS trends. The author believes to generate a robust and reliable model, several experimental data should be utilized. However, the model generated has shown prediction on the geopolymer data and the under-prediction of the models that have been derived from rock and cement based.

Finally, this thesis work based on the 3 days, 10 days, 62^o C temperature and atmospheric pressure cured geopolymer results concludes that:

- The neat geopolymer has shown good strength.
- The impact of SP has shown an insignificant impact on the neat geopolymer after 10 days.
- The impact of Nanoparticles after 3 and 10 days has shown an insignificant impact on the neat geopolymer.
- After 3 days, Human hair has shown an impact on the neat geopolymer.
- The less concentration of carbon finer has shown a good impact. Increasing the concentration exhibited a weakening effect.

Please note that by changing the curing conditions, one may achieve different results. To further use the formulated geopolymer for practical application, more research needs to be done as outlined in the summary and future works.

7 FUTURE WORK

For further work, this author suggests the following activities:

- **Realistic slurry preparation and testing.** In reality, cement slurry used in the petroleum well is formulated among others with an accelerator, retarder, and loss control additive. In this thesis, cement was synthesized with water and cement powder. Similarly, geopolymers are formulated with solid precursors and binders. It is therefore important to investigate in the future the impact of the mentioned additives in geopolymer and compare them with cement as well. By doing so, one can improve the hydration process of geopolymers.
- **Higher Temperatures and Pressures**: The downhole conditions of oil and gas wells vary, and it is expected that to be able to develop an optimal performing cementing material, this material should be able to withstand high temperatures and pressures. For further work in this research, this author proposes that the plugs should be subjected to higher temperatures (above 62^{o}C used in this work) and at higher pressure conditions.
- **Human Hair**: There exist different textures of human hair and this author suggests that to accurately determine the effect of human hair on the strength of geopolymer, several other hair textures should be used as additives and tested.
- **Scan Electron:** This author suggests that for future works relating to this research topic, it is important that the internal structures of the geopolymer plugs are viewed with a scan electron microscope to be able to understand the process of geopolymerization undergone by the plugs.
- **Repetition Of Tests:** Tests on the geopolymer plugs should be repeated severally to eliminate possible errors and have a better conclusion on the results obtained.
- **Curing Time:** This author suggests that the curing time for the geopolymer plugs should be spread over a large range (3, 7, 14, 21, 28, and even more) as the plugs in this thesis were predominantly cured for 3 and 10 days. This will help study the effect of the various additives on the strength development of the geopolymer slurries.
- **Size of the Plugs:** It would be interesting to scale up the size of the plugs and compare them with the results obtained in this thesis.
- **Tensile test:** To gain more insight into the strength of the geopolymer, it would be interesting to perform the Brazilian test and compare it with cement.

8 References

[1] Irina Slav, Oil Price.Com: Https://Oilprice.Com/Energy/Energy-General/The-Complete-Guide-To-Cementing.Html

[2] Mtaki T. Maagi, Samwel D. Lupyana, Gu Jun, "*Nanotechnology in the petroleum industry: focus on the use of nano-silica in oil well cementing applications – A review"*, Journal of Petroleum Science and Engineering.

[3] Well integrity in drilling and well operations NORSOK STANDARD D-010 Rev. 3, August 2004

[4] T. Vralstad, A. Saasen, E. Fjar, T. Oia, J. D. Ytrehus, and M. Khalifeh, *"Plug & abandonment of offshore wells: Ensuring long-term well integrity and cost-efficiency"* J. Pet. Sci. Eng., vol. 173, pp. 478–491, Feb. 2019, doi: 10.1016/j.petrol.2018.10.049

[5] Birgit Vigenes and Bernt Aadnøy, "*Well Integrity Issues Offshore Norway"*. Society of Petroleum Engineers (SPE) Production & Operations, Volume 25, Issue 02, pages 145 - 150, https://doi.org/10.2118/112535-PA, 2010.

[6] Ngoc Lan Mai a , Nguyen-Hieu Hoang b , Ha T. Do a, Monika Pilz b, Thuat T. Trinh c, "*Elastic and thermodynamic properties of the major clinker phases of Portland cement: Insights from first principles calculations"*. ELSEVIER, February 2021.

[7] Wikipedia, Portland Cement, Available from: https://en.wikipedia.org/wiki/Portland_cement.

[8] The constructor (Building ideas), "*Geopolymer concrete: Properties, Composition and Applications"*, Available from: https://theconstructor.org/concrete/geopolymer-concrete-ecofriendly-construction-material/9430/

[9] Hemn Unis Ahmed, Azad.A. Mohammed, Serwan Rafiq, Ahmed S. Mohammed, Amir Mosavi, And Hamah Sor and, Shaker M. A. Qaidi, "*compressive strength of*

sustainable Geopolymer concrete composites: A state-of-the-art review", MDPI JOURNALS Vol 13, December 2021.

[10] Dimas, D, Giannopoulou, I, and Panias, D, Polymerization in sodium silicate solutions: a fundamental process in polymerization technology, Journal of material science, Volume 44, July 2009.

[11] Jadambaa Temuujin, Enkhtuul Surenjav, Claus Henning Ruescher, Jan Vahlbruch, "*Processing and uses of fly ash addressing radioactivity (critical review)"*, Elsevier; Chemosphere, Volume 216, February 2019, pg 866-882.

[12] Peiliand Cong, Yaqian Cheng, "*Advance sin geopolymer materials: A comprehensive review*," Journal of traffic and transportation Engineering, Volume 8, June 2021.

[13] Silica Powder, properties and benefits, Available from https://www.bm.com.sa/2020/02/11/silica-powder-properties-and-benefits/.

[14] Mo Alkaysi, Sherif El-Tawil, Zhichao Liu, Will Hansen, "*Effects of silica powder and cemnt type on durability of ultra-high-performance concrete (UHPC)"*, Elsevier; Cement and concrete composites, Volume 66, February 2016.

[15] Muhammad I. M. Rjoub, "*Effect of silica powder on the bond between building stone and pumice concrete",* Civil Engineering journal, Available from; www.CivilJournal.org, volume 7, February 2021.

[16] Srinivasa Reddy, Karnati Vamsi Krishna, M V Seshagiri Rao, Shrihari S, "*Effect of molarity of sodium hydroxide and molar ratio of alkaline activator solution on the strength development of geopolymer concrete",* E3S Web of conferences 309, 2021.

[17] Ganesan C., Ramesh Babu, and PL Meyappan, "*Influence of Alkaline activator ratio on compressive strength of GGBS based geopolymer concrete*", IOP conference series: Materials science and Engineering, 2019.

[18] Sathish Kumar, N Ganesan, P V Indira, "*Effect of molarity of sodium hydroxide and curing method on the compressive strength of ternary blend geopolymer concrete"*, IOP Conference Series; Earth and environmental science, August 2011.

[19] George Mattew and Binu M. Isaac//E*ffect of molarity of sodiumhydroxide on the aluminosilicate content in laterite aggregate of laterised geopolymer concrete//* Journal of building engineering, Vol. 32, November 2020.

[20] Minhao Dong, Mohamed Elchalakani, Ali Karrech, "*Development of high strength one-part geopolymer mortar using sodium metasilicate"*, Construction and Building Materials, Volume 10, March 2020

[21] Bashar S. Mohammed, Sani Haruna, M.M.A. Wahab, M.S. Liew, and Abdulrahman Haruna, "*Mechanical and microstructural properties of high calcium fly ash one-part geopolymer cement made with granular activator"*. Elsevier, Heliyon, Volume 5, Issue 9, September 2019, e02255, https://doi.org/10.1016/j.heliyon.2019.e02255.

[22] Liew Y. M., Kamarudin H., Mustafa Al Bakri, Binhussain M., Luqman M., Khairul Nizar, Ruzaidi C. Y., "*Influence of solids-liquid activator ratios on kaolin cement powder"*, international conference on physics and technology, 2011.

[23] Avinash Ojha, Praveen Aggarwal, "*Fly Ash Based Geopolymer Concrete; a comprehensive Review"*, Spring Nature Publishers, March 2021.

[24] Chakradhara R. Meesala, Nikhil K. Verma, Shailendra Kumar, "*Critical review on fly ash based geopolymer concrete"*, available from: https://doi.org/10.1002/suco.201900326, November 2019.

[25] Hardjito D, Wallah SE, Sumajouw DMJ, Rangan BV. "*Factors influencing the compressive strength of fly-ash based geopolymer concrete"*. *Civ Eng Dimens*. 2004b;**6**:88–93

[26] Shankar HS, Khadiranaikar RB. "*Performance of geopolymer concrete under severe environmental condition"s*, International Journal of Civil and Structural Engineering, 2012, Vol 3.

[27] Yasir S, Iftekar G. "*Study of properties of Fly ash based geopolymer concrete"*, International Journal of Engineering, 2015

[28] Benny Joseph, George Mattew, "*Influence of aggregate content on the behavior of fly ash based geopolymer concrete"*, 2020

[29] Palomo A., M. W. Grutzeck, M. T. Blanco, "*Alkali- activated fly ashes: A cement for the future, Elsevier",* Cement and concrete research, Volume 29, August 1999

[30] Prinya Chindaprasirt, Tanakorn Phoo-ngernkham, Sakonwan Hanjitsuwan, Suksun Horpibulsuk, Anurat Poowancum, Borwonrak Injorhor, "*Effect of calcium-rich compounds on the setting time and strength development of alkali-activated fly ash cured at ambient temperature*", Elsevier; case studies in construction materials, Volume 9, December 2018.

[31] Nath Pradip, Sarker Prabir Kumar, "*Flexural strength, and elastic modulus of ambient-cured blended low-calcium fly ash geopolymer concret"e*, Web of Science; construction and building materials, Volume 130, January 2017.

[32] Singh,B, Rahman, MR, Paswan, R, Bhattacharyya, SK, "*Effect of activator concentration on the strength, ITZ and drying shrinkage of fly ash/slag geopolymer concrete*." Web of science; construction and building materials, August 2016.

[33] Hardjito Djwantoro, Rangan B. Vijaya, "*Development, and properties of low calcium fly ash-based geopolymer concrete",* Available from: http://www.geopolymer.org.

[34] Olivia Monita, Nikraz Hamid, "*strength and water permeability of fly ash geopolymer concrete"*, Journal of engineering and applied sciences, Available from; http://www.arpnjournals.com/jeas/research_papers/rp_2011/jeas_0711_525.pdf. 2011.

[35] Steenie Edward Wallah, "*Drying shrinkage of heat-cured fly ash based geopolymer concrete",* Journal of Modern applied science, Vol 3, December 2009.

[36] Wallh Steenie, Rangan Vijaya, "*Low calcium fly ash based geopolymer concrete: long term properties, espace-curtin's institutional repository",* Available from; http://hdl.handle.net/20.500.11937/34322.

[37] Sukmak Patimapon, De Silva Pre, Horpibulsuk Suksun, Chindaprasirt Prinya, "*Sulfate resistance of clay portland cement and High calcium fly ash geopolymer",* Journals of materials in civil engineering, Volume 27, May 2015.

[38] Sanni Shankar, Khadiranaikar R. B., "*Performance of geopolymer concrete under severe environmental conditions",* international journal of civil and structural engineering, Volume 3, 2012.

[39] Baharev T.," *Durability of geopolymer materials in sodium and magnesium sulfate solutions",* Web of science- cement and concrete research, Volume 35, June 2005.

[40] Ali Nazari, Jay G. Sanjayan, 2014 "*Hybrid effects of alumina and silica nanoparticles on water absorption of geopolymers: Application of Taguchi approach",* Centre for Sustainable Infrastructure, Faculty of Science, Engineering and Technology, Swinburne University of Technology, Victoria 3122, Australia, October 2014.

[41] N.B. Singh, S.K. Saxena, and Mukesh Kumar, "*Effect of nanomaterials on the properties of geopolymer mortars and concrete".* Elsevier, Materials Today: Proceedings, Volume 5, Issue 3, Part 1, 2018, Pages 9035-9040, https://doi.org/10.1016/j.matpr.2017.10.018

[42] Tanakorn Phoo-ngernkham, Prinya Chindaprasirt, Vanchai Sata, Sakonwan Hanjitsuwan, and Shigemitsu Hatanaka, "*The effect of adding nano-SiO2 and nano-Al2O3 on properties of high calcium fly ash geopolymer cured at ambient temperature",* Materials, and Design, Volume 229, September 2013.

[43] Mehmet Kaya, "*The effect of micro-SiO_2 and micro-AL_2O_3 additive on the strength properties of ceramic powder-based geopolymer paste, journal of material cycles and waste management*," November 2021-

[44] Tao Wang, Xiamgqian Fan, Changsheng Gao, Chiyu Qu, Jueding Liu and Guanghui Yu, "*The influence of Fiber on the mechanical properties of geopolymer concrete; A Review."* https://doi.org/10.3390/polym15040827, February 2023.

[45] Dong Zhang, Kang Hai Tan, Aravind Dasari, Yiwei Weng, *"Effect of natural fibers on thermal spalling resistance of ultra-high-performance concrete, cement and concrete composites"*, Volume 109, May 2020.

[46] Liew Y. M., Kamarudin H., Mustafa Al Bakri, Binhussain M., Luqman M., Khairul Nizar, Ruzaidi C. Y.," *Influence of solids-liquid activator ratios on kaolin cement powde"r*, international conference on physics and technology, 2011.

[47] Marzena Kurpinska, Magdalena Pawelska- Mazur, Yining Gu and Filip Kurpinska, *'The impact of natural Fibers' characteristics on mechanical properties of cement composites"*" Available online, https://www.nature.com/articles/s41598-022-25085-6#Abs1, 2022

[48] NORCEM AS. Available from: https://www.norcem.no/no.

[49] V.K., Gomti Nagar, Lucknow, India. "*Chemical Composition of Fly Ash*." 2014, Concrete-Techgroup, Accessed: 03.06.2020; Available from: http://concretebasics.org/articles/chemical-composition-fly-ash-concrete/.

[50] Sigma-Aldrich. *Sodium hydroxide*. Accessed: 28.06.2020; Available from: https://www.sigmaaldrich.com/catalog/product/sigald/221465?lang=en&region=

[51] Manvendra Verma, "*Sodium hydroxide effect on the mechanical properties of flyash-slag based geopolymer concrete*", https://onlinelibrary.wiley.com/doi/full/10.1002/suco.202000068

[52] "Aluminum Oxide Al2O3 Nanopowder / Nanoparticles (Al2O3, 100% alpha, 99+%, 80nm)." https://www.us-nano.com/inc/sdetail/208 (accessed Mar. 17, 2020).

[53] ZOLTEK. "What is Carbon Fiber?" [Online]. Available: https://zoltek.com/carbon-fiber/what-is-carbon-fiber/ [Accessed: Aug. 04, 2022]

[54] Erling Fjar, R.M. Holt, A.M. Raaen, and P. Horsrud *Petroleum Related Rock Mechanics.* Elsevier, Volume 53, 2nd edition, Published: January 2008.

[55] E. B. Nelson and D. Guillot, Eds. *Well Cementing*, 2nd ed. Sugar Land, Texas, USA: Schlumberger, 2006. [Online]. Available: https://www.slb.com/resource-library/book/well-cementing

[56] P. Horsrud, "*Estimating Mechanical Properties of Shale from Empirical Correlations," SPE Drilling & Completion*, vol. 16, no. 02, pp. 68–73, Jun. 2001, Paper SPE-56017-PA, doi: 10.2118/56017-PA. [Online]. Available: https://onepetro.org/DC/article/16/02/68/75206/Estimating-Mechanical-Properties-of-Shale-From [Accessed: Jul. 12, 2022]

[57] H. Nerhus, "*Effect of nanoparticles and elastomers on the mechanical and elastic properties of G-class Portland cement: Experimental and Modelling studies*.," M.S. thesis, Department of Energy and Petroleum Engineering (IEP), University of Stavanger, Stavanger, Norway, 2020. [Online]. Available: https://uis.brage.unit.no/uis-xmlui/handle/11250/2685503 [Accessed: Jul. 12, 2022]

[58] Sjur Sato Fimreite, '*Experimental studies: Formulation of a new geopolymer and investigation of effects of nanoparticles*' M.S. thesis, Department of Energy and Petroleum Engineering (IEP), University of Stavanger, Stavanger, Norway, 2020'

[59] Nelson, E., & Guillot, D. (2006). *Well Cementing, Second Edition.* Schlumberger.

9 Appendix

Appendix table 3: Data for 14 M geopolymer + SP 3 day

	Ref + 0g SP									
Plug	Mass	Diameter	Length	Vol	Density	Sonic	Vp	M (Gpa)	UCS (Max Load	UCS (MPa)
Ref #1	93.677	32.8	61.35	5.1838E-05	1807	24.4	2514	11.4	27.09	32
Ref #2	91.299	32.8	60.97	5.1517E-05	1772	24.5	2489	11.0	18.88	22
Ref #3	87.431	32.8	56.9	4.8078E-05	1819	22.7	2507	11.4	29.69	35
						Average	2503.2	11.3	25.2	29.8
	Ref+ 5g SP									
Plug	Mass	Diameter	Length	Vol	Density	Sonic	Vp	M (Gpa)	UCS (Max Load	UCS (MPa)
Ref+1+5g	94.273	32.8	61.38	5.1864E-05	1818	27.8	2208	8.9	19.43	23
Ref #2+5g	94.651	32.8	61.78	5.2202E-05	1813	25	2471	11.1	17.14	20
Ref #3+5g	84.186	32.8	55.02	4.649E-05	1811	22.4	2456	10.9	20.93	25
						Average	2378.45	10.29	19.17	22.68
	Ref+ 10g SP									
Plug	Mass	Diameter	Length	Vol	Density	Sonic	Vp	M (Gpa)	UCS (Max Load	UCS (MPa)
Ref+#1+10g	91.129	32.8	60.55	5.1162E-05	1781	24.5	2471	10.9	27.03	32
Ref+#2+10g	93.238	32.8	60.7	5.1289E-05	1818	24.3	2498	11.3	27.18	32
Ref+#3+10g	87.757	32.8	56.66	4.7876E-05	1833	22.2	2552	11.9	23.19	27
						Average	2507	11	26	31

	Ref+ 5g SP REPEAT (14 M)									
Plug	Mass	Diameter	Length	Vol	Density	Sonic	Vp	M (Gpa)	UCS (Max Load	UCS (MPa)
Ref+1+5g	91.234	32.8	58.43	4.9371E-05	1848	23.2	2519	11.7	22.91	27
Ref #2+5g	91.664	32.8	58.72	4.9616E-05	1847	23.5	2499	11.5	22.23	26
Ref #3+5g	93.028	32.8	59.57	5.0334E-05	1848	23.8	2503	11.6	20.24	24
						Average	2506.73	11.61	21.79	25.79

Appendix table 4: Data for 12 M geopolymer + SP 3 days

	Ref-0 Silica Powder									
Plug	Mass	Diameter	Length	Vol	Density	Sonic	Vp	M (Gpa)	UCS (Max Load, N)	UCS (MPa)
Ref #1	93.56	32.8	61.44	5.19145E-05	1802	26.5	2318	9.7	12.31	15
Ref #2	92.58	32.8	60.45	5.1078E-05	1813	24.8	2438	10.8	19.9	24
Ref #3	83.9	32.8	55.41	4.68194E-05	1792	23.6	2348	9.9	12.84	15
						Average	2368	10.11	15.02	17.77
	Ref- 5 SilicaPowder									
Plug	Mass	Diameter	Length	Vol	Density	Sonic	Vp	M (Gpa)	UCS (Max Load, N)	UCS (MPa)
Ref+1+5g	92.75	32.8	60.79	5.13653E-05	1806	25.9	2347	9.9	17.43	21
Ref #2+5g	93.41	32.8	61.53	5.19906E-05	1797	25.8	2385	10.2	17.45	21
Ref #3+5g	85.04	32.8	55.49	4.6887E-05	1814	22.7	2444	10.8	18.54	22
						Average	2392	10.33	17.81	21.07
	Ref- 10 SilicaPowder									
Plug	Mass	Diameter	Length	Vol	Density	Sonic	Vp	M (Gpa)	UCS (Max Load, N)	UCS (MPa)
Ref+#1+10g	93.67	32.8	61.03	5.15681E-05	1816	26.5	2303	9.6	19.85	23
Ref+#2+10g	94	32.8	61.34	5.183E-05	1814	26	2359	10.1	17.34	21
Ref+#3+10g	96.05	32.8	62.61	5.29031E-05	1816	26.5	2363	10.1	23.27	28
						Average	2342	9.95	20.15	23.85

Appendix table 5: Data for 12 M geopolymer + SP 10 days

	Ref									
Plug	Mass	Diameter	Length	Vol	Density	Sonic	Vp	M (Gpa)	UCS (Max Lo	UCS (MPa)
Ref #1	87.151	32.8	61.49	5.1957E-05	1677	24.5	2510	10.6	25.46	30
Ref #2	86.617	32.8	60.61	5.1213E-05	1691	24.3	2494	10.5	24.83	29
Ref #3	72.196	32.8	58.4	4.9346E-05	1463	20.1	2905	12.4	26.67	32
						Average	2636.50	11.15		30.36
	Ref + 5G SP									
Plug	Mass	Diameter	Length	Vol	Density	Sonic	Vp	M (Gpa)	UCS (Max Lo	UCS (MPa)
Ref+5g SP	83.438	32.8	57.73	4.878E-05	1711	22.7	2543	11.1	24.49	29
Ref+5g SP	84.904	32.8	59.19	5.0013E-05	1698	22.8	2596	11.4	23.86	28
Ref+5g SP	81.609	32.8	57	4.8163E-05	1694	22.9	2489	10.5	26.79	32
						Average	2542.77	11.00		29.64
	Ref + 10G SP									
Plug	Mass	Diameter	Length	Vol	Density	Sonic	Vp	M (Gpa)	UCS (Max Lo	UCS (MPa)
Ref+#1+10g SP	83.192	32.8	57.93	4.8949E-05	1700	23.2	2497	10.6	25.55	30
Ref+#1+10g SP	80.418	32.8	55.46	4.6862E-05	1716	22	2521	10.9	29.22	35
Ref+#1+10g SP	84.058	32.8	58.29	4.9253E-05	1707	23.6	2470	10.4	26.05	31
						Average	2495.94	10.64	26.94	31.88

Appendix table 6: Data for 12 M geopolymer + NP 3 days

	Ref + 0,1 AL2O3									
Plug	Mass	Diameter	Length	Vol	Density	Sonic	Vp	M (Gpa)	UCS (Max Lo	UCS (MPa)
Ref #1+0,1	85.402	32.8	58.8	4.9684E-05	1719	24.2	2430	10.1	20.47	24
Ref #2+0,1	85.965	32.8	59.33	5.0132E-05	1715	24.6	2412	10.0	31.11	37
Ref #3+0,1	84.089	32.8	57.9	4.8923E-05	1719	24.5	2363	9.6	22.41	27
						Average	2401.60	9.91		29.19
	Ref + 0,3 AL2O3									
Plug	Mass	Diameter	Length	Vol	Density	Sonic	Vp	M (Gpa)	UCS (Max Lo	UCS (MPa)
Ref+1+0,3	77.043	32.8	53.58	4.5273E-05	1702	21.6	2481	10.5	25.16	30
Ref #2+0,3	83.64	32.8	57.8	4.8839E-05	1713	23.1	2502	10.7	29.09	34
Ref #3+0,3	81.86	32.8	57.84	4.8873E-05	1675	23.5	2461	10.1	22.51	27
						Average	2481.33	10.45		30.28
	Ref + 0,5 AL2O3									
Plug	Mass	Diameter	Length	Vol	Density	Sonic	Vp	M (Gpa)	UCS (Max Lo	UCS (MPa)
Ref+#1+0,5	83.866	32.8	59.03	4.9878E-05	1681	24.1	2449	10.1	28.82	34
Ref+#2+0,5	78.288	32.8	54.82	4.6321E-05	1690	23	2383	9.6	25.64	30
Ref+#3+0,5	77.15	32.8	54.42	4.5983E-05	1678	21.1	2579	11.2	11.31	13
						Average	2470.67	10.28		25.95

Appendix table 7: Data for 12 M geopolymer + NP 10 days

	Ref + 0,1 AL2O3									
Plug	Mass	Diameter	Length	Vol	Density	Sonic	Vp	M (Gpa)	UCS (Max Lo	UCS (MPa)
Ref #1+0,1	85.402	32.8	58.8	4.9684E-05	1719	24.2	2430	10.1	20.47	24
Ref #2+0,1	85.965	32.8	59.33	5.0132E-05	1715	24.6	2412	10.0	31.11	37
Ref #3+0,1	84.089	32.8	57.9	4.8923E-05	1719	24.5	2363	9.6	22.41	27
						Average	2401.60	9.91		29.19
	Ref + 0,3 AL2O3									
Plug	Mass	Diameter	Length	Vol	Density	Sonic	Vp	M (Gpa)	UCS (Max Lo	UCS (MPa)
Ref+1+0,3	77.043	32.8	53.58	4.5273E-05	1702	21.6	2481	10.5	25.16	30
Ref #2+0,3	83.64	32.8	57.8	4.8839E-05	1713	23.1	2502	10.7	29.09	34
Ref #3+0,3	81.86	32.8	57.84	4.8873E-05	1675	23.5	2461	10.1	22.51	27
						Average	2481.33	10.45		30.28
	Ref + 0,5 AL2O3									
Plug	Mass	Diameter	Length	Vol	Density	Sonic	Vp	M (Gpa)	UCS (Max Lo	UCS (MPa)
Ref+#1+0,5	83.866	32.8	59.03	4.9878E-05	1681	24.1	2449	10.1	28.82	34
Ref+#2+0,5	78.288	32.8	54.82	4.6321E-05	1690	23	2383	9.6	25.64	30
Ref+#3+0,5	77.15	32.8	54.42	4.5983E-05	1678	21.1	2579	11.2	11.31	13
						Average	2470.67	10.28		25.95

Appendix table 8: Data for 12 M geopolymer + Carbon Fiber 3 days

	Ref + CF									
Plug	Mass	Diameter	Length	Vol	Density	Sonic	Vp	M (Gpa)	UCS (Max Lo	UCS (MPa)
Ref #1+0,1 C	91.271	32.8	59.12	4.9954E-05	1827	25.4	2328	9.9	20.82	25
Ref #2+0,1CF	91.293	32.8	58.98	4.9836E-05	1832	25.3	2331	10.0	21.55	26
Ref #3+0,1CF	92.236	32.8	59.5	5.0275E-05	1835	25.2	2361	10.2	16.24	19
							2339.97	10.03		23.12
	Ref + CF									
Plug	Mass	Diameter	Length	Vol	Density	Sonic	Vp	M (Gpa)	UCS (Max Lo	UCS (MPa)
Ref+1+0,3 CF	97.814	32.8	66.33	5.6046E-05	1745	29.5	2248	8.8	16.82	20
Ref #2+0,3 C	99.277	32.8	67.13	5.6722E-05	1750	31	2165	8.2	14.03	17
Ref #3+0,3CF	70.293	32.8	48.9	4.1319E-05	1701	22.2	2203	8.3	17.84	21
							2205.55	8.43		19.21

Appendix table 9: Data for 12 M geopolymer + Human hair for 3days

	Ref + HH									
Plug	Mass	Diameter	Length	Vol	Density	Sonic	Vp	M (Gpa)	UCS (Max Lo	UCS (MPa)
Ref+#1+0,1 H	95.444	32.8	64.66	5.4635E-05	1747	29.3	2207	8.5	17.72	21
Ref+#2+0,1 H	96.623	32.8	65.48	5.5328E-05	1746	30.5	2147	8.0	15.72	19
Ref+#3+0,1H	78.524	32.8	53.7	4.5375E-05	1731	24.8	2165	8.1	14.08	17
							2173.01	8.22	15.84	18.75
	Ref + HH									
Plug	Mass	Diameter	Length	Vol	Density	Sonic	Vp	M (Gpa)	UCS (Max Lo	UCS (MPa)
Ref+#1+0,3 H	92.035	32.8	59.52	5.0292E-05	1830	25.3	2353	10.1	18.39	22
Ref+#2+0,3 H	90.09	32.8	58.51	4.9439E-05	1822	25.7	2277	9.4	17.95	21
Ref+#3+0,3H	91.519	32.8	59.15	4.998E-05	1831	25.8	2293	9.6	15.75	19
							2307.29	9.73	17.36	20.55

Appendix table 10: Data for cement for 4days and 10days

	10 days in oven Cement									
Plug	Mass	Diameter	Length	Vol	Density	Sonic	Vp	M (Gpa)	UCS (Max Lo	UCS (MPa)
Ref #1+0,1	93.237	32.8	65.89	5.5675E-05	1675	21.6	3050	15.6	25.02	30
Ref #2+0,1	92.855	32.8	65.59	5.5421E-05	1675	21.6	3037	15.4	19.55	23
Ref #3+0,1	95.2	32.8	66.2	5.5937E-05	1702	20.2	3277	18.3	21.4	25
							3121.42	16.44		26.02
	4 days in oven Cement									
Plug	Mass	Diameter	Length	Vol	Density	Sonic	Vp	M (Gpa)	UCS (Max Lo	UCS (MPa)
Ref #1+0,1	95	32.8	64.3	5.4331E-05	1749	21.3	3019	15.9	20.42	24
Ref #2+0,1	93.6	32.8	63.4	5.3571E-05	1747	21.2	2991	15.6	17.62	21
Ref #3+0,1	86	32.8	58.4	4.9346E-05	1743	19.4	3010	15.8	19.63	23
								15.79		22.75

Appendix table 11: Data for water absorption

TIME	Mass	% Cement water absorption
0	96.891	
24	104.62	7.98
48	104.68	8.04
72	104.75	8.11
96	104.82	8.18
120	105.05	8.42

TIME	Mass	% Geopolymer water absorption
0	90.2	
24	91.74	1.71
48	91.45	1.39
72	91.27	1.19
96	91.14	1.04
120	91.07	0.96

Appendix table 12: Data for Leakage test

	3 days		3+3 days		3+3+4 days	
	Geoplymer	Cement	Geoplymer	Cement	Geoplymer	Cement
Weight of pipe without water	191.84	183.84	186.13	186.66	185.18	187.65
weight of pipe with water	217.34	206.11	213.52	210.79	211.51	211.92
weight of cup w/o water	16.50	16.45	16.50	16.45	16.50	16.45
Wt of fluid added on the top	25.5	22.27	27.39	24.13	26.33	24.27
Wt of pipe with water	216.67	205.9	213.41	210.49	211.36	211.53
Wt of cup with water	16.50	16.45	16.50	16.45	16.50	16.45
Wt of pipe after removel of water	194.29	194.2	191.49	194.28	191.5	194.29
Wt of fluid on the top	22.380	11.700	21.920	16.210	19.860	17.240
Wt of fluid leakage	0.00	0.00	0.00	0.00	0.00	0.00
Wt of fluid absorbed in the plug	2.45	10.36	5.36	7.62	6.32	6.64
Wt of fluid evapuration	0.67	0.21	0.11	0.30	0.15	0.39

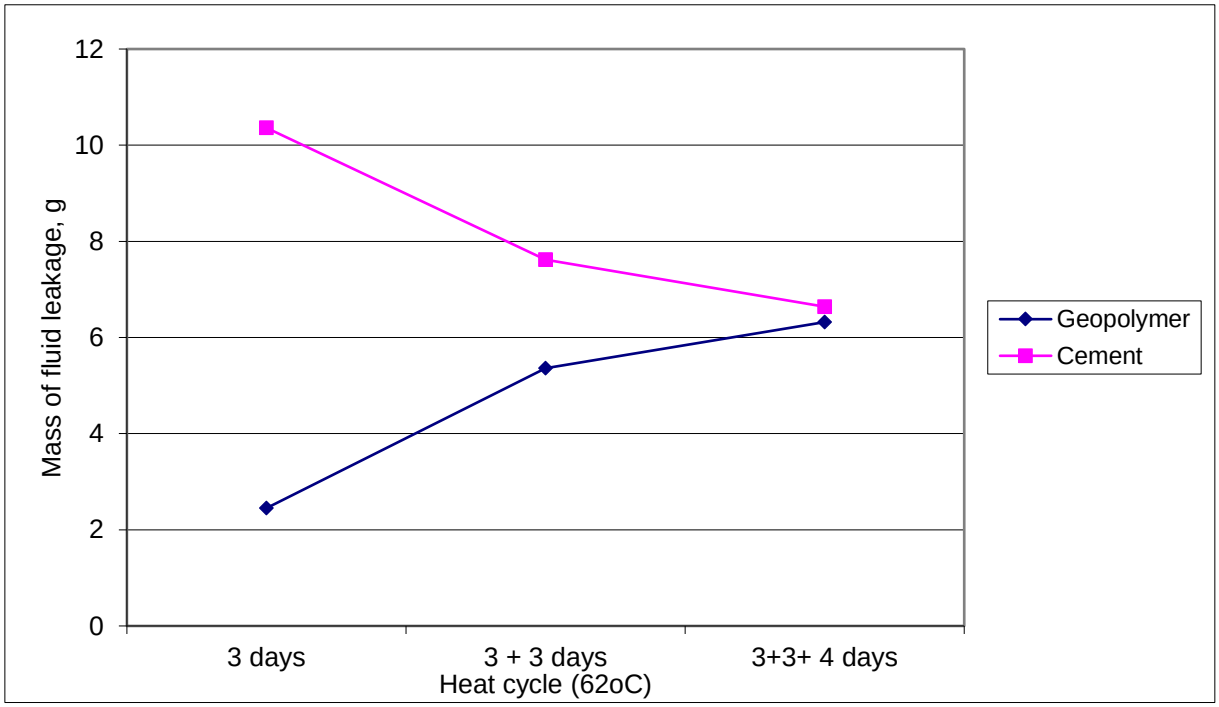

Diagram showing the rate of leakagewith respect to time for the geopolymer and cement plug

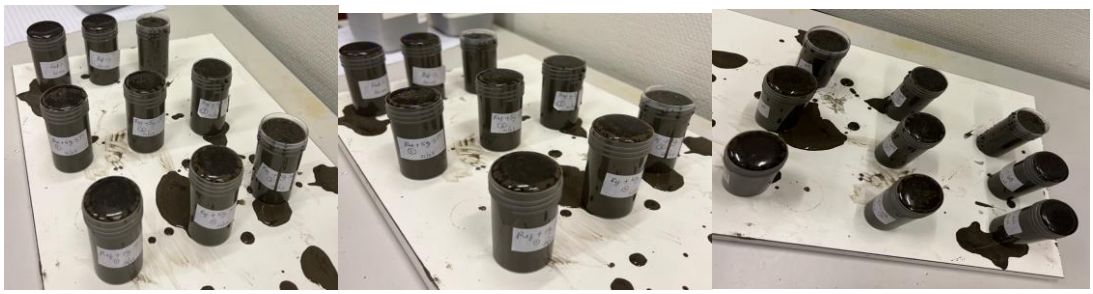

The diagram shows well-labelled plugs which are being cured for 24 hours before going into the oven

The diagram shows plugs containing SP which have been properly polished and ready for testing

The diagram shows plugs containing NP which have been properly polished and ready for testing

The diagram shows polished neat geopolymer to be used to test for water absorption

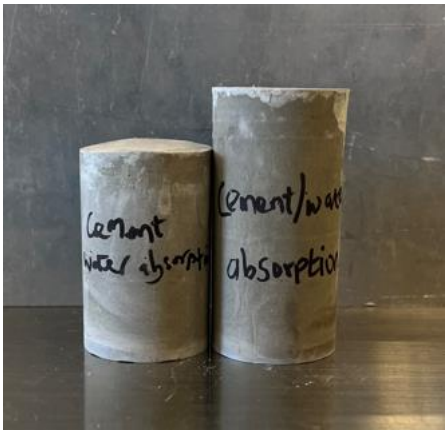

The diagram shows polished neat cement to be used to test for water absorption

The diagram shows the condition of the cement plug after the complete leakage test cycle

The diagram shows the condition of the cement plug after the complete leakage test cycle